Progress in Polymer Science 122 (2021) 101453

Contents lists available at ScienceDirect

Progress in Polymer Science

journal homepage: www.elsevier.com/locate/progpolymsci

Functional polymers for lithium metal batteries

Sipei Li[a,b,1], Francesca Lorandi[a,1], Han Wang[c], Tong Liu[a], Jay F. Whitacre[c,d,*], Krzysztof Matyjaszewski[a,*]

[a] Department of Chemistry, Carnegie Mellon University, 4400 Fifth Avenue, Pittsburgh, Pennsylvania, 15213, USA
[b] Aramco Research Center – Boston, Aramco Services Company, Boston, Massachusetts, 02139, USA
[c] Department of Materials Science and Engineering, Carnegie Mellon University, 5000 Forbes Avenue, Pittsburgh, Pennsylvania, 15213, USA
[d] Scott Institute for Energy Innovation, Carnegie Mellon University, 5000 Forbes Avenue, Pittsburgh, Pennsylvania, 15213, USA

ARTICLE INFO

Article history:
Received 11 May 2021
Revised 3 August 2021
Accepted 3 September 2021
Available online 8 September 2021

Keywords:
Lithium metal batteries
Polymer electrolytes
Composite electrodes
Artificial solid lectrolyte interfaces
Polymer binders
Polymer separators
Anode coatings

ABSTRACT

Rechargeable batteries that use Li metal as anode are regarded as the most viable alternative to state-of-the-art lithium ion batteries (LIBs), since Li metal batteries (LMBs) are capable of higher-density energy storage. The Nobel Prize in Chemistry 2019 awarded to J. B. Goodenough, S. M. Whittingham, and A. Yoshino for their contributions to the development of LIBs, drew increasing attention to the design of LMBs. Due to the highly reactive nature of metallic lithium and the need to tweak the design of cathode, electrolyte and anode, the industrial success of LMBs has yet to be achieved. In a battery cell, polymeric materials were traditionally used only as separators, cathode binders and packaging materials. In contrast, the enormous progress achieved in a century of polymer chemistry has enabled a large variety of application of polymers in numerous areas of material science. The design and implementation of functional polymers in LMBs is crucial to enhance their practical performance, safety and durability, paving the way to LMB commercialization. This review describes recent advances in the synthesis and tailoring of functional polymer materials to improve the stability of LMBs. The role and application of polymers in different parts of an LMB are presented, including anode, cathode, electrolyte and anode/electrolyte interphases.

Abbreviations

AAO	Anodized aluminum oxide
ASEI	artificial solid electrolyte interphase
ATRP	atom transfer radical polymerization
BAMB	bis(allylmalonato) borate
BASP	brush-arm star polymers
BCPE	block copolymer electrolyte
Bis-αCCs	bis(α-alkylidene carbonate)s
BMITFSI	butyl-3-methylimidazolium bis (trifluoromethanesulfonyl)imide
β-CDp	β-cyclodextrin polymer
CB	carbon black
CE	Coulombic efficiency
CEI	cathode electrolyte interphase
CMC	carboxymethylcellulose
CNF	cellulose nanofiber
C-NF	carbon nanofiber
CNT	carbon nanotube
CPE	composite polymer electrolyte
CPL	composite protective layer
CROP	cationic ring opening polymerization
CTAB	cethyltrimethyl ammonium bromide
$Đ$	molecular weight dispersity
DAA	N-(3, 4-dihydroxyphenethyl)acrylamide
DDQ	2, 3-dichloro-5, 6-dicyano-1, 4-benzoquinone
DeTAB	decyltrimethyl ammonium bromide
DIB	1,3-diisopropenylbenzene
DMAc	dimethylacetamide
DNW	double network
DOL	1,3-dioxolane
DP	degree of polymerization
DPCE	disparete-polymers protected ceramic electrolyte
DPPG	diaminopoly(propylene glycol)
DSN	dynamic single Li-ion conducting network
DVIMBr	1-vinyl-3-al-lylimidazolium bromide
EDL	electric double layer
EDOT	3,4-ethylenedioxythiophene
EO	ethylene oxide
FEC	fluoroethylene carbonate
FRP	free radical polymerization

* Corresponding author.
[1] These authors contributed equally

https://doi.org/10.1016/j.progpolymsci.2021.101453
0079-6700/

FTEG	1H,1H,11H,11H-perfluoro-3,6,9-trioxaundecane-1,11-diol
G3	triethylene glycol dimethyl ether
G4	Tetraethylene glycol dimethyl ether
GA	gum Arabic
Ga-LLZO	$Li_{6.25}Ga_{0.25}La_3Zr_2O_{12}$
GMA	glycidyl methacrylate
GO	graphene oxide
GPE	gel polymer electrolyte
HF	hydrofluoric acid
HOMO	highest occupied molecular orbital
HPMC	hydroxypropylmethyl cellulose
ICE	internal combustion engine
IL	ionic liquid
LA132	polyacrylic rubber latex
LAGP	$Li_{10}Al_{10.5}Ge_{1.5}(PO_4)_3$
LATP	$Li_{1.3}Al_{0.3}Ti_{1.7}(PO_4)_3$
LCO	lithium cobalt oxide ($LiCoO_2$)
LFP	lithium iron phosphate ($LiFePO_4$)
LIB	lithium ion battery
LICGC	LiO_2-Al_2O_3-SiO_2-P_2O_5-TiO_2-GeO_2
LiFSI	lithium bis(fluorosulfonyl)imide
LiMTFSI	lithium 1- [3-(methacryloyloxy)propyl sulfonyl]-1-(trifluoromethylsulfonyl)imide)
LiPAA	lithium polyacrylic acid
LiPSP	lithium polysulfidophosphate
LiTFSI	lithium bis(trifluoromethanesulfonyl)imide
LLAZO	$Li_{6.28}La_3Al_{0.24}Zr_2O_{12}$
LLCZNO	$Li_7La_{2.75}Ca_{0.25}Zr_{1.75}Nb_{0.25}O_{12}$
LLTO	$Li_{0.33}La_{0.557}TiO_3$
LLZO	$Li_7La_3Zr_2O_{12}$
LLZTO	$Li_{6.4}La_3Zr_{1.4}Ta_{0.6}O_{12}$
LMB	lithium metal battery
LNMO	$Li_{1.2}Ni_{0.2}Mn_{0.6}O_2$
LSPS	$Li_{10}SnP_2S_{12}$
LTO	lithium titanate ($Li_4Ti_5O_{12}$)
LUMO	lowest unoccupied molecular orbital
MOF	metal organic framework
MP	microparticle
MW	molecular weight
N/P	negative to positive electrode capacity ratio
NCA	$LiNi_{0.8}Co_{0.15}Al_{0.05}O_2$
NCM111	$LiNi_{1/3}Co_{1/3}Mn_{1/3}O_2$
NCM532	$LiNi_{0.5}Co_{0.3}Mn_{0.2}O_2$
NCM622	$LiNi_{0.6}Co_{0.2}Mn_{0.2}O_2$
NCM811	$LiNi_{0.8}Co_{0.1}Mn_{0.1}O_2$
NMP	nitroxide mediated polymerization
NMPy	N-methyl-2-pyrrolidone
NP	nanoparticle
oCVD	oxidative chemical vapor deposition
OEGDE	poly(ethylene glycol)diglycidyl ether
OIPC	organic ionic plastic crystal
OTf	trifluoromethane sulfonate (triflate)
P(SF-DOL)	poly(vinylsulfonyl fluoride-*ran*-2-vinyl-1,3-dioxolane)
PAA	polyacrylic acid
PAA-NH_4	ammonium polyacrylic acid
PAL	polyacrylate latex
PAM	polyacrylamide
PAN	polyacrylonitrile
PANI	polyaniline
PBzMA	polybenzylmethacrylate
PC	polycarbonate
PCEA	poly(2-chloroethyl acrylate)
PCL	polycaprolactone
PDADMA	polydiallyldimethylammonium
PDMS	polydimethylsiloxane
PE	polymer electrolyte
PEt	polyethylene
PEALiFSI	poly(ethylene-*co*-acrylic lithium(fluoro sulfonyl)imide)
PEDOT	poly(3,4-ethylenedioxythiophene)
PEDOT:PSS	poly(3,4-ethylenedioxythiophene) polystyrene sulfonate
PEGDA	poly(ethylene glycol) diacrylate
PEGDGE	poly(ethylene glycol) diglycidyl ether
PEGMA	poly(ethylene glycol)methacrylate
PEI	polyehtyleneimine
PEO	poly(ethylene oxide)
PEO_X-PC	poly(ethylene oxide carbonates)
PFE	perfluoroether
PFPE	perfluoropolyether
PFPE-DMC	methyl carbonate-terminated perfluoropolyether
PI	polyimide
PIL	poly(ionic liquid)
PIM	polymer of intrinsic microporosity
PLiSTFSI	polystyrenesulfonyllithium (trifluoromethylsulfonyl)imide
PMEA	poly(ethylene glycol)methyl ether acrylate
PMMA	poly(methyl methacrylate)
PNMA	poly(N-methyl-malonic amide)
PO	propylene oxide
PolyFAST	polymeric fluorinated aryl sulfonimide tagged (FAST) anion
POSS	polyhedral oligomeric silesquioxanes
PP	polypropylene
PPC	polypropylene carbonate
PPS	polyphenylene sulfide
PPy	polypyrrole
PPyPU	polypyrrole-polyurethane
PS	polystyrene
PSS	poly(styrenesulfonate)
PTFE	polytetrafluoroethylene
PTHF	polytetrahydrofuran
PTMEG	poly(tetramethylene ether glycol)
PU	polyurethane
PVA	polyvinyl alcohol
PVC	poly(vinylene carbonate)
PVK	poly(N-vinylcarbazole)
PVDF	polyvinylidene fluoride
PVDF-HFP	poly(vinylidene fluoride-co-hexafluoropropylene)
PVP	polyvinylpyrrolidone
RAFT	reversible addition-fragmentation chain-transfer
rGO	reduced graphene oxide
ROMP	ring opening metathesis polymerization
ROP	ring opening polymerization
RPC	reactive polymer composite
SBMA	2-methacryloyloxy ethyl dimethyl -3-sulfopropylammonium hydroxide
SBR	styrene butadiene rubber
SEI	solid electrolyte interphase
SEM	scanning electron microscope
SEO	polystyrene-*b*-poly(ethylene oxide)
SHE	standard hydrogen electrode
SIL	solvate ionic liquid
SLIC	single Li-ion conducting
SLMA	semiliquid lithium metal anode
SP	silly putty
SPAN	sulfur-polyacrylonitrile composite
SPE	solid polymer electrolyte
TEM	transmission electron microscopy
T_g	glass transition temperature
t_{Li+}	transference number
THF	tetrahydrouran

TMC	trimethylene carbonate
TOM	trimethoxyehtylene
UPyMA	ureidopyrimidinone methacrylate
VC	vinylene carbonate
YSZ	yttria stabilized zirconia

1. Introduction

For over a hundred years, our society has been powered by internal combustion engines (ICEs), which are heat engines where chemical energy is directly transformed into mechanical energy via the combustion of fuels and oxidizers [1]. Unfortunately, ICEs have low energy efficiency (<40%) and are evidently causing a dramatic level of environmental pollution [2]. Thus, sustainable energy generation, conversion, and storage methods are urgently needed. Rechargeable batteries can reversibly convert chemical energy directly into electricity at a much higher energy efficiency, generate much less greenhouse gases than ICE and are key tools to fight against global warming [3]. In 2019, the Nobel Prize in Chemistry was awarded to Goodenough, Whittingham and Yoshino, honoring the development of rechargeable lithium ion batteries (LIBs) [4]. This prestigious recognition has drawn even more consensus on the role of rechargeable batteries as necessary and most promising replacement for ICEs.

The history of commercial rechargeable batteries dates back to the early 1900s when battery chemistries such as Lead-Acid battery, Ni-Cd battery and Ni-metal hydride (Ni-MH) battery were commercialized for mobile and stationary applications [5]. In the 1970s, Whittingham developed an intercalation cathode, TiS_2, that could operate in conjunction with lithium metal as anode [6]. In the 1980s, Goodenough developed another intercalating cathode material, lithium cobalt oxide ($LiCoO_2$, more commonly referred to as LCO), which had higher energy density than TiS_2 [7]. In 1985, Yoshino paired LCO with an intercalating carbon anode made of petroleum coke [8], which resulted in a device with more stable cycling performance and sufficiently high energy density. The pioneering contributions from the three Nobel laureates and many other scientists and engineers in both industry and academia led to the creation of LIBs, which have a profound impact on our daily life.

A state-of-the-art LIB uses graphite as the anode, a layered metal oxide as the cathode and liquid organic solvents, such as carbonate-based solvents, together with lithium salts as the electrolyte. Such configuration typically gives a cell-level energy density of about 200-250 Wh/Kg, which is only slightly improved in comparison to the first-generation LIBs released by SONY in 1991. Moreover, the energy density remains far from the one of gasoline, which is around 13,000 Wh/Kg [9]. While recent advances in LIB design including Si-based anodes [10–12] and layered metal oxide cathodes [13,14] show promising performance, the energy density of LIBs is approaching a bottleneck. Therefore, the question that needs to be addressed is whether the energy density of rechargeable batteries can keep up with the explosive technology expansion. Currently, the most credited solution relies on replacing the graphite anode (with a theoretical capacity of 375 mAh/g) with lithium metal. In fact, lithium metal has the lowest redox potential (-3.04 V vs standard hydrogen electrode, SHE), high theoretical capacity (3860 mAh/g) and low market price [15].

Lithium metal was already used as anode material in the earliest prototypes of lithium secondary batteries, including the device originally developed by Whittingham in the 1970s. In the late 1980s, Moli Energy released the first commercial lithium battery that used lithium metal as anode. However, shortly after the release, the company had to recall all sold cells because of continuous accidents including fires and explosions, marking a halt in the study of lithium metal anodes [16]. The development of advanced characterization techniques and material preparation approaches, along with better understanding of the mechanisms of lithium deposition acquired in the 21st century, raised the possibility of obtaining safe and stable devices based on lithium metal anodes. Therefore, the revival of lithium metal anode has become a necessity. In pursuit of reliable rechargeable lithium metal batteries (LMBs), many governments across the World started their own programs to accelerate related research. For example, the United States established the *Battery500* consortium in 2016, Japan started the *Research and Development Initiative for Scientific Innovation of New Generation Battery (RISING)* project in 2009, and China launched the *Made in China 2025* project in 2015 [17]. Many global battery manufacturers such as Tesla, Toyota, Samsung, CATL and LG Chem, and several promising tech start-ups such as QuantumScape, SolidEnergy Systems, and Ionic Materials have invested vast amounts of resources in developing LMBs.

An LMB uses a thin layer of lithium foil as the anode, aprotic organic lithium solution as the electrolyte, lithiated layered metal oxides or sulfur or oxygen in the presence of binders, as the cathode (Fig. 1). It should be noted that an anode-free set-up is also possible [18], albeit more challenging, whereby Li^+ ions are initially stored in a lithiated cathode material and directly plated on the Cu current collector during the first charge. The stability of anode, electrolyte and cathode affects the composition and properties of the artificial solid electrolyte interphase (ASEI) that forms between the anode and the electrolyte, as well as of the cathode electrolyte interphase (CEI) that forms on the particle surface of cathode active materials in contact with the electrolyte, polymer binders and conductive agent (Fig. 1). The success of rechargeable LMBs hinges on the integrated operation of all components [19], i.e. anode, electrolyte, cathode, SEI, CEI and binders. Thus, problems associated with any of these parts need to be addressed.

Due to its intrinsic “hostless” nature, a lithium metal anode undergoes vast volume change during cycling. For example, the deposition of Li at a current density of 1 mAh/cm^2 corresponds to a thickness increase of 4.95 μm at the electrode. High volume changes can lead to non-uniform deposition of lithium and breakage of the naturally formed SEI. To minimize the volume variation of the lithium electrode, various anode engineering approaches have been reported, including the fabrication of lithium/alloy hybrid anodes and the infusion of molten lithium into a conductive scaffold [20]. Recently, polymer materials have emerged as soft hosts for making composite lithium anodes, exhibiting unique advantages over inorganic materials-based approaches [21].

In addition to physical interfacial instability due to the variation of volume change, the SEI that spontaneously forms via chemical and electrochemical reactions between lithium and the liquid electrolyte is intrinsically unstable. The SEI brittleness and non-uniform composition lead to “hotspots” that favor lithium depositions, and “cold-spots” that block the lithium transport. Such inhomogeneity can cause the growth of detrimental lithium dendrites [22]. Polymer materials have highly tunable mechanical properties, dielectric permittivity and functionalities, therefore being ideal candidates for the ex situ fabrication of artificial SEIs, i.e. protective coatings on the anode that compensate for the flaws of natural SEIs [22].

Besides the occurrence of side reactions with lithium metal that result in formation of unstable SEIs, conventional liquid electrolytes also suffer from i) low transference number (t_{Li+}, defined as the fraction of current carried by Li ions) that can induce the formation of gradients in the concentration of lithium ions promoting the growth of dendrites; ii) poor mechanical strength, therefore being unable to physically prevent the penetration of lithium dendrites; iii) high flammability that can lead to safety concerns in

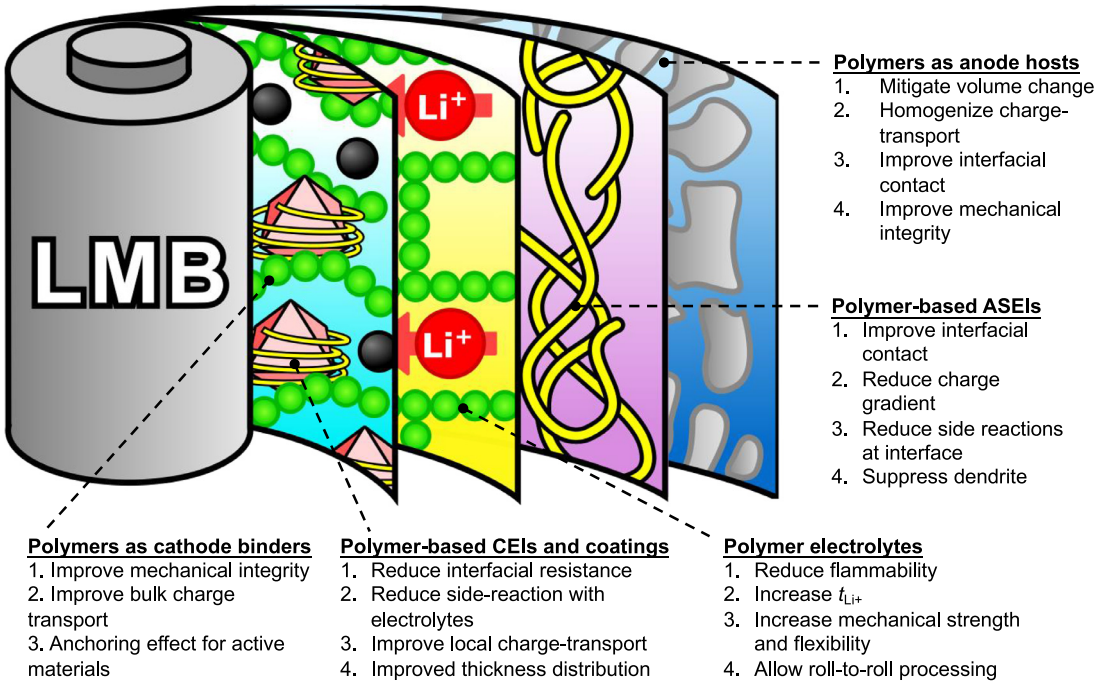

Fig. 1. Illustration of a LMB including its critical components (anode, electrolyte, cathode, binders, SEI and CEI) and the roles that polymer materials could play for each component.

case of short-circuits. Solid polymer electrolytes (SPEs) can overcome the drawbacks of liquid electrolytes [23]. Compared to other electrolyte compositions, such as liquid electrolytes with high salt concentration [20] and solid ceramic electrolytes [24], SPEs benefit from relatively low costs and facile processability. Therefore, SPEs are regarded as key enablers for next-generation solid-state LMBs. In addition to dry SPEs, an alternate approach is by adding small amount of solvent or plasticizers to form gel polymer electrolytes (GPEs), with enhanced conductivities.

Two categories of cathode materials are used for high-energy-density LMBs: i) lithiated layered metal oxide (also adopted for current LIBs) and ii) non-lithiated high-energy-density materials, such as sulfur and oxygen. Paring a lithium metal anode with high-energy-density cathode materials, such as Li-rich and Ni-rich cathodes, eliminates the need for modifying the original production infrastructure of LIBs. However, electrolyte decomposition in highly oxidative environments and structural instability of cathode materials in the delithiated stage (i.e. metal ions dissolution) can lead to rapid capacity loss [21,25]. A sulfur cathode has a very high theoretical specific capacity of 1670 mAh/g. However, the implementation of a sulfur cathode is limited by the low active material loading and the polysulfide shuttle effect, i.e. the dissolution of intermediate active materials in the electrolytes [26]. Lithium-air (O_2) batteries have an ultra-high theoretical energy density of 3500 Wh/Kg. However, the chemical instability of conventional organic electrolytes against oxygen reduction products (e.g., superoxide or peroxide) and the slow kinetics of oxygen reduction and peroxide oxidation have to be solved in order to deploy these devices [27]. Polymer materials have long been used as cathode binders, providing mechanical stability, prompt adhesion and improved distribution of active materials and conductive agents. Furthermore, novel polymers are being developed and used as protective layers (CEI) or framework for cathode active materials to further provide ionic/electronic conductivity, chemical/electrochemical stability, continuous surface coverage, and mechanical integrity.

During the past 100 years since when Staudinger proposed the concept of macromolecules in 1920 [28], polymer science has witnessed a rapid development, culminated in the invention of advanced controlled polymerization techniques. These revolutionary polymerization methods were developed around the same time of the commercialization of LIBs, and include nitroxide mediated polymerization (NMP) [29], acyclic diene metathesis polycondensation [30] and ring opening metathesis polymerization (ROMP) [31] in 1980s, atom transfer radical polymerization (ATRP) in 1995 [32,33], and reversible addition−fragmentation chain-transfer (RAFT) polymerization in 1998 [34]. Together with advanced modification chemistries, such as click chemistries [35–39], these synthetic tools enabled scientists to design polymer materials with predetermined molecular weight (MW) and low dispersity [40–44], precisely defined morphologies, compositions [45–52], and functionalities [47,53–58]. Therefore, it became possible to readily synthesize polymers that meet the property requirements of each part of an LMB [59–61]. In this review, recent advances in materials for LMBs are examined from the perspective of polymer chemistry. Specifically, chemistries and applications of polymer materials in the area of polymer electrolytes (Section 2), polymer artificial solid electrolyte interphases (ASEIs) (Section 3), polymer/lithium composite anodes (Section 4), and polymer-based cathode electrolyte interphases (CEIs) and binders for cathode materials – layered metal oxide (Section 5) and sulfur (Section 6) – are presented. Lithium-air batteries and Li-O_2 batteries have been previously discussed in literature [62–67], and will not be covered in this review. In addition to LMBs, there are other promising energy storage techniques such as silicon-anode-based LIBs, sodium ion/metal batteries, zinc-air batteries, etc, which have been comprehensively discussed in previous reviews and will not be covered herein [68–74]. The aim of this review is to provide a comprehensive overview for polymer scientists who contribute or intend to contribute to the field of energy storage, as well as for battery scientists who are interested in tailoring polymer properties to develop safe and long-term stable high-energy LMBs.

2. Polymer electrolytes for LMBs

2.1. General characteristics of polymer electrolytes

Commercial LIBs use liquid electrolytes, which are typically composed of a lithium salt with bulky anion, such as $LiPF_6$, and aprotic organic solvents with high dielectric constant. The most common electrolytes include ethylene carbonate and a dialkyl carbonate, e.g. dimethyl carbonate, diethyl carbonate. These solvents are highly flammable and their instability increases at high temperatures, potentially causing thermal runaway and hazardous failure of the battery [75,76]. Therefore, non-flammable electrolytes with enhanced thermal and electrochemical stability are imperative for safer energy storage devices.

Conventional liquid electrolytes are even more detrimental when employed in LMBs [77,78]. The contact between the highly reactive Li metal and aprotic organic electrolytes results in the formation of a conducting SEI on Li metal. The SEI typically has non-uniform composition and poor mechanical strength, therefore being prone to fracturing during battery cycling, exposing fresh Li to the electrolyte, and thus causing further electrolyte decomposition [77]. Moreover, the SEI inhomogeneity induces the formation of preferential nucleating sites during Li deposition, which results in growth of Li dendrites. During prolonged plating/stripping cycles, dendrite proliferation and electrolyte consumption ultimately cause battery failure. Dendrites can penetrate through the cell, causing an internal shortage that can lead to fires and explosion because of the combustible nature of the electrolyte. In addition, liquid electrolytes generally have low t_{Li+}, which indicates poor charge-transport efficiency [79].

Therefore, different strategies were explored to design safe electrolytes with improved compatibility with Li metal, including varying the composition of liquid electrolytes to form better SEIs, and developing solid or quasi-solid electrolytes, with desirable electrochemical and mechanical stability [77]. Polymer-based electrolytes and ceramic lithium ion conductors are the most widely investigated alternatives to liquid electrolytes, and their encouraging performances are attracting the interest of EV manufacturers and boosting their implementation in practical devices [76,78–80].

Typical ceramic electrolytes include garnet-type electrolytes, such as $Li_7La_3Zr_2O_{12}$ (LLZO) and NASICON-type electrolytes, such as $Li_{1.5}Al_{0.5}Ge_{1.5}(PO_4)_3$ (LAGP). Ceramic electrolytes generally have high Li transference number, high ionic conductivity (σ) that can be comparable or even higher than that of conventional liquid electrolytes ($> 10^{-3}$ S/cm at r.t.), and high shear modulus [78]. The latter was predicted to be key to uniform Li electrodeposition and inhibition of dendrites in LMBs [81]. In particular, Monroe and Newman's model indicated that optimal electrolytes have a shear modulus of $>$ 6 GPa, or about twice the shear modulus of Li metal.

However, ceramic electrolytes are highly brittle and have poor interfacial contact with electrodes that can result in large interfacial resistance and poor cycling performance [78]. Furthermore, they are not exempt from dendrite growth that can occur through grain boundaries or interconnected pores [82]. In contrast, polymer electrolytes typically exhibit good mechanical integrity and flexibility, as well as sufficient surface stability and interfacial contact with electrodes [12,76]. Moreover, polymer electrolytes are easily processed in thin films, manufactured from readily available precursors and their structure can be largely tuned, which results in tunable mechanical properties and electrochemical performance.

Nevertheless, some challenges remain to be solved for practical use of polymer-based electrolytes and particularly for their implementation in high-voltage LMBs. i) The conductivity of polymer electrolytes must be improved to reach practical targets (e.g. $\sigma > 4 \times 10^{-4}$ S/cm at r.t. as established by the U.S. Department of Energy) [83]. ii) A lithium transference number close to unity should be achieved to ensure efficient charge transport. iii) The polymer electrolyte should have high shear modulus to suppress dendrite growth, while maintaining desirable flexibility and electrode wetting. iv) The electrolyte should be amenable of large-scale roll-to-roll productions. Furthermore, wide electrochemical stability window (from 0 to $>$ 4.5 V vs Li^+/Li – all potential values reported in this review are referred to Li^+/Li, unless otherwise specified) is necessary to pair the electrolyte with high-voltage cathodes. Polymer electrolytes for Li-S batteries should also slow down or block the shuttling of polysulfides that form on the cathode side [84].

In order to have good conductivity for Li ions, the polymer matrix should: i) possess sites able to coordinate to Li ions with sufficient strength to promote the dissolution of the salt, but at the same time enabling Li^+ to hop between the sites; ii) have high dielectric constant to favor charge separation in the salt; iii) have low glass transition temperature (T_g) and low crystallinity at room temperature, corresponding to high backbone flexibility and facile segmental motion [85].

While most polymers have shear moduli lower than the ideal value of 6 GPa, recent studies suggest that "soft" electrolytes can still enable stable Li plating/stripping on Li metal anode [77,79]. While electrolytes with high modulus can suppress dendrites by exerting pressure during deposition, electrolytes with high Li transference number promote efficient and uniform Li^+ transport, preventing formation of charge concentration gradient and anions decomposition [86]. Moreover, nanostructured electrolytes can confine the Li deposition to a length scale smaller than the length scale of the most stable nucleates [87]. Therefore, the ability of precisely engineering the composition and architecture of polymer materials through advanced polymerization techniques is essential to reach a breakthrough in polymer electrolytes for high-energy, safe and stable Li metal batteries.

This Section discusses some of the most relevant and most investigated types of polymer electrolytes, including recently developed and promising materials, highlighting the synthetic strategies that are enabling to overcome key challenges for high-performing electrolytes.

2.2. Solid polymer electrolytes (SPEs)

2.2.1. PEO-based solid electrolytes

In the late '70s, alkali metal salts dispersed in poly(ethylene oxide) (PEO) were first used as solid electrolytes [88]. Since then, PEO has been the most investigated polymer for polymer-based electrolytes. The ability of PEO/salt mixtures to conduct Li^+ depends on the amorphous region of the polymer. PEO has relatively low T_g ($\sim$ -60°C) and the ethylene oxide (EO) units are capable of complexing to Li^+, facilitating the dissolution of the salt. However, PEO has poor mechanical stability at $T >$ 60°C and relatively high degree of crystallinity at r.t., which results in low conductivity, 10^{-8}-10^{-7} S/cm. Moreover, the strong interactions between Li^+ and EO units diminishes the Li transference number (0.1-0.2), and PEO-based electrolytes tend to be unstable at high voltages ($>$ 3.8 V) [89].

Therefore, several efforts were made to engineer the structure and composition of PEO-based SPEs to meet the requirements for long-term stable LMBs. At the same time, other polymers were extensively investigated for their use as solid-state electrolytes. On the other hand, plasticizers and inorganic fillers were introduced in polymer electrolytes to enhance their conductivity and/or mechanical strength, forming gel polymer electrolytes (GPEs) and composite polymer electrolytes (CPEs), respectively (see Section 2.3 and 2.4).

In the past decades, advancements in polymer chemistry enabled to finely tune polymer morphology and architecture, opening new possibilities to explore structure-properties relationships

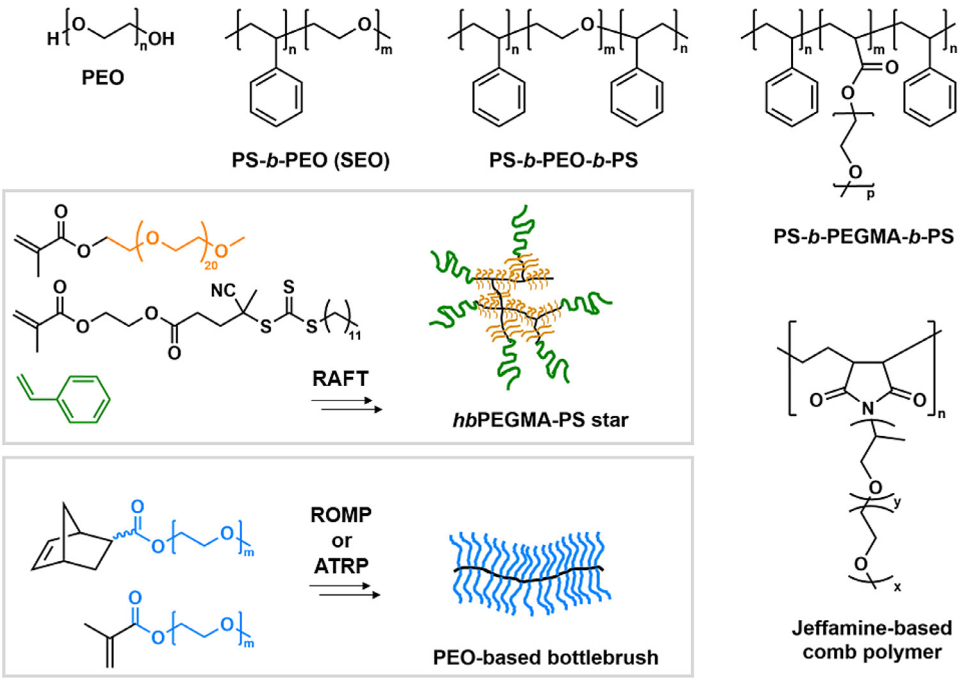

Fig. 2. Examples of PEO-based polymers with different architectures used as SPEs.

in polymer electrolytes [12,59,60,90]. The design of block copolymer electrolytes (BCPEs) has attracted great interest as it allows for decoupling the electrical and mechanical properties, due to the self-assembly of these materials into periodic structures with nanosized domains [91–94]. In PEO-based BCPEs, the conductive pathways are provided by an EO-containing block, while the other block contributes to the mechanical strength. The nanostructure of BCPEs depends on the Flory-Huggins interaction parameter, on the degree of polymerization and chain architecture, as well as on the relative block volume. However, doping with Li salt and the complexation of Li^+ with EO-units can modify the copolymer morphology and the properties of the domains, affecting the conductivity and mechanical strength of the electrolyte. Thus, the molar ratio of Li ions to EO units (r = [Li]/ [EO]) needs to be carefully optimized in BCPEs, together with the copolymer composition.

Polystyrene-*b*-PEO (PS-*b*-PEO, or SEO) diblock copolymers and PS-*b*-PEO-*b*-PS triblock copolymers (Fig. 2) have been widely studied as BCPEs. SEO is synthesized by anionic polymerization, whereas the triblock copolymer is usually prepared by transforming the terminal hydroxyl group of PEO into initiating sites for subsequent controlled radical polymerization, e.g NMP or ATRP [93,95,96]. In contrast to PEO homopolymers where the ionic conductivity decreased with increasing the molecular weight M_n, the conductivity of SEO (with r = 0.02-0.1) increased with M_n(PEO) (for M_n > 10k) until reaching a plateau, and a similar behavior was reported for the triblock copolymer [91,95]. This was attributed to the existence of a dead zone excluded from the Li^+ transport at the PEO/PS interface, which was reduced in size with increasing M_n(PEO) [95]. Recent analysis of Li electrodeposition through SEO/lithium bis(trifluoromethanesulfonyl)imide (LiTFSI) electrolytes showed that the formation of globular protrusions and mossy lithium was more significant at high current densities and relatively high r, and it was strongly favored by the presence of impurities on the Li surface [97,98]. PS-*b*-PEO-*b*-PS/LiTFSI can reach ionic conductivity of $\sim 10^{-3}$ S/cm at 70°C (r = 0.05), with good oxidative stability up to 4.5 V, enabling to achieve 91% Coulombic efficiency during charge/discharge cycles of a high-voltage Li/NCM532($LiNi_{0.5}Co_{0.3}Mn_{0.2}O_2$) cell at 0.1C and 70°C [96].

Comb polymers with short PEO side chains have been used in SPEs, in order to locate the Li^+ coordinating units into dynamic side chains, thus suppressing the crystallization of the PEO-based units and enhancing the conductivity [92]. BCPEs with a central block of poly(ethylene glycol) methacrylate (PEGMA) between PS blocks (Fig. 2) were prepared by NMP and Ru-catalyzed ATRP using difunctional initiators [99,100]. PS-*b*-PEGMA-*b*-PS/$LiClO_4$ (r = 0.05) had high conductivity $\sigma = 2 \times 10^{-4}$ S/cm at room temperature [99]. However, the electrochemical stability of this type of comb BCPEs was generally lower than the corresponding PS-*b*-PEO-*b*-PS electrolytes [100]. Methacrylate monomers, such as benzyl and methyl methacrylate, have been used to build triblock copolymer electrolytes with a central PEGMA block by ATRP [101,102]. These BCPEs with pre-determined MW of each block and low dispersity, $Đ < 1.2$, exhibited room temperature conductivity of $\sim 10^{-5}$ S/cm and wide electrochemical stability window.

Different architectures have been explored to further enhance the segmental motion of polymer chains and increase the electrolyte conductivity. Hyperbranched star PEs (Fig. 2) were built by a two-step RAFT polymerization, to first generate an hyperbranched PEGMA-based core, subsequently extended with styrene. The star polymers showed 5-16 times higher conductivity than PEGMA-PS linear BCPEs with similar compositions due to the suppressed crystallization, and Young's modulus ranging from 0.5 to 1.4 MPa at 60°C [103]. Li/$LiFePO_4$ (LFP) batteries with the hyperbranched star PE delivered stable capacity for over 100 cycles at 0.2C and 60°C. Fluorinated star-branched PEs were synthesized by ATRP from a hyperbranched polystyrene core extended with trifluoroethyl methacrylate and PEGMA, and exhibited high oxidative stability, up to 4.9 V [104].

Methacrylate and norbornene monomers with PEO side chains were used to prepare polymer brushes (Fig. 2) with different backbone and side chain length by free radical polymerizations (FRP), ATRP and ROMP, respectively [105,106]. The polymer brushes mixed with LiTFSI exhibited 10-time higher conductivities than linear PEO-based PEs with similar MW. Indeed, the brush structure has the advantage of enabling the synthesis of high MW polymers, while maintaining short and dynamic PEO side chains.

Brush-first ROMP was used for the synthesis of PEO-based brush-arm star polymers (BASPs) with different degree of polymerization of PEO [107]. The method comprised the polymerization of linear norbornene-terminated macromonomers to produce bottlebrush polymers that were subsequently cross-linked by addition of a bis-norbornene to yield BASPs. Systematic analysis of the effect of polymer architecture on the conductivity revealed that the macromonomer and BASPs with equivalent Li salt loading had comparable ability of dissociating Li salts. Recently, a Yamamoto homocoupling reaction has been exploited to polymerize 2,5-dichlorophenolic monomers functionalized with short PEO chains [108]. The self-assembly of *p*-phenylene backbones resulted in stacked structures with phase separated soft EO domains, and their morphology was preserved upon addition of Li salt.

Cross-linked polymers have shown promising performance as electrolytes for LMB, because of their increased mechanical strength and the capability of nanostructured networks of confining and homogenizing the Li electrodeposition. As proposed by Tikekar et al., limiting the deposition of active metals to uniform nanoscale structures can prevent the growth of dendrites because interfacial forces, such as surface tension, are strongest on small length scales [77]. Thus, uniform Li plating/stripping can be achieved at lower material modulus than the value predicted by Monroe and Newman. Crosslinked PEO-based SPEs were synthesized via thermally induced cationic ring opening polymerization (CROP) of the epoxide monomer poly(ethylene glycol) diglycidyl ether, using $LiBF_4$ as initiator in the presence of moisture [109]. The solvent-free polymerization could be performed *in situ* on the cathode surface, reaching quantitative conversion in 1 h at 80°C. Upon mixing with LiTFSI ($r = 0.045$), the SPE had T_g ~-55°C, σ ~10^{-4} S/cm at r.t. and electrochemical stability up to 5.5 V, which enabled to measure a Coulombic efficiency (CE) of 99.4% in a Li/NCM111($LiNi_{1/3}Mn_{1/3}Co_{1/3}O_2$) battery cycled at 0.2C. Cross-linked PEO based SPEs with highly uniform mesh size could be prepared by thiol-ene click chemistry under mild conditions, by reacting poly(ethylene glycol) diallyl ether with a tetrathiol crosslinker, in the presence of a photoinitiator and LiTFSI [110]. The SPE networks showed conductivity of 5×10^{-5} S/cm at r.t. and ~10^{-3} S/cm at 90°C, with moduli of ~0.9 MPa. PEO-based networks were also prepared by electron beam irradiation of poly(ethylene glycol) dimethyl ether in the presence of an hyperbranched polymer with acryloyl groups, and LiTFSI [111]. The SPE with optimized composition showed σ ~2×10^{-4} S/cm at r.t. and Young's modulus of 0.22 MPa and resulted in high capacity Li/LTO($Li_4Ti_5O_{12}$) cells.

Among PEO based PEs, polyetheramines that follow under the trademark Jeffamine® have attracted great interest as they comprise EO and propylene oxide (PO) units, the latter contributing to reduce the crystallinity and thus enhancing the conductivity upon suitable balance of EO and PO groups [112]. The use of Jeffamines as electrolytes dates back to the '90s, however their room temperature conductivity was relatively low ($< 10^{-5}$ S/cm). More recently, comb SPEs based on a rigid polyimide backbone with Jeffamine side chains (Fig. 2) and LiTFSI or lithium bis(fluorosulfonyl)imide (LiFSI) were prepared by thermal ring-opening and closure reactions [113]. The electrolyte with the highest conductivity ($\sigma = 7.9 \times 10^{-5}$ S/cm at 30°C) showed promising performance in Li/LFP cell. The synthetic procedure was further optimized to obtain a flowable Jeffamine-based PE, as evidenced by the loss modulus prevailing over the storage modulus at different temperatures [114]. The flowable electrolytes showed slightly higher conductivity and oxidative stability than the corresponding SPEs, and more durable performance in LMB due to the improved interfacial contact between electrodes and electrolyte.

Finally, layered electrolytes were constructed in order to overcome the poor stability of PEO-based systems at high voltages. Dimethylacetamide (DMAc) was studied as an additive for liquid electrolytes capable of improving their oxidative stability [115]. Thus, poly(N-methyl-malonic amide) (PNMA), which contains repeating DMAc units, was used together with PEO to form double-layer SPEs, with PNMA in contact with the cathode material and PEO for the anodic side. The SPEs showed good stability up to 4.75 V and 91% capacity retention was measured after 100 cycles of a Li/LCO cell at 0.2C and 65°C.

2.2.2. Polycarbonate-based solid electrolytes

In order to overcome the typical drawbacks of PEO, such as low oxidative stability, several polymer materials based on non-ether backbones have been explored, including polyacrylonitrile, poly(vinyl alcohol), polysiloxanes, as well as their copolymers with other polymer classes. [85,116–118] Polycarbonate (PC)-based electrolytes are among the most studied PEO alternatives [85]. PCs coordinate to Li ions primarily through the carbonyl group oxygen, and this interaction is weaker than the complexation between Li^+ and EO units. Thus, polycarbonates generally display enhanced conductivity compared to polyethers. Aliphatic PCs have relatively low crystallinity, which additionally contributes to achieving good conductivity. They exhibit high Li transference number and good stability at high voltages (> 4 V) [119]. On the other hand, PCs have poor stability against Li metal, analogously to their small molecule liquid counterparts. The degradation of PC-based SPEs, including polypropylene carbonate (PPC, **Fig. 3**), when in contact with Li metal at high temperatures can result in decreased interfacial and bulk resistance, due to a decrease in polymer crystallinity and formation of small molecule products with high conductivity [120,121]. However, the electrolyte degradation abates its mechanical integrity and favors dendrites proliferation. Furthermore, PPC in contact with an LFP cathode can cause the reduction of Fe^{3+} to Fe^{2+}, hampering the battery capacity, unless the cathode electrolyte interphase is engineered to minimize side reactions [122].

Polycarbonates can be synthesized by ring opening polymerization (ROP) of cyclic carbonates or by copolymerizations using CO_2 as renewable feedstock, thus with the additional benefit of serving for CO_2 utilization [85,123]. The copolymerization strategy enables to introduce selected functionalities into the polymer structure and tune the electrolyte properties. Poly(β-oxocarbonate)s (Fig. 3) have been synthesized by room temperature organocatalyzed polyaddition of CO_2-sourced bis(α-alkylidene carbonate)s (bis-αCCs, Fig. 3) with PEO-diols of different molar masses [123,124]. Longer PEO chains resulted in SPEs with higher conductivity. By introducing a dihydroxy methacrylate into the synthetic procedure, a semi-interpenetrated network SPE was prepared by UV-induced crosslinking. The network had Young's modulus of 13 MPa, σ ~10^{-5} S/cm at r.t. and electrochemical stability up to 5 V. Alternatively, combinations of a dithiol with bis-αCCs and PEO were used to prepare SPEs with tunable content of linear and cyclic carbonate segments (Fig. 3) [125]. The presence of as low as 18 mol% of cyclic groups enhanced the conductivity and the oxidative stability (5.6 V) of the electrolyte, although a small amount of plasticizer (10 wt%) was needed to enable r.t. operation in Li/LFP batteries.

Aiming to combine the advantages of PEO and PC-based electrolytes, poly(ethylene oxide carbonates) (PEO_X-PC, Fig. 3) were synthesized by polycondensation between ethylene oxide diols of various length and dimethyl carbonate [126]. PEO_X-PC with $M_n = 25k$ and 30 wt% LiTFSI showed $\sigma \approx 4 \times 10^{-5}$ S/cm at r.t. By adding a methacrylate based diol into the polycondensation mixture, a crosslinkable PEO_X-PC derivative (Fig. 3) was prepared to subsequently obtain a free-standing SPE upon UV curing [127]. The crosslinked SPE showed similar conductivity to the corresponding linear material, electrochemical stability up to 4.9 V and improved mechanical strength.

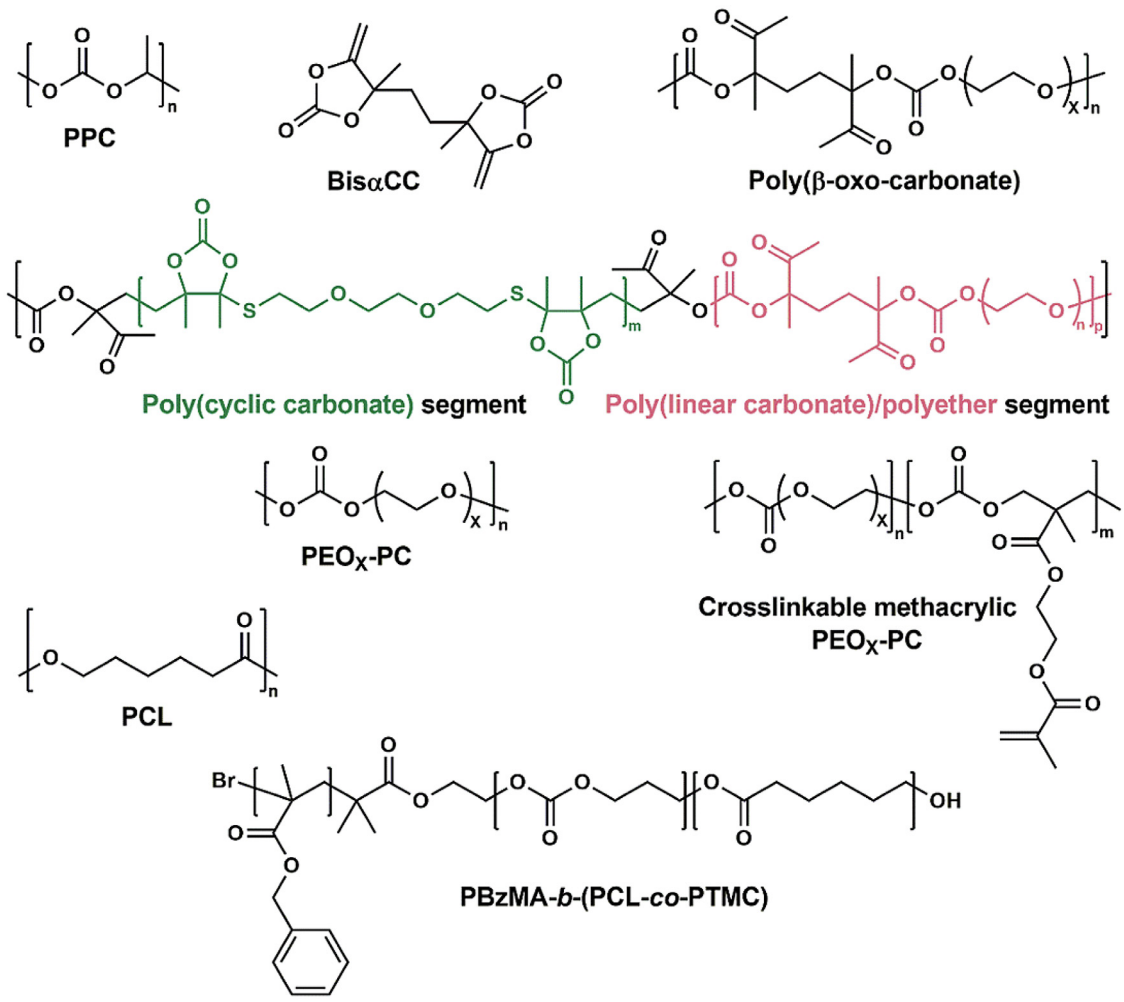

Fig. 3. Structures of some polycarbonates and polyesters and their copolymers employed as solid polymer electrolytes.

2.2.3. Polyester based solid electrolytes

Polyester-based electrolytes share similarities with both PEO and polycarbonates. Polyesters can coordinate to Li^+ ions through the oxygen atoms in the C=O groups. They have low T_g and a semi-crystalline structure at moderate temperature, which hampers the ionic conduction [85]. Among numerous explored strategies to increase the conductivity of polyester-based electrolytes, the variation of polymer architecture by copolymerization or crosslinking resulted in SPEs with good electrochemical and mechanical properties.

Polycaprolactone (PCL, Fig. 3) is one of the most studied polyesters for SPEs, benefiting from a facile synthesis by ROP of ε-caprolactone and eventual biodegradability. While the semi-crystallinity of PCL at room temperature limits its use, statistical copolymerization of PCL with trimethylene carbonate (TMC) led to largely amorphous copolymers with high MWs (~300k) [128]. PCL-*co*-PTMC with 20 wt% TMC units and 36 wt% LiTFSI displayed r.t. conductivity of 4×10^{-5} S/cm and Li transference number of 0.62 at 40°C, indicative of improved conduction ability compared to common PEO-based electrolytes. However, these copolymers have poor structural integrity and can be prone to dendrite penetration in LMBs. Thus, crosslinked SPEs were prepared by UV curing of PCL-*co*-PTMC in the presence of di- and tri-acrylate crosslinkers and a photoinitiator [129]. Improved mechanical stability, with no substantial effect on conductivity and good cycling performance in Li/LFP cells were obtained. In an alternative approach, a block copolymer electrolyte with a hard block of poly(benzyl methacrylate) (PBzMA) that reinforced the PCL-*co*-PTMC (Fig. 3) was synthesized by sequential ATRP and ROP [130]. The BCPE with 20 wt% PBzMA and 16.7 wt% LiTFSI showed $\sigma = 10^{-5}$ S/cm at r.t., $t_{Li+} = 0.64$ and a high Young's modulus of 0.2 GPa below 40°C.

2.2.4. Poly(ionic liquids)-based solid electrolytes

Poly(ionic liquid)s (PILs) have emerged as attractive materials for rechargeable battery electrolytes, as they combine the low-flammability and high electrochemical stability window of ionic liquids to the mechanical strength, flexibility and tunable design of polymers [131]. In PIL electrolytes, cations or anions are immobilized onto the polymer backbone and this affects the mobility of Li^+ and counterions. While PILs are often used upon addition of an IL as plasticizer to form GPEs, solid PIL electrolytes were also studied. Comb-like structures bearing cationic side chains were generally preferred, particularly piperidinium ions that gave better electrochemical stability. Block copolymers and other architectures were explored to achieve better mechanical properties in PIL-based SPEs.

Recently, a solid PIL-in-salt electrolyte system was developed, based on poly(diallyldimethylammonium bis(fluorosulfonyl)imide) (PDADMA FSI) [132]. Increasing the salt concentration in electrolyte systems can increase the ionic conductivity and Li transference number. FSI-based salts have high solubility, enhanced alkali ion transport, and tend to form SEIs with good uniformity and conductivity. In the PDADMA FSI system, the molar ratio of PIL to LiFSI could be varied from 2/1 to 1/6. Ratios as high as 1/4 and 1/6

resulted in the formation of microphases and decreased conductivity, likely due to the presence of non-conductive phases. However, SPEs with 2/1, 1/1 and 1/1.5 PIL/LiFSI ratios showed conductivity increasing with LiFSI content and stability up to 5 V. The PIL-in-salt with 1/1.5 ratio enabled good cycling stability of Li/LFP and Li/NCM cells with practical high loading of active material.

2.2.5. Charge-transfer-complex-based solid polymer electrolytes

When lithium salts are dissociated in a polymer matrix, the transport of charges occurs via a translational method, whereby moving ions are always coupled with the segmental motion of solvating polymer chains. Therefore, polymers with relatively low glass transition temperatures, such as PEO, are generally employed for SPEs. Consequently, the mechanical strength of the SPE usually needs to be sacrificed in order to enhance its conductivity. Therefore, it is critical to develop a strategy toward SPEs with simultaneously high conductivity and strength to fabricate solid-state batteries. In a patent filed by Zimmerman et al. [133] a novel type of polymer electrolytes was reported, based on the formation of charge-transfer complexes. The electrolyte comprised the electron-donating semicrystalline polymer poly(phenylene sulfide) (PPS), a p-type dopant, and lithium salt. Upon doping PPS with 2,3-dichloro-5,6-dicyano-1,4-benzoquinone (DDQ), the polymer and dopant formed a charge-transfer complex in a regularly stacked lamella phase, with lithium ions moving within the highly polarized matrix. PPS has a T_g of over 80 °C and a melting point $>$ 250 °C, yet the electrolyte achieved a superionic conductivity of 10^{-4} ~10^{-3} S/cm at room temperature. Hatakeyama-Sato et al. further showed that when either PPS or a more soluble dimethyl substituted PPS were mixed with tetrachloro-1,4-benzoquinone (chloranil), in the presence of as little as 10 wt% LiTFSI, the resulting SPEs had conductivities of ~10^{-3} S/cm at r.t. [134]. To explain this phenomenon, it was proposed that when the HOMO level of the donor approaches the LUMO level of the acceptor, the charge-transfer complex becomes electrically ionic and helps to dissociate the lithium ions [135]. An interface conduction model suggested that the charge transport occurs at the interface of crystals where the binding energy is weaker than in bulk [136]. Polymer charge-transfer complex electrolytes opened new avenues for designing SPEs with robustness and high conductivities.

2.2.6. Toward more sustainable polymer electrolytes

The need for sustainable alternative to conventional polymers derived from fossil feedstocks is relevant to the application of polymers in energy storage devices, where the use of naturally abundant resources and the potential for biodegradation can reduce costs and improve the device recycling [137–139]. Cellulose is among the most abundant and studied natural polymers, with a large number of functionalities that can be exploited for transformations. Polymer brushes with a cellulose-based backbone and EO units in the side chains were prepared by partial oxidation of cellulose, followed by reaction with PEO mono-methyl ether, or by esterification of cellulose with 2-bromopropionyl bromide in order to introduce ATRP initiating sites for the subsequent ATRP of PEGMA [140,141]. The cellulose-PEGMA bottlebrush electrolyte showed high r.t. conductivity (8×10^{-5} S/cm), oxidative stability up to 4.9 V and high stretchability [141]. The high conductivity was attributed to the ordered nanolayered structure of the brushes, promoted by the rigid and rod-like cellulose backbones, which tend to form ordered nanochannels that enhance the Li^+ transport. A similar strategy was used to functionalize lignin and grow polymers with multi-arm star architecture, via ATRP of PEGMA and glycidyl methacrylate (GMA). The GMA units were introduced to allow for subsequent crosslinking with poly(ethylene glycol) diglycidyl ether (PEGDGE), under photoacid catalyzed conditions. The crosslinked polymers could be used as either SPE or binder in LMBs [142].

2.3. Gel polymer electrolytes (GPEs)

2.3.1. Characteristics and manufacturing of gel polymer electrolytes

Gel polymer electrolytes typically comprises a polymer framework as host material, a Li salt and a solvent as plasticizer. The latter should present good chemical and electrochemical stability and high dielectric constant, thus carbonate molecules and ionic liquids (ionogels) are the most commonly employed plasticizers [76,143]. GPEs generally present greater conductivity and improved interfacial properties compared to SPEs. Moreover, GPEs have high flexibility and elasticity, which allow for better containment of volumetric changes occurring at the electrode and are well-suited for wearable devices. However, the presence of relatively high fractions of liquid plasticizers decreases the membrane strength and thermal stability. Therefore, inorganic fillers are often used to form composite GPEs with improved mechanical properties. In addition, in GPEs the melting point of the solvent can be significantly lowered when the solvated electrolyte is trapped in a confined environment. As a consequence, the GPE can exhibit sufficiently high conductivity at sub-zero temperatures, widening the application range of the electrolyte [144].

GPEs are prepared via physical or chemical procedures. Dry polymers can be soaked in the liquid of choice to form the GPE, or the polymerization mixture can contain the plasticizer that is incorporated in the electrolyte during the gelation or polymerization process. The second method ensures better contact with the polymer (and eventual fillers) and do not require excessive amount of liquid solvent [143].

Plasticizers are commonly added to polymer networks to improve their flexibility, conductivity, and interfacial contact with electrodes. Crosslinked PEO-based electrolytes are typically plasticized with liquid carbonates or with glymes, in order to improve the room temperature conductivity [110,145]. Cross-linked poly(tetrahydrofuran) (PTHF) plasticized with dimethylformamide (18 wt%) had σ ~10^{-4} S/cm at r.t. [146]. THF was crosslinked by UV irradiation in the presence of 2-isocyanatoethyl methacrylate. PTHF is less coordinating to Li^+ than PEO due to the smaller number of oxygen in the chain, and this resulted in increased conductivity.

Double network (DNW) GPEs were synthesized by using commercial poly(vinylidene fluoride-co-hexafluoropropylene) (PVDF-HFP) as long-chain network and poly(ethylene glycol) diacrylate (PEGDA) to form the short-chain network by UV crosslinking [147]. The DNW was soaked in a carbonate-based liquid electrolyte and the DNW-GPE exhibited $\sigma = 8.1 \times 10^{-4}$ S/cm at r.t. Moreover, the double network showed higher modulus and fracture energy than PVDF-HFP-based GPEs. While PVDF-HFP is a common material for rechargeable batteries, a PVDF-perfluoroether (PFE) based GPE showed a remarkably high conductivity of 3×10^{-3} S/cm at r.t. [148]. PVDF-PFE copolymer had a PVDF backbone with PFE side chains and was synthesized by thermally initiated free radical polymerization. Then, the copolymer (M_n = 49,000) was dissolved in acetone and an IL-based electrolyte (PFE/LiTFSI = 2) followed by solvent evaporation to form the highly conductive GPE.

The combination of ionic liquids and block copolymer can led to materials with controlled nanostructures and exceptional mechanical properties [149]. The nature of the IL and monomers and the composition of the block copolymers and their miscibility primarily determine the material properties. RAFT polymerization of a styrene/divinylbenzene mixture from PEO functionalized with a chain transfer agent was conducted in the presence of the IL butyl-3-methylimidazolium TSFSI (BMITFSI) and LiTFSI [150]. The polymerization induced self-assembly approach resulted into nanoscale

domains, with continuous morphology ensured by the crosslinking between PS and divinylbenzene. BMITFSI was immiscible with PS and therefore partitioned into the PEO domains, together with LiTFSI. This one-step process gave bicontinuous and nanostructured membranes with conductivity $> 10^{-3}$ S/cm at r.t. and shear modulus approaching 1 GPa.

2.3.2. Electrolytes from in-situ polymerizations

Inducing the polymerization of liquid electrolyte mixtures into the assembled battery during initial charge/discharge cycles is an emerging strategy toward high-performing LMBs [151]. The main advantage of this *in situ* polymerization approach is that polymers grown into assembled cells can better wet the electrodes, thus considerably reducing the interfacial resistance. In addition, the simple manufacturing and relatively low cost facilitate the scale up of this method. *In situ* polymerization of some liquid electrolytes commonly used in battery research was recently investigated. Key components of the initial electrolyte mixture are the polymerization initiator and/or catalyst, as their amount and nature affect the degree and rate of polymerization, as well as the composition and properties of the resulting quasi-solid or solid system.

1,3-Dioxolane (DOL) has been studied as precursor for *in situ* polymerization in LMBs. Ether-based liquid electrolytes, typically composed of DOL, dimethoxy ethane and LiTFSI, in contact with Li metal forms a solid electrolyte interphase with more favorable properties and composition than the SEI formed by carbonate electrolytes [152]. The outer layer of this spontaneous SEI largely contains short oligomers with elastomeric character and C-O-C linkages, thus displaying favorable conductivity and flexibility. DOL can be polymerized by ROP in the presence of Al salts, and this reaction was exploited by Archer et al. to transform a liquid electrolyte into a solid one *in situ* during the battery cycling [151]. During charge/discharge cycles, $Al(OTf)_3$ initiated the ROP of DOL, and the polyDOL content and MW depended on the loading of Al salt. The *in situ* generated polyDOL electrolyte enabled good interfacial contact and long-term stable cycling. Furthermore, by combining $Al(OTf)_3$ and AlF_3 it was possible to improve the anodic stability of the electrolyte [153]. Indeed, AlF_3 helped preventing the oxidation of Al current collectors, by creating an Al^{3+} saturated environment with immobilized $TFSI^-$. Additionally, AlF_3 contributed to a more stable cathode electrolyte interphase, thus extending the cycle life of high-voltage Li/NCM622($LiNi_{0.6}Co_{0.2}Mn_{0.2}O_2$) cells.

The properties of polyDOL-based electrolytes could be improved by tuning the composition of the initial liquid mixture to form random copolymers. In the presence of $LiPF_6$, mixtures of DOL ($>$ 30 wt%) and ethylene carbonate could be polymerized, forming viscous gels with inhibited crystallinity, and high oxidative stability up to 4.7 V, which increased with the DOL content. Similarly, by using $LiBF_4$ as a source of BF_3 initiator, DOL was randomly copolymerized with trimethoxyethylene (TOM) [154]. Adjusting the monomer ratio and the temperature, the crystallization in the copolymers was suppressed, thus increasing the diffusion coefficient of Li^+ and the conductivity ($\sim 10^{-5}$ S/cm at r.t. for DOL/TOM 8/2 solid copolymer). The electrolyte was electrochemically stable up to 4.4 V, and a Li/LFP cell with in-situ polymerized electrolyte showed $>$ 91% capacity retention after 400 cycles at 0.5C and 40°C.

PTHF could also be formed *in situ* in Li/LFP cells, by starting from THF/$LiClO_4$ and BF_3 as initiator, while poly(vinylene carbonate) (PVC) was formed inside a Li/LCO operating at high temperature, by adding a thermal radical initiator to the VC/$LiClO_4$ liquid electrolyte [155,156]. Therefore, the *in situ* polymerization strategy is emerging as a versatile tool to achieve quasi-solid or solid-state polymer electrolytes with optimal interfacial contact with Li metal anode.

2.3.3. Solvate ionic liquids (SILs)

Mixtures of lithium salt and oligomeric ethylene glycol under specific compositions results in strong chelation of lithium cations by the ethylene glycol repeating units to form solvate, with very little amount of free oligomers. Such unique formulations exhibit similar characteristics to ionic liquids, thus being termed solvate ionic liquids (SILs) [157,158]. Typically, SILs are formed between lithium salt bearing anions with weak Lewis basicity and glymes with 3 or 4 repeating unit. The greater the ionic association of the salt, the less likely the chelation between Li^+ and glymes. Thus, the tendency to form SILs decrease in the order LiTFSI $>$ LiOTf (lithium triflate) $>$ $LiNO_3$. The most prominent SILs are combinations of LiTFSI with either tri(ethylene glycol) dimethyl ether (G3) or tetra(ethylene glycol) dimethyl ether (G4), i.e. [Li(G3)]TFSI and [Li(G4)]TFSI. Due to the absence of free glymes, SILs have several advantages compared to glymes: i) negligible vapor pressure; ii) reduced flammability; iii) enhanced oxidative stability; iv) reduced corrosion of aluminum current collector [159]; v) reduced dissolution of electroactive materials, such as lithium polysulfide in Li-S batteries [160].

When SILs are mixed with long-chain polymers, the interaction between Li^+ and the polymer backbone is due to the preservation of chelated $[Li(glyme)]^+$. Therefore, the ion transport is decoupled from the polymer segmental motion, resulting in enhanced ionic conductivity. For example, Kitazawa et al, prepared a gel polymer electrolyte comprising [Li(G4)TFSI] and PS-poly(methyl methacrylate) (PMMA)-PS triblock copolymer. The electrolyte properties depended on the self-assembly of the PS-PMMA-PS triblock copolymer in the presence of the SIL, whereby the SIL-phobic PS segments served as physical crosslinkers, and the SIL-philic PMMA segments as conductive phase. The ionogel showed similar mechanical properties to an elastomer, and room temperature conductivity of $10^{-4} \sim 10^{-3}$ S/cm [161].

2.4. Composite polymer electrolytes (CPEs)

Composite polymer electrolytes are solid or quasi-solid PEs with added inorganic fillers. The presence of fillers can improve the mechanical, thermal and electrochemical stability of PEs, as well as their Li transference number, and wetting ability toward metal electrodes [162]. Importantly, fillers increase the conductivity of PEs, since they act as crosslinking centers that disrupt the polymer crystallinity, increasing the segmental motion, as well as increasing local ionic concentration by confining lithium ions at nanointerfaces [163,164]. Moreover, Lewis acid-base interactions between Li^+, anions and chemical groups on the filler surface can promote salt dissociation and offer new Li^+ conduction pathways [165].

Typical fillers can be divided into non-conductive or conductive fillers, where the latter have intrinsic Li ion conductivity. While ceramic fillers are most commonly used, other materials have been recently introduced in polymer electrolytes, including metal organic frameworks (MOFs) and organic fillers such as organic ionic plastic crystals (OIPCs) [74,166]. Besides the nature of the filler, its alignment and orientation are crucial to create channels for fast Li^+ conduction [162]. Moreover, blends of polymers and ceramic particles can be non-uniform because of particle aggregations and this can limit the relative amount of filler and the enhancement of mechanical and electrochemical properties. Conversely, by covalently linking polymer chains to the surface of fillers, the filler loading can be largely increased without observing aggregation, therefore allowing for better tunability of the electrolyte properties [60,167,168].

2.4.1. Non-conductive fillers

Several metal oxide nanoparticles, such as SiO_2, ZrO_2 or Al_2O_3 have been widely used as reinforcing fillers for PEO and other

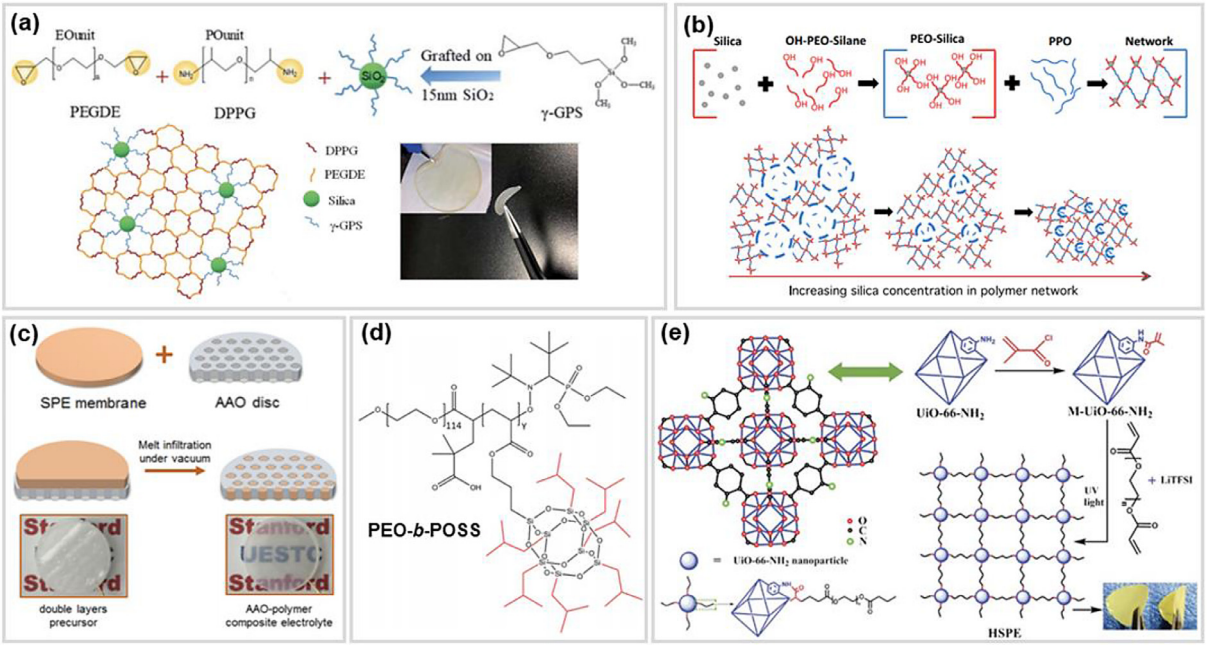

Fig. 4. Examples of composite polymer electrolytes prepared by (a,b) grafting polymers onto SiO_2 nanoparticles. [171], Copyright 2019. Reprinted with permission from Royal Society of Chemistry; [87], Copyright 2018. Reprinted with permission from the National Academy of Sciences. (c) infiltration of polymer melt in anodized aluminum oxide with vertically aligned nanochannels. [173], Copyright 2018. Reprinted with permission from American Chemical Society. (d) forming PEO-*b*-oligomeric silsesquioxanes (POSS) block copolymer; [174], Copyright 2019. Reprinted with permission from American Chemical Society; (e) crosslinking of a vinyl-functionalized metal organic framework (MOF). [175], Copyright 2018. Reprinted with permission from Royal Society of Chemistry.

polymer electrolytes. One of the main advantages of SiO_2 is represented by the possibility of synthesizing the inorganic particles *in situ* into the polymer matrix [169,170]. By *in situ* hydrolysis of tetraethyl orthosilicate in PEO/$LiClO_4$, a PEO-monodisperse ultrafine SiO_2 CPE was prepared, with chemical bonds between the OH-terminated PEO chains and the OH- groups on the surface of SiO_2 NPs. The CPE showed wide electrochemical stability window (up to 5.5 V) and high $\sigma = 4 \times 10^{-5}$ S/cm at r.t., due to the strong covalent interaction between PEO and NPs that dramatically suppressed the polymer crystallinity. Alternatively, polymers were grafted onto SiO_2 NPs by first functionalizing the NPs with 3-glycidoxypropyltrimethoxy silane through a hydrolysis/condensation process (Fig. 4a) [171]. The functionalized NPs were crosslinked by ring-opening reactions with PEGDGE, and α,ω-diamino poly(propylene glycol) (DPPG). The grafting strategy prevented the agglomeration of the nanofillers and enabled to obtain a membrane with storage modulus of ~9 MPa and good extensibility.

In another strategy, alkoxy silane terminated oligomeric PEO-OH were used to graft PEO oligomers onto SiO_2 nanoparticles in water [87]. The resulting densely grafted SiO_2-PEO-OH was used as crosslinker for PPO chains ($M_n \sim 3000$) functionalized with isocyanate end groups, forming cross-linked hairy NPs with high degree of crosslinking (Fig. 4b). The pore size of the crosslinked membrane could be tuned by changing the volume fraction of nanoparticles and it was correlated to the electrochemical performance of the electrolytes. In particular, the membranes with pore sizes of 20 and 100 nm (soaked into a carbonate liquid electrolyte) were able to promote smooth Li electrodeposition on Li metal, and prevent dendrite growth, as observed by optical microscopy under application of high current density. In contrast, dendrite growth was observed for pore sizes of 500 and 1000 nm. These observations are in agreement with the ability of crosslinked PEO-based GPEs made by thiol-ene chemistry to suppress Li dendrites, supporting that crosslinked electrolytes with a smaller mesh size than the size of Li nucleate can effectively promote uniform Li electrodeposition [110].

3D continuous inorganic nanostructures allow for achieving high content of the inorganic component in CPEs. Highly interconnected SiO_2-aerogel has been used as porous host structure for crosslinked PEO formed by UV-curing of a mixture of PEGDA, succinonitrile and LiTFSI, infused into the aerogel pores [172]. The CPE (with 22 wt% SiO_2) exhibited high r.t. conductivity (6×10^{-4} S/cm) and elastic modulus of 0.43 GPa. The high conductivity was mainly attributed to the ultrafine and well-distributed SiO_2 domains with large internal surface area that promoted Lewis acid–base interaction with the anions, enhancing the dissociation of Li salt. The presence of aligned channels in the continuous inorganic structure can further promote rapid transport of Li^+. Thus, the nanochannels of anodized aluminum oxide (AAO) were filled with PEO/LiTFSI by melt infiltration, to form a CPE with vertically aligned pathways for Li ions (Fig. 4c) [173]. The CPEs exhibited conductivity as high as 5×10^{-4} S/cm, much higher than PEO/Al_2O_3 blends with similar composition. Moreover, the conductivity could be tuned by modifying the surface chemistry of AAO or by changing the polymer composition.

Polyhedral oligomeric silsesquioxanes (POSS) are silica NPs with empirical formula $RSiO_{1.5}$ (R = H, or an organic functional group), which have been employed to form polymer electrolytes with different architectures [176–180]. PEO-*b*-POSS BCPEs (Fig. 4d) were synthesized by NMP of acryloisobutyl POSS monomer, from the functionalized PEO macroinitiator [181]. The BCPEs showed mainly lamellar morphology, independently on the composition. Importantly, PEO-*b*-POSS/LiTFSI ($r = 0.1$) showed 50 times higher conductivity and 5 orders of magnitude higher Young's modulus than SEO/LiTFSI with similar compositions. The bulkiness of POSS bearing a silica-like core surrounded by a shell of organic groups gives rise to unusual physical properties due to the high degree of conformational asymmetry and relative stiffness [174]. Thus, POSS-based hybrid BCPEs emerge as promising materials for solid-state batteries.

Additionally, nanoparticles such as SiO_2 or Al_2O_3 can possess negative surface charges, attracting Li cations to form a positively charged outer layer of the electric double layer (EDL). When the nanoparticles are close enough to each other in a mesoporous environment, the EDLs overlap, drastically enhancing the concentration and transference number of lithium ions, which results in enhanced conductivity [163,164]. The filler surface can also be positively charged, as in yttria stabilized zirconia (YSZ) nanoobjects that possess oxygen vacancies acting as Lewis acid sites, which strongly interact with the salt anions, enhancing the mobility of Li^+ [165]. YSZ nanowires (15 wt%) dispersed in a polyacrylonitrile (PAN)/$LiClO_4$ matrix, resulted in a CPE with high conductivity and double Li transference number compared to pure PAN.

Metal organic frameworks are increasingly explored as additives for polymer electrolytes, favored by the large variety of reported MOF structures and their microporous and ordered nature that can promote fast and uniform Li migration [166]. For similar reasons, covalent organic frameworks has also found application in energy storage devices [182]. MOFs have been used as host for polymer electrolytes, Li salt and eventual plasticizers, as well as to covalently link polymer chains [175,183]. The latter strategy was realized by synthesizing vinyl-functionalized MOF nanoparticles and crosslink them under UV irradiation in the presence of PEGDA and a photoinitiator (Fig. 4e). The polymer-linked MOF electrolyte showed higher conductivity and improved interfacial stability with Li metal electrodes, compared to similar MOF/polymer blends.

2.4.2. Conductive fillers

Conductive fillers employed in CPEs are mainly represented by garnet- and perovskite-type ceramics with high Li^+ conductivity. Embedding conductive ceramics into polymer matrix can not only improve mechanical and electrochemical stability, but also offer additional ionic conductive pathways for fast and uniform Li^+ transport [162].

Ceramic particles of garnet-type LLZO are frequently used as fillers, due to their Li transference number close to unity, high r.t. conductivity and facile doping with different elements. Micro-sized cubic LLZO pellets embedded in a UV crosslinked PEO/LiTFSI matrix in the presence of tetraglyme as plasticizer, formed a non-flammable, self-standing, homogeneous membrane with high $\sigma > 10^{-4}$ S/cm at r.t (LLZO 20 wt%) [184]. The size of ceramic fillers and their homogeneous distribution affects the conductivity and the performance of CPEs. Nanosized $Li_{6.25}Ga_{0.25}La_3Zr_2O_{12}$ (Ga-LLZO, 40-50 nm) homogeneously dispersed in a PEO matrix (Ga-LLZO 16 vol%) above a percolation threshold value formed a continuous space charge region [185]. Thus, fast channels for Li^+ ion transport were obtained and the CPE exhibited wide electrochemical window and good stability against Li metal. Ga-LLZO nanoparticles have been used to prepare self-healable CPEs, by homogeneously dispersing the NPs into a self-healing polymer electrolyte matrix, composed of fatty acids and urea linkages [186]. The CPE with 30 wt% Ga-LLZO formed a viscoelastic, flexible and conformal membrane with uniform pathways for Li^+ flux and $\sigma \sim 10^{-3}$ S/cm at r.t. In a Li/LTO cell the CPE enabled stable cycling with 99% capacity retention for 120 cycles at 0.2C. The filler loading is crucial to determine the properties of the electrolyte, particularly membrane flexibility and handling. PEO-$Li_{6.4}La_3Zr_{1.4}Ta_{0.6}O_{12}$ (LLZTO) CPEs with largely different compositions were prepared by hot pressing [187]. The polymer-in-ceramic (10 wt% LLZTO) and ceramic-in-polymer (80 wt% LLZTO) showed high conductivity and oxidative stability. The ceramic-in-polymer was more flexible and suitable for small-scale flexible energy storage devices, while the polymer-in-ceramic with high mechanical strength and safety was more appropriate for use in electric vehicles.

Conductive ceramics based on sulfides generally have lower density and higher conductivity than oxides. $Li_{10}SnP_2S_{12}$ (LSPS) was dispersed in a PEO matrix via a solvent casting method [188]. The CPE with only 1 wt% LSPS improved the conductivity, Li transference number, tensile strength, and elongation at break of PEO. Inorganic sulfide glasses (Li_2S–P_2S_5) have been also used to form composite electrolytes. These materials have high shear moduli (~20 GPa) and ionic conductivity [189]. Sulfide glasses were covalently linked to diol-terminated perfluoropolyether (PFPE) to form hybrid electrolytes in the presence of LiTFSI. The materials had modulus of >2 MPa, stability up to 5 V, and Li transference number of 0.99, due to the single Li ion conducting character of sulfide glasses (see Section 2.5).

Besides nanoparticles, other filler conformation ranging from mono- to tridimensional structures were observed to greatly influence electrolyte performance. 1D nanofibers have large surface area and provide continuous pathway for Li ion conduction. LLZO nanofibers formed by electrospinning and dispersed in a PVDF-HFP matrix formed a CPE (10 wt% LLZO) with $\sigma \sim 10^{-3}$ S/cm at r.t., high voltage stability (up to 5.2 V) and high mechanical strength [190]. In addition, the orientation of fillers is crucial for the electrochemical and mechanical properties. PAN-based electrolytes with well-aligned $Li_{0.33}La_{0.557}TiO_3$ (LLTO) nanowires prepared by electrospinning exhibited one order of magnitude higher r.t. conductivity than when disordered nanowires where introduced in the PAN matrix [191]. An alternative approach to form continuous and highly conductive pathways in CPEs consists of forming 3D interconnected and porous ceramic networks [192]. $Li_{6.28}La_3Al_{0.24}Zr_2O_{12}$ (LLAZO) nanofibers were functionalized with silane-acrylates via a hydrolysis process, in order to subsequently create a crosslinked matrix of polymer grafted nanofibers, using PEGDA as crosslinker [193]. The crosslinked structure and the covalently linked polymers and ceramics resulted in homogenous, well-percolated networks for fast Li^+ transport. Moreover, this strategy enabled to achieve a filler content of 50 wt% and the CPE exhibited Young's modulus of 30 MPa and conductivity of 5×10^{-4} S/cm at r.t.

An emerging class of solid electrolytes are organic ionic plastic crystal-based electrolytes (OIPC) [74,76]. They are long-range ordered crystalline lattices with plastic-like mechanical behavior that can be considered solid analog of ILs, possessing good conductivity, low-flammability and wide electrochemical stability window. In order to display sufficient mechanical integrity and flexibility for application in Li metal batteries, OIPCs are mixed with polymers and/or inorganic fillers. PVDF nanoparticles were coated through a powder pressing method with LiFSI and [C_2mpyr] [FSI] ((N-ethyl-N-methyl-pyrrolidinium bis(fluorosulfonyl)imide) OIPC [194]. The amount of OIPC was increased up to 50 wt%, resulting in high Li transference number, electrochemical stability up to 5.3 V and no evidence of dendrite growth in Li/NCM devices cycled up to 4.6 V.

2.5. Single Li-ion conducting polymer electrolytes

One of the most recent examples of a crossover between polymer science and battery technology is the development of single Li-ion conducting (SLIC) polymer electrolytes [195]. PEs have Li transference number generally lower than 0.5 because of their dual-ion conducting character. In PEs, the motion of cations is coupled to the segmental motion of polymers, and therefore the anions are more mobile than Li^+ and t_{Li+} is lower than 0.5. The low value of t_{Li+} generates concentration gradients over the electrodes during charge/discharge cycles, harnessing the dendrite growth and leading to battery failure. Therefore, SLIC-PEs have been developed in which anions are immobilized on the polymer backbone, thus achieving high t_{Li+} values. The anions immobilization prevent the anions depletion near the anode and thus alleviate the Li^+ concentration gradient, extending the cycle life of the battery. It was

considered that even modestly high t_{Li+} (e.g., ~0.7) would result in higher attainable state of charge at high charge rate, which will dramatically benefit cell performance for high rate applications, such as electric vehicles (EV) [196].

2.5.1. SLIC with covalently immobilized anions

The immobilization of anions onto polymer backbones is attained by either post-polymerization modification or by synthesizing monomers bearing an anionic group for their subsequent (co)polymerization. The post-polymerization approach generally relies on highly efficient coupling reactions, such as amidation or alkyne-azide cycloadditions, however its use is limited by the difficulty of achieving complete functionalization of high MW polymers [197]. Therefore, the (co)polymerization of a functionalized monomer is typically preferred.

Strong ion pairs have been chemically linked onto polymer backbones, including sulfonate-based, acrylate-based, and borate-based ion pairs. However, the strong ionic association between Li^+ and the electron-rich counter ions resulted in SLIC-PEs with low conductivity. In contrast, bulky TFSI anions are capable of inducing high delocalization of Li^+, because of the strong electron-withdrawing fluorine atoms and the resonance structures of the sulfonyl groups. Therefore, since the seminal report of Bouchet et al. of a SLIC polystyrene, formed by attaching $TFSI^-Li^+$ ion pairs onto the *p*-position of a phenyl group (PLiSTFSI), a variety of SLIC-PEs based on the $TFSI^-Li^+$ ion pair have been developed [198]. Rigid polystyrene backbones have poor ionic conductivity, therefore a synthetic procedure was defined to prepare a PEO-based SLIC polymer (Fig. 5). OH-terminated PEGMA was reacted with pentynoic acid to form an alkyne-functionalized PEGMA that underwent a Cu-catalyzed alkyne-azide cycloaddition reaction with an azide molecule bearing a $TFSI^-$ group [199]. The resulting PEGMA-$TFSI^-Li^+$ macromonomer was polymerized by metal-free ATRP, targeting degree of polymerization (DP) ranging from 7 to 30. The SLIC-PE with DP = 7 (M_n = 7500) showed very high Li transference number (0.99) and conductivity of 10^{-4} S/cm at 90°C, while its shear modulus was 1 MPa at r.t. Kinetic modeling and cycling performance suggested that the electrolyte could suppress the growth of dendrite, thus supporting that electrolytes with relatively low shear moduli can suppress dendrites if able of promoting uniform and efficient Li^+ transport [86].

Since block copolymer electrolytes provide tunable mechanical and electrochemical properties, an interest was devoted to the synthesis of SLIC BCPEs. Triblock copolymers of PLiSTFSI-*b*-PEO-*b*-PLiSTFSI, generally prepared by NMP, exhibited high Li transference number (~0.9), and higher conductivity and mechanical strength than their PS-*b*-PEO-*b*-PS analog, and better cycling performance [198]. Analysis of ion transport and morphology of the triblock PEs and PLiSTFSI-*b*-PEO diblock copolymers showed a complex interplay between the volume fraction of PEO block capable of ion transport and the fraction of PLiSTFSI block where the ions were stored [200]. Similar block copolymers with a methacrylic anionic block (LiMTFSI) were prepared by RAFT polymerization and showed high transference number and conductivity [201].

The introduction of single Li-ion conducting units improved the Li transport in polymer electrolytes with a large variety of structures. SLIC poly(ethylene oxide carbonates) (Fig. 5) were synthesized by a 2-step melt polycondensation process between PEO,

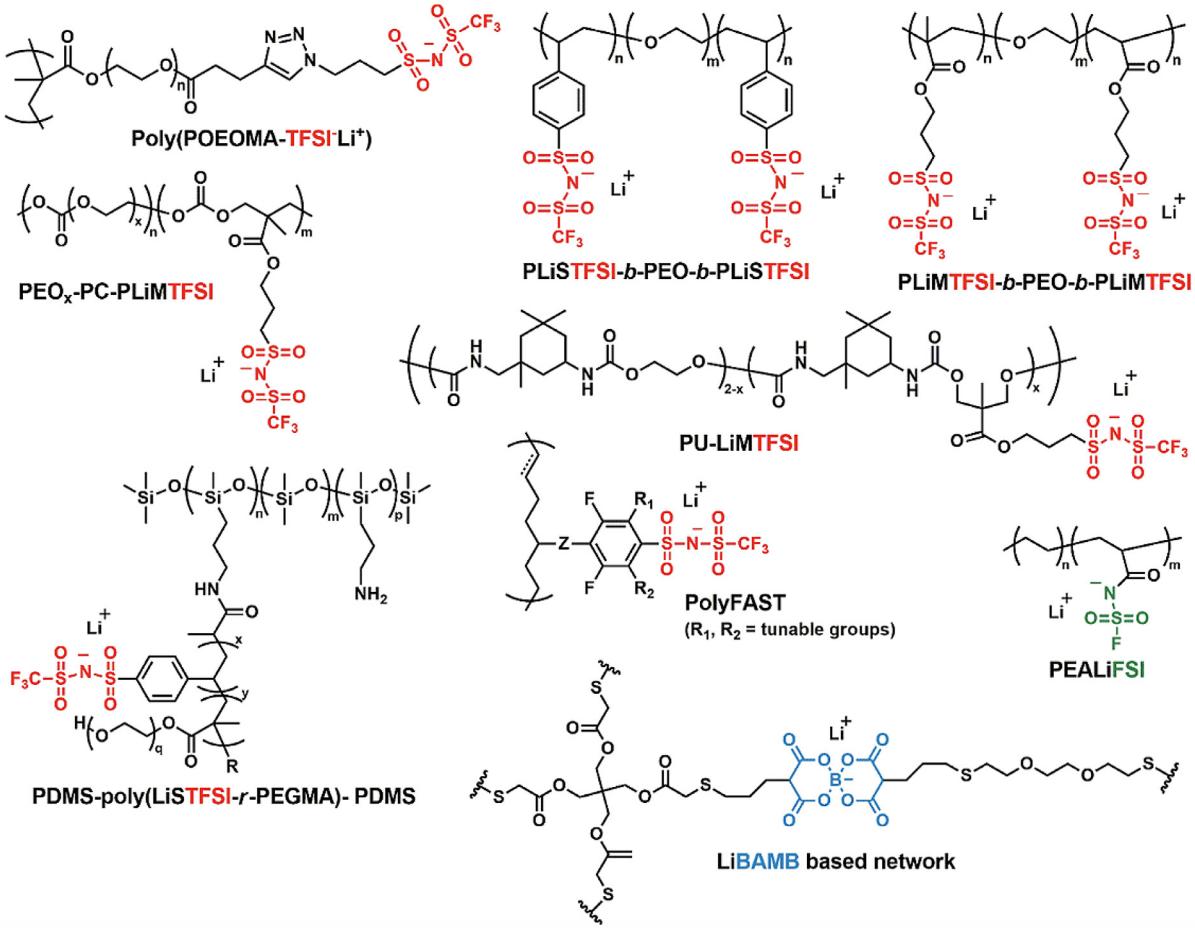

Fig. 5. Examples of single Li-ion conducting polymer electrolytes.

dimethyl carbonate and a functional diol bearing a sulfonimide group [202]. The SLIC PEO_x-PC showed Li transference number of 0.89, while the corresponding PEO_X-PC with dual ion conductivity showed $t_{Li+} = 0.23$. The SLIC electrolyte exhibited promising performance in a Li/NCM cell. SLIC polyurethanes (PU) were prepared by combining isophoronediisocyanate, PEO blocks and an ester functionalized anionic diol having a pendant TFSI group (Fig. 5) [203]. Upon addition of propylene carbonate as plasticizer, the SLIC-PU showed $t_{Li+} = 0.93$ and conductivity of 6.5×10^{-5} S/cm at r.t. Stretchable SLIC electrolytes were made by exploiting the elasticity of poly(dimethylsiloxane) (PDMS) [204]. Thus, a grafted copolymer was prepared by using PDMS with pendant reactive amine units as backbone to form a macro(chain transfer agent) for the subsequent RAFT copolymerization of PEGMA and PLiSTFI or PLiMTFSI, followed by addition of a PDMS crosslinker (Fig. 5). The resulting network showed good extensibility and tunable properties by changing the molar ratio of the elastic PDMS crosslinker and grafted block copolymers.

While sulfonyl imide anions are the most common among SLIC-PEs because of their highly delocalized negative charge, other anionic units were used as well. A copolymer of poly(ethylene-*co*-acrylic lithium (fluoro sulfonyl)imide) (PEALiFSI, Fig. 5) exhibited high t_{Li+} (0.81), thermal stability, heat and flame retardancy and self-healing properties [205]. Its high conductivity (5.84×10^{-4} S/cm) at room temperature was attributed to the weak interaction of Li^+ with the acrylic (fluoro sulfonyl)imide counterion. SLIC networks based on the bis(allylmalonato) borate (BAMB) anion were prepared via one-step photoinitiated thiol–ene click reaction of LiBAMB, pentaerythritol tetrakis(2-mercaptoacetate), and 3,6-dioxa-1,8-octanedithiol, in the presence of gamma-butyrolactone and electrospun PVDF to enhance the mechanical strength (Fig. 5) [206]. The resulting network had $t_{Li+} = 0.92$ and high ionic conductivity, $>10^{-3}$ S/cm at r.t.

Similarly to traditional PEs with double-ion conductivity, SLIC-PEs can be reinforced by adding fillers. This offers the opportunity of using or designing fillers that possess single-ion conducting units. SLIC mesoporous silica was synthesized through a sol-gel process and subsequent functionalization with PEO-trimethoxysilane and TFSI-terminated trimethoxysilane [207]. The SLIC composite was immersed in a PEO matrix (30 wt% silica) to form an electrolyte with good conductivity and mechanical strength and t_{Li+} of 0.9.

SLIC-PEs can be mixed with glymes to form single Li-ion poly(solvate ionic liquids) with enhanced oxidative stability. ROMP was used to design a library of SLIC-SILs based on a polymeric fluorinated aryl sulfonimide tagged (polyFAST) anions (Fig. 5). [208,209] The polymers were highly electron-deficient due to the electron-pulling fluoride groups. The electron density and conductivities of the polymer were modularly tuned by introducing O-, N- and S-based nucleophiles on the aromatic rings, via nucleophilic aromatic substitution. By mixing with G4 at a stoichiometry ratio of 1/1 (Li/G4), the resulting SLIC-SIL showed ionic conductivity of $\sim 10^{-4}$ S/cm at 80°C with oxidative electrochemical stability of up to 5.0 V and exceptional low-temperature performance [210].

2.5.2. Anion-trapping polymer electrolytes

The design of SLIC polymer electrolytes is one of several proposed strategies to regulate the anions in PEs to improve the Li^+ conduction and transfer number. Another strategy consists of partial trapping anions through Lewis acid units introduced into the electrolyte. [79,211] The preferential interaction of anions with the Lewis acidic sites results in enhanced Li^+ conductivity and transference number.

The strong Lewis acid character of boron (B) has been exploited to design anion-trapping PEs, whereby B-containing oligomers acted as plasticizers in polymer matrices, or boron species were embedded into polymer structures. PEO-borate ester (B-PEO, Fig. 6) was extensively employed as plasticizer for PEs, improving their conductivity by increasing the segmental mobility. However, only limited enhancement of t_{Li+} was generally reported. Conversely, when B-PEO was covalently grafted to a Si-doped PEO-based network, t_{Li+} was observed to increase (up to 0.8) with increasing the fraction of covalently bound B-PEO in the PE [212]. It was proposed that in non-covalent systems, B atoms were partially shielded by the surrounding polymer chains, decreasing their anion-trapping ability. Covalently linking B-PEO to a polymer network suppressed the shielding and improved the electrolyte transference number.

Several synthetic approaches were developed to design organoboron polymers, including alkylborane and boric ester type polymers, boric acid ester polymers and boroxine ring containing polymers [213]. Hydroboration polymerization of oligo(ethylene oxide) diallyl ether and dehydrocoupling polymerization of oligo(ethylene oxide) using mesitylborane were employed to prepare alkly borane and boric ester type polymers (Fig. 6), respectively [214]. Upon doping with different lithium salts, conductivities up to 3×10^5 S/cm and t_{Li+} ranging from 0.35 to 0.82 were measured. Alkylborane type polymer exhibited higher t_{Li+} values due to the stronger Lewis acidity of the alkylborane unit. An acrylate monomer containing a boric acid ester unit in the side chain was synthesized by reacting catechol, trimethoxyborane and tetra(ethylene glycol) acrylate [215]. The monomer was used to form polymer networks under UV light irradiation in the presence of an ether based monomer and crosslinker, a Li salt and photoinitiator. The presence of Lewis acid boric acid ester sites enhanced the t_{Li+} for different Li salts. Moreover, B-containing PILs were prepared by hydroboration polymerization of a bifunctional molten salt (1,3-diallylimidazolium bromide) followed by anion exchange reaction with LiTFSI [216]. An equimolar amount of LiTFSI and organoboron units resulted in σ = 2-3 $\times 10^{-5}$ S/cm at 50°C and t_{Li+} as high as 0.87. Of note, boronic esters and boroxine can exhibit dynamic behavior and therefore are ideal building block for PEs bearing dynamic covalent bonds (Section 2.6 and 3.2), thus being self-healable and degradable, [217] while displaying high t_{Li+} due to their Lewis acidic nature.

GPEs and CPEs containing B-based species were also designed to enhance the transport of Li ions. Linear and branched B-containing crosslinkers (Fig. 6) were synthesized through transesterification reactions and used to form cross-linked GPEs by thermal polymerization in the presence of carbonate solvents and LiTFSI [218]. By optimizing the composition, a GPE with $\sigma = 8.4 \times 10^{-4}$ S/cm at r.t. and $t_{Li+} = 0.76$ was obtained, which was electrochemically stable up to 4.52 V and enabled to achieve a capacity retention of 89.7% after 400 cycle of a Li/LFP cell. In addition, B-based nanocomposite electrolytes were prepared by mixing oligomeric borate ester electrolytes with 10 nm-diameter SiO_2 NPs and fumed silica with 7 nm diameter [219]. A small fraction of SiO_2 (1 vol%) was sufficient to increase both the conductivity and transference number, due to the adsorption of anions on the oxide surface, enhancing the Li^+ mobility.

In addition to organoboron polymers, perfluorinated analogs of PEO, i.e. perfluoropolyethers (PFPEs), have attracted great interest as electrolytes for LMBs. Hydroxyl terminated PFPE oligomers of different MW are commercially available and susceptible of chemical modification, for example by reaction with methyl chloroformate to obtain methyl carbonate-terminated PFPEs (PFPE-DMC, Fig. 6) [75]. In the presence of LiTFSI, the electrolytes showed non-flammability and very high lithium transference number (0.91-1). The latter was attributed i) to the ability of F-atoms in the oligomers to strongly interact with fluorinated TFSI anions reducing their mobility, and ii) to the delocalization effect of fluorine moieties that decreased the nucleophilicity of O-atoms, resulting

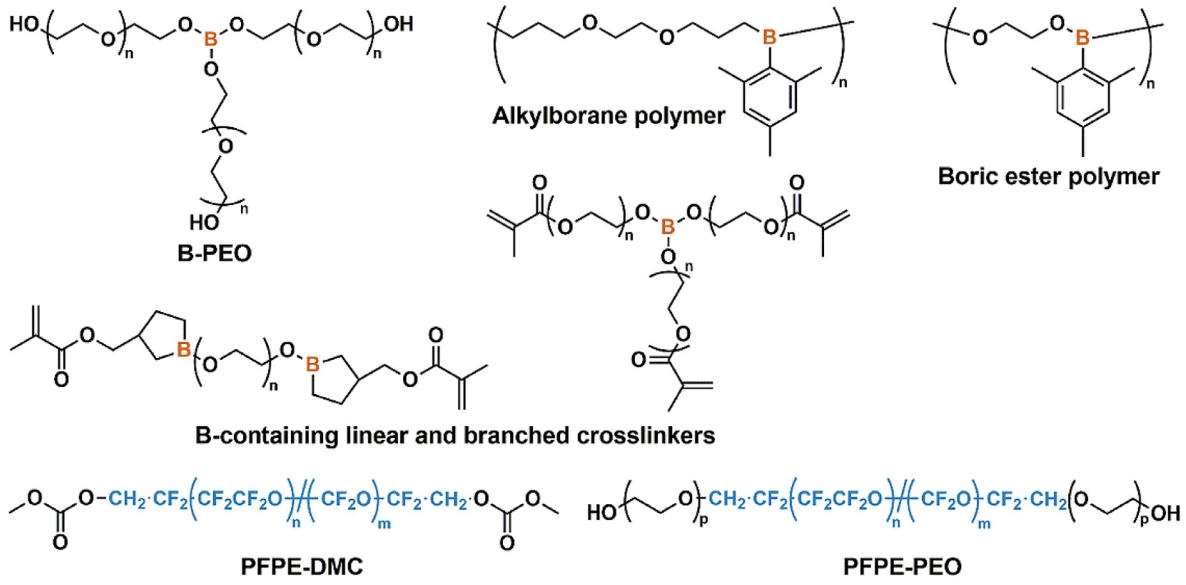

Fig. 6. Structures of anion-trapping organoboron polymers and oligomers, and perfluoropolyether-based polymers.

in both increased Lewis acidity of the polymer backbone and enhanced Li^+ mobility. In LMBs, PFPE-DMCs prevented the corrosive effect of LiTFSI on Al current collectors at high potential, thus avoiding eventual cracks and detachment of the active material [220]. This beneficial effect is due to the interactions between polymers and $TFSI^-$ and enabled stable long-term cycling of Li/Li symmetric cells. Crosslinked PFPEs were synthesized by UV curing of a PFPE-urethane dimethacrylate in the presence of a photoinitiator and LiTFSI, to obtain solid electrolytes with the preserved benefits of PFPE oligomers [221]. The crosslinked SPEs enabled to solubilize higher amount of Li salt.

Recently, short triblock copolymers of PEO-PFPE-PEO were synthesized (Fig. 6), whereby the presence of PEO increased the ionic conductivity while decreasing the Li transference number, due to preferential partitioning of LiTFSI into PEO segments [222]. Moreover, short oligoether-PFPE-oligoether structures, with different lengths of the PFPE block or the ether blocks showed very high oxidative stability, up to 5.6 V [223]. This enabled stable cycling of a LMB with high-voltage $LiNi_{0.8}Co_{0.1}Mn_{0.1}$(NCM811) cathode, for >100 cycles at 0.1C and 0.2C.

2.6. Polymer electrolytes based on dynamic networks

The design of polymer electrolytes with dynamic bonds has great potential for application in LMBs. Dynamic polymers based on either covalent or non-covalent reversible chemistries can exhibit different properties, including self-healing ability, stimuli responsiveness and adhesive properties [66,224]. Great progress has been made in the last decade in the development of these smart materials, particularly by exploring a large variety of reversible covalent chemistries to redesign thermosets from permanently cross-linked polymers into reprocessable and recyclable materials [225,226].

Self-healing cross-linked PEs are attractive materials for LMBs, because their ability to self-recover upon damages can confer greater safety and durability to the device [227]. In contact with Li metal, self-healing PEs can mitigate the dendrite formation by forming adaptable interfaces with improved electrode adhesion. To be effective, the electrolyte should be able of rapid self-healing at the operative temperature of the device, without the need for external stimuli, while also displaying sufficient conductivity, mechanical strength and electrochemical stability. Self-healing polymers based on H-bonding interactions typically exhibit fast recovery upon damages, therefore being suitable for applications as battery electrolytes. Supramolecular networks based on H-bonds were prepared by RAFT copolymerization of an ureidopyrimidinone containing methacrylate monomer (UPyMA) and PEGMA (Fig. 7a). The storage modulus of the polymers increased with increasing the UPyMA content due to the improved interaction among polymer chains via quadruple H-bonding [228]. Upon mixing with LiTFSI ($r = 0.05$), the SPE exhibited Young's modulus of 0.12 MPa at r.t. and $\sigma \sim 10^{-4}$ S/cm at 60°C, and upon cut was able of complete self-healing in 2 h at r.t. without stimuli. A Li/LFP cell cycled at 0.1C and 60°C retained 91% capacity after 100 cycles.

Different strategies were adopted to improve the properties of ureidopyrimidinone-based electrolytes. Composite self-healing PEs were designed by mixing UPy-functionalized SiO_2 nanoparticles with the UPyMA-PEGMA copolymer (Fig. 7b) [229]. UPy-SiO_2 NPs were formed by reacting amino-terminated SiO_2 NPs with isocyanate-functionalized UPy. The CPE with 10 wt% UPy-SiO_2 showed slightly improved conductivity and mechanical properties compared to the pure copolymer, and a blend of copolymer and non-functionalized SiO_2 NPs. Alternatively, dual network PEs comprising both covalent cross-linking and H-bonds were prepared by RAFT copolymerization of UPyMA-PEGMA, and polyethylene glycol-bis-carbamate dimethacrylate cross-linker [230]. The optimized PE had a modulus of 0.4 MPa, oxidative stability up to 5.2 V, and the urethane groups contributed to increasing the conductivity. Moreover, an ionic liquid monomer bearing an UPy-group in the side chain was used to synthesize pIL copolymers (Fig. 7c) [231]. The ionogels had high ionic conductivity (10^{-3} S/cm at r.t.) and were able of self-heal in 1 h at 55°C, however its mechanical strength was relatively poor. In contrast, block copolymer micellar ionogels showed a Young's modulus of 0.12 MPa, $\sigma \sim 2 \times 10^{-3}$ S/cm at r.t. and self-repaired in 3 h at r.t. [232]. The copolymers were made by RAFT polymerization and contained a polystyrene block and a statistical block with N,N-dimethylacrylamide and acrylic acid units, responsible for the formation of H-bonding interactions.

Amino-terminated PEO and a thermoplastic polyurethane formed self-healing PEs, thanks to the intramolecular H-bonds between urea and ester groups [235]. The optimized electrolyte achieved complete self-healing in 60 s upon cut, high flexibility, $\sigma = 2 \times 10^{-4}$ S/cm, and oxidative stability up to 5 V, enabling high capacity in a Li/NCM battery. The incorporation of covalent

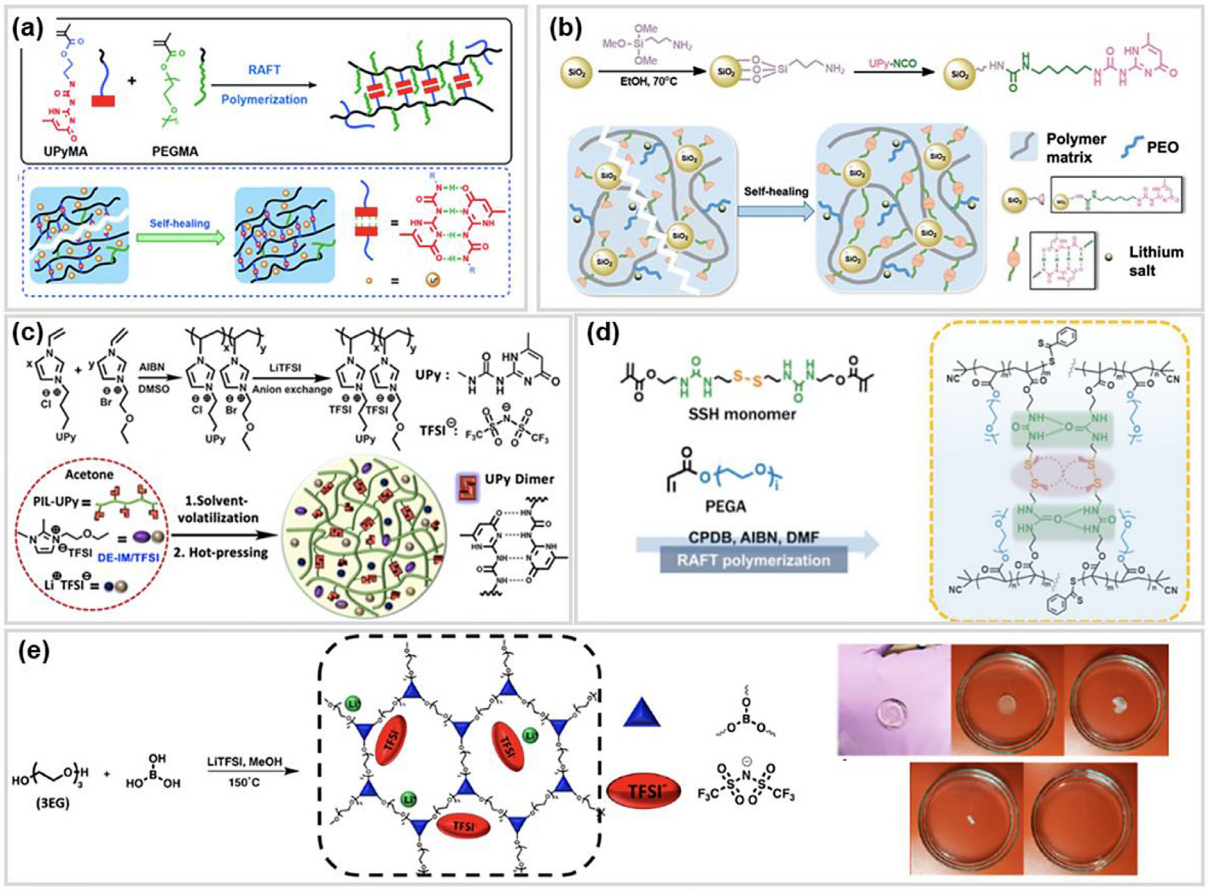

Fig. 7. Self-healing polymer electrolytes based on H-bonding through ureidopyrimidinone units, including (a) UPyMA-PEGMA copolymers. [228], Copyright 2018. Reprinted with permission from Royal Society of Chemistry; (b) UPy-SiO_2 NPs in UPyMA-PEGMA copolymer matrix. [229], Copyright 2018. Reprinted with permission from Royal Society of Chemistry; (c) ionogels based on UPy-functionalized IL monomer. [231], Copyright 2019. Reprinted with permission from American Chemical Society; (d) H-bonding via urea groups and covalent disulfide bonds. [233], Copyright 2020. Reprinted with permission from American Chemical Society; and (e) vitrimer-like materials with boronic ester linkages. [234], Copyright 2019. Reprinted with permission from American Chemical Society.

dynamic bonds in supramolecular networks leads to improved mechanical strength and self-healing behavior. PEs with both disulfide and H-bonds were made by RAFT polymerization of poly(ethylene glycol) methyl ether acrylate (PMEA) and a crosslinker containing urea and S-S groups (Fig. 7d) [233]. The PEs were able to self-heal from cut damage in 30 min at r.t.

PEO-based networks with dynamic disulfide bonds were synthesized by thiol oxidation of a bisthiol monomer and tetrathiol cross-linker, in the presence of H_2O_2 and NaI [236]. Upon addition of LiTFSI, the electrolytes exhibited conductivities of $\sim 10^{-6}$ S/cm and storage modulus of about 0.5-1 MPa at r.t. ($r = 0.1$). The stimuli-responsiveness of these materials was demonstrated by measuring stable conductivity and adhesive shear strength upon intermittent UV-irradiation. On the other hand, dynamic chemistries that do not require catalysts or (photo)thermal activation are preferable for application in LMBs. Evans et al. developed PEO-based network electrolytes with boronic-ester linkages by condensation of triethylene glycol and boric acid, in the presence of LiTFSI (Fig. 7e) [234]. The polymer network in the absence of salt exhibited a solid-liquid transition and associative exchange mechanism, indicative of a vitrimer-like behavior. The B atom showed Lewis acidic character, thus interacting with $TFSI^-$, increasing the Li transference number. The self-healing behavior was proven under application of an alternating voltage, and the network could be completely dissolved in water in 30 min, to recover the initial components. Therefore, this electrolyte set the premise for degradable and recyclable PEs for Li batteries.

2.7. Summary

The replacement of conventional liquid electrolytes in LMBs with polymer electrolytes can improve safety, while increasing the cycling life by contributing to regulate the morphology of Li deposits. Moreover, PEs benefit from high tunability, facile manufacturing and improved interfacial contact in comparison to inorganic solid electrolytes.

PEO is the most employed polymer for Li-based batteries, and various strategies were proposed to overcome its typical drawbacks, including high crystallinity and low stability at high potentials. On the one hand, comb polymers carrying ethylene oxide units in the side chains have decreased crystallinity and enhanced conductivity. On the other hand, block copolymers allow for decoupling transport and mechanical properties by exploiting phase separation to obtain more robust membranes with sufficient ionic conductivity. Additionally, cross-linked PEs exhibit improved mechanical strength to resist the penetration of dendrites, while the presence of nanosized meshes enable to confine and homogenize the electrodeposition of Li.

Polycarbonate-based electrolytes typically have superior conductivity, transference number and oxidative stability to PEO-based polymers, however they are poorly stable against Li metal. Poly(ionic liquid)s have larger electrochemical window and tun-

able charged units that can affect the Li^+ transport. ILs are also often used as plasticizers, as well as glymes and liquid carbonates, to enhance the conductivity of polymers, forming GPEs. In particular, the combination of ILs and block copolymers can form nanostructured materials with exceptional conductivities and mechanical strength, depending on the miscibility and ratios of the components. Additionally, solvate ionic liquids are formed by combining glymes and Li salts to obtain strongly chelated structures with improved electrochemical and thermal stability. Mixtures of SILs and polymers result in ionogel with high ionic conductivities.

To achieve Li transference number approaching units, polymer electrolytes can be design to possess Lewis acid sites that partially trap anions, such as in the case of organoboron polymers. Similarly, F atoms in perfluoropolyether-based electrolytes strongly interact with TFSI anions, enhancing the mobility of Li^+. Alternatively, anions can be immobilized onto polymer chains, to form single Li-ion conducting polymer electrolytes with transference number approaching unity. Poly(styrene-TFSI) was the first developed SLIC polymer, however SLIC (meth)acrylate units can overcome the rigidity of styrene. In alternative, the introduction of various functionalities on the aromatic rings allowed for tuning the conductivity of resulting SLIC-PEs.

Composite membranes based on polymer matrices, inorganic fillers and Li salt exhibit improved mechanical strength and pathways for rapid and uniform Li^+ transport, created by the homogeneous and/or ordered distribution of fillers. Charged and conductive fillers highly enhance the Li^+ conductivity and transference number. An alternative strategy to simultaneously achieve high conductivity and mechanical strength consists of forming charge-transfer complexes, by mixing suitable polymers and p-type dopants. In the presence of Li salt, the resulting solid electrolytes can exhibit superionic conductivity.

Recent trends in the design of PEs include the use of bio-derived polymers, such as cellulose, as well as reprocessable and degradable polymers, toward more sustainable electrolytes. Moreover, polymer networks presenting dynamic bonds result in self-healing electrolytes that ensure durability and stability to the device. Finally, in situ polymerizations that occur inside the assembled battery from liquid precursors offer the advantage of facile manufacturing, although it remains challenging to achieve high conversions and controlled properties of the resulting gels.

3. Polymer-based artificial solid electrolyte interphase (ASEI)

3.1. General characteristics of solid electrolyte interphase (SEI) in LMBs

The concept of an electronically insulating and ionically conducting passivation layer or solid electrolyte interphase on the graphite anode of LIBs was first introduced by Peled in 1979 [237]. Extensive studies of the SEI were carried out by Peled et al. and Aurbach et al. in the '90s [238,239]. The SEI is regarded as the most important but less understood component in a rechargeable Li battery, as great efforts were devoted to measuring and optimizing the SEI properties [240]– [241].

In LMBs, the lithium metal anode reacts with most organic electrolytes (such as carbonate-based electrolyte or ether-based electrolyte) and a passivation layer (i.e. SEI) forms on the lithium surface. Similar to the case of LIBs, a dense and intact SEI is necessary in an LMB to restrict the electron tunneling and protect additional lithium from reacting with the electrolyte. However, the spontaneously formed SEI is unstable, brittle and easy to crack. Fractures in the SEI causes re-exposure of fresh lithium to the electrolyte as the cycling continues, ultimately leading to depletion of both lithium metal and electrolyte, resulting in low Coulombic efficiency [242]. In order to overcome the weaknesses of spontaneous SEIs, a promising strategy consists of constructing an artificial SEI (ASEI) membrane that can be purposely added onto the lithium surface. The key features of an effective ASEI include: i) pressure-driven or density-driven mechanical suppression of dendrites and resistance to volume changes during lithium plating/stripping; ii) fast and uniform lithium ion transport to ensure low interfacial resistance and uniform Li electrodeposition; iii) chemical and physical stability against both lithium metal and electrolytes [22,243,244].

Some liquid electrolyte additives such as VC or fluoro ethylene carbonate (FEC) were found to increase the stability of the anode/electrolyte interface due to the tendency of forming oligomers upon attack of radical anions. The thin layers of oligomers were less prone to side reactions with the electrolyte, suggesting that polymers could be good building blocks for ASEIs [245]. Taking advantage of their tunable functionalities, physical and mechanical properties, facile fabrication/processing and good thin film formability, several polymers were exploited as ASEIs (Fig. 8). Moreover, hybrid system composed of polymers and inorganics were employed to further enhance the properties of polymer-based artificial SEIs, in particular their mechanical properties and conductivities.

According to their structure and physicochemical properties, polymer-based ASEIs could be divided in three categories: i) polymers with high mechanical strength or viscoelastic behavior; ii) polymers with high conductivity, transference numbers or dielectric constant; iii) reactive polymers that generate stable interfaces upon contact with lithium metal. In this section, polymer and polymer/inorganic composite materials pertaining to these three categories are discussed, together with their application with both liquid and solid electrolytes. Macromolecular approaches to engineer the surface of separators will also be discussed in this section.

3.2. Polymer-based ASEIs for liquid electrolyte

3.2.1. Mechanically robust polymer ASEIs

Two approaches were adopted to harness the mechanical properties of polymers toward effective ASEIs: i) a pressure-driven approach based on "hard" ASEIs with high shear modulus; ii) a density-driven approach based on polymers with viscoelastic nature.

"Hard" polymer ASEI with high shear modulus. The kinetic model proposed by Monroe and Newman suggested that polymer materials with a Poisson's ratio similar to PEO could suppress the roughening of Li surfaces when their shear modulus is at least 1.8 times higher than that of lithium [81]. Tikekar et al. later showed that lower shear modulus could stabilize the interface when possessing high transference number, high ionic conductivity and high interfacial surface tension [77]. Ionically conductive polymers typically have low shear modulus (< 1 GPa). Therefore, composite polymer/organic ASEIs are generally preferred. A Kevlar-fiber/PEO composite with a shear modulus of 1.8 GPa successfully suppressed the growth of lithium dendrite [246]. Similarly, a composite protective layer composed of Al_2O_3 particles and PVdF-HFP copolymer formed an effective ASEI, with inorganic Al_2O_3 providing sufficient mechanical strength while PVDF-HFP imparted fast Li^+ transport by forming a gel polymer electrolyte with liquid electrolytes. The shear modulus of such protective layer was ~1.8 times higher than that of the Li metal, effectively suppressing the dendrites growth. The Li/LCO cell incorporating CPL exhibited excellent cycling stability up to 400 cycles at 1 mA/cm^2 (1 C) [247]. In contrast to non-covalent blends of polymers and inorganics, designing hybrid layers with polymers covalently anchored onto the inorganic surface is a promising strategy to tune the inorganic content while limiting the aggregation of inorganics, so that hybrid ASEIs with high uniformity can be obtained. Polymer/nanoparticle hybrid core-shell structures with high electrochemical stability were

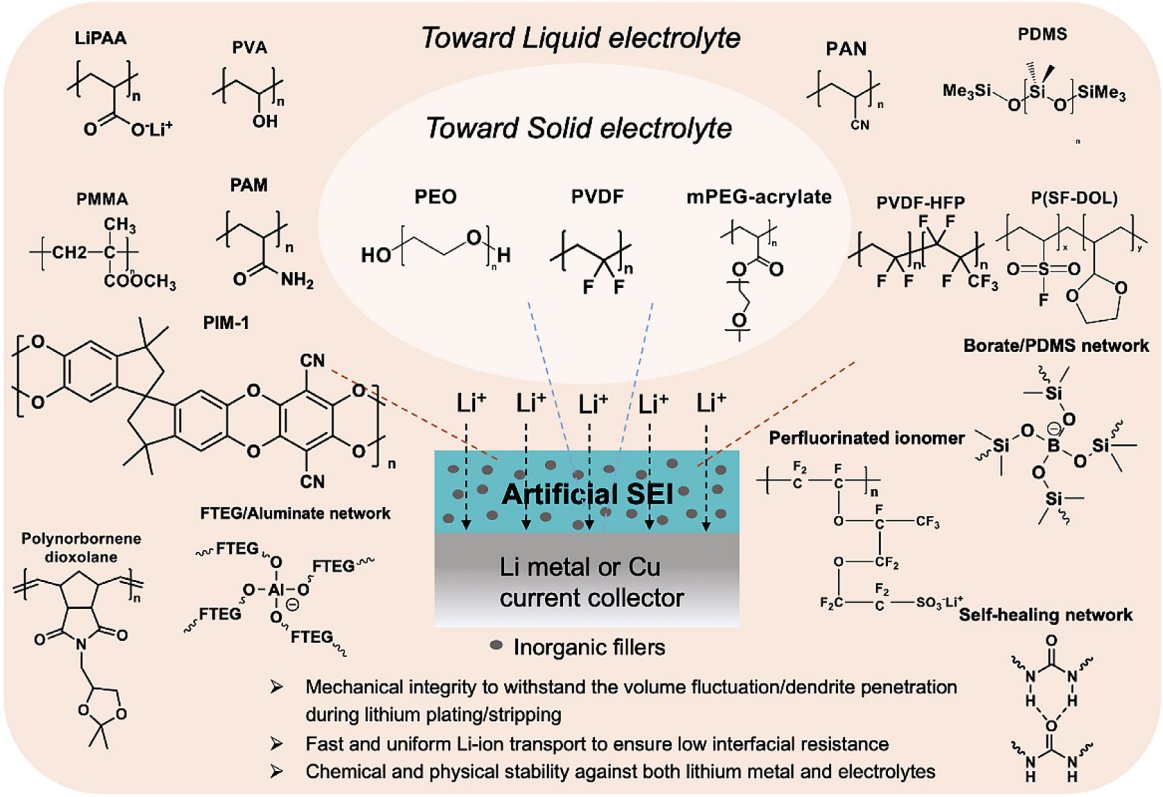

Fig. 8. Key features and examples of polymers for polymer ASEI.

prepared by copolymerizing MMA in presence of SiO_2 NPs, which were surface-modified with vinyl bond, via seeded emulsion polymerization (Fig. 9a). The high modulus of the SiO_2 NPs (68 GPa) imparted sufficient strength to suppress the dendrite growth while nano-sized pores were able to block the nucleation and penetration of lithium dendrites [87,248]. The PMMA shell enhanced the toughness and flexibility of the membrane, and favored the uniformity of the preparation slurry, to obtain a homogeneous distribution of NPs after solvent removal. Compared to an uncoated electrode, the electrode coated with such hybrid ASEI maintained Coulombic efficiency of ~85% after 40 cycles of at current density of 1 mA/cm^2 and practical areal capacity of 4 mAh/cm^2 with conventional LiPF6-based carbonate electrolyte (BASF Selectilyte LP40) [249].

"Soft" polymer ASEI with viscoelasticity. On the other hand, soft elastic or viscoelastic polymers could also greatly improve lithium deposition and interface stability. By using a coarse-grained molecular model to study the effect of polymer bond on the morphology of lithium deposits, it was found that only when the bond strength falls in the range of elastic/viscoelastic polymers the ASEI can prevent the penetration of lithium protuberances while adapting to the large volume change of the electrode [250]. In line with this discovery, many soft polymers were employed as effective ASEIs.

PDMS-based materials exhibit intriguing properties thanks to the chemical inertness and mechanical flexibility of PDMS (Young's modulus 360-870 KPa), which therefore is a suitable building block for an ASEI. PDMS was treated with hydrofluoric acid (HF) to create nanoporosity that could serve as pathways for Li^+ transport. The nanopore size was tuned by varying the HF etching time. Nanopores of 40-100 nm gave optimal ASEIs, while larger pores resulted in direct contact between lithium metal and electrolyte, losing the protective effect. The nanoporous PDMS ASEI enabled a Coulombic efficiency of 95% in a LMB for over 200 cycles at 0.5 mA/cm^2 current density. By depositing the PDMS ASEI on Cu current collector an average Coulombic efficiency of 98.2% was measured in 100 cycles at 0.5 mA/cm^2 [251]. Pang et al. created a PDMS/Li_3PS_4 hybrid membrane that took advantage of the PDMS matrix to improve the electrochemical stability of the ceramic electrolyte Li_3PS_4. (Fig. 9b) The compact packing of the ceramic phase formed percolative Li^+-conducting channels. The PDMS phase provided sufficient adaptability to accommodate the surface roughness/volume change during lithium plating/stripping, while preventing direct contact between lithium metal and Li_3PS_4, and the reduction of liquid electrolytes. Such hybrid ASEI enabled Li plating with 95.8% efficiency over 200 cycles and stable operation of a Li/LTO cell for 2,000 cycles [252].

Silly putty (SP), a popular kids' toy, is made of PDMS crosslinked by transient boron-mediated bonds. The dynamics of bond breaking and reforming in polymer chains makes it a smart material, with "solid-liquid"-like properties: SP responds as an elastic solid to fast deformations while displaying flowable character when gently touched, as typical of viscoelastic materials. When in contact with a lithium electrode, SP could withstand sudden dendrite tip rupture while accommodating to the volume fluctuation. By using SP as ASEI, the resulting conformal interface improved the lithium morphology and cycling stability, and inhibited non-uniform Li deposition and dendrite growth. In the presence of SP-coating, a LMB maintained an average CE of 97.6% for over 120 cycles at 0.5 mA/cm^2, whereas in the absence of coating the CE dropped below 90% after 75 cycles [253]. Another viscoelastic ASEI was prepared by exploiting the condensation reaction between branched oleic acids and diethylene triamine, followed by treating with urea to generate a supramolecular self-healing polyamides

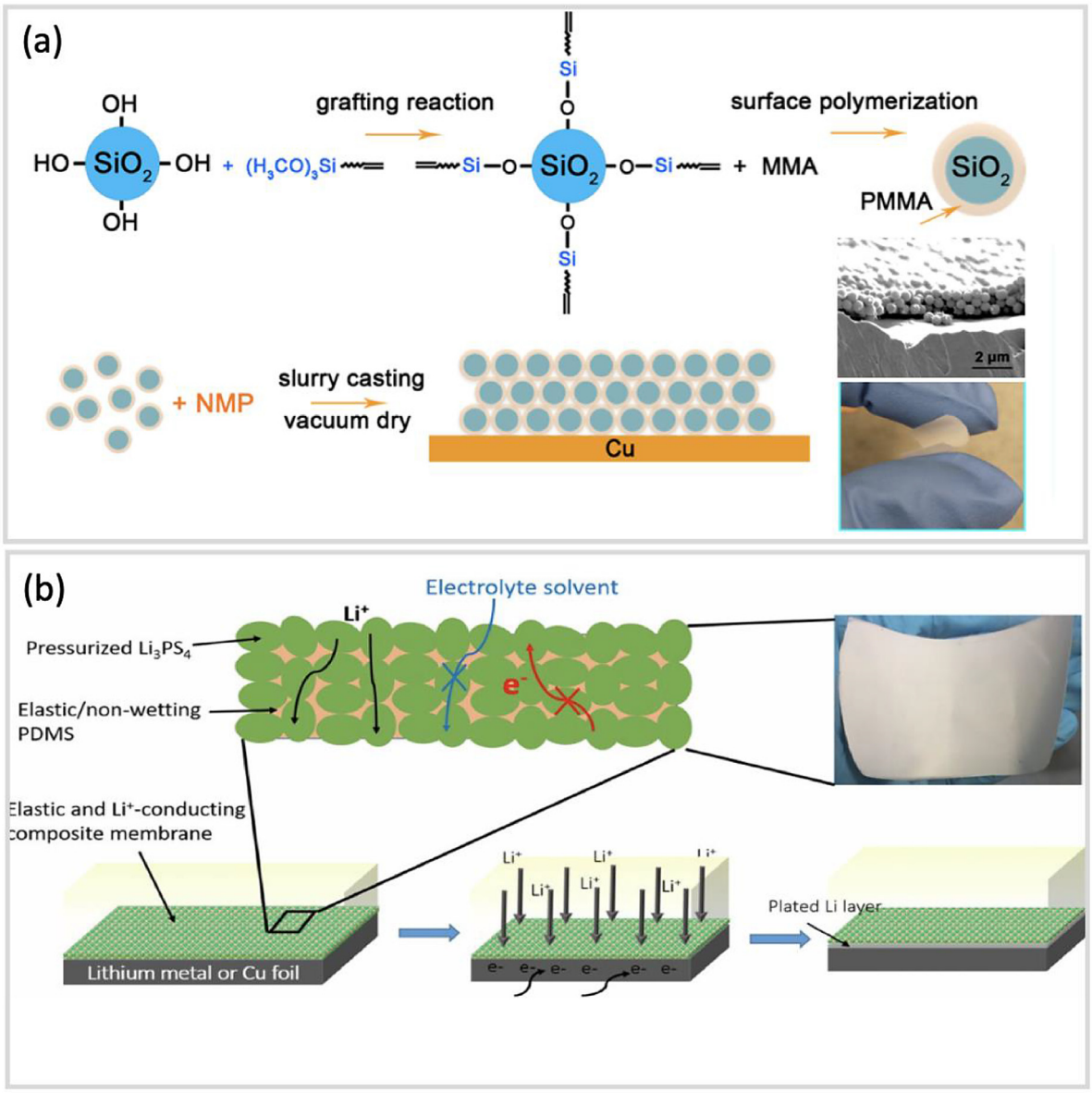

Fig. 9. (a) Preparation of silica/PMMA core-shell hybrids via surface radical polymerizations, followed by vacuum drying to make an ASEI; and TEM image and digital picture the hybrids ASEI. [249], Copyright 2017. Reprinted with permission from American Chemical Society. (b) Illustration of preparation of PDMS/Li_3PS_4 hybrids ASEI. [252], Copyright 2018. Reprinted with permission from the National Academy of Sciences.

with a high density of hydrogen bonds [254,255]. The viscoelasticity, healing speed and mechanical strength were tuned by adjusting the crosslinking densities. Uniform Li electrodeposition and high CE (97%) was obtained on Li metal coated with a 4 μm thick self-healing ASEI and cycled at 5 mA/cm^2 with Coulombic efficiency of 97% [254].

3.2.2. Polymer ASEI with improved ion transport properties

The electrochemical properties of polymer ASEIs are critical, as the coating should create channels for lithium ions migration while blocking the electron-tunneling that can reduce the electrolyte. The spontaneous SEI on the lithium metal anode is heterogeneous, leading to uneven distribution of ionic conductivity across the SEI. Hotspots with faster conductivity promote faster lithium deposition and formation of dendrites [22]. If the ionic conductivity of the ASEI is much lower than that of the liquid electrolyte, lithium still preferentially deposits at defects or hotspots, intensifying the inhomogeneity of the layer [256]. Therefore, polymer-based ASEIs with uniform distribution of fast ion transport paths and high transference number are crucial for suppressing dendrites [77]. These properties can be affected by the structure, composition, functionality, and porosity of the polymer being used, and will be discussed in this section.

Polymer ASEIs with high dielectric constant. Polymers with higher dielectric constant promote stronger dissociation of lithium ions. By comparing different polymer coatings including PEO, PVDF-HFP, PVDF, PU, PDMS and polyamides, it was found that polymer coatings with higher dielectric constant, such as PVDF-HFP and PVDF, increased the exchange current (i.e. the equilibrium current where the rate of the forward reaction is equal to the rate of the backward reaction at the metal electrode) and interfacial energy, leading to larger deposits of lithium [257]. β-phase PVDF is the most polar form of PVDF, with full trans conformation with H and F atoms located on the opposite sides of the polymer backbone. The highly polar β-phase PVDF has high dielectric constant (8∼13) compared to other fluoropolymers. The alignment of

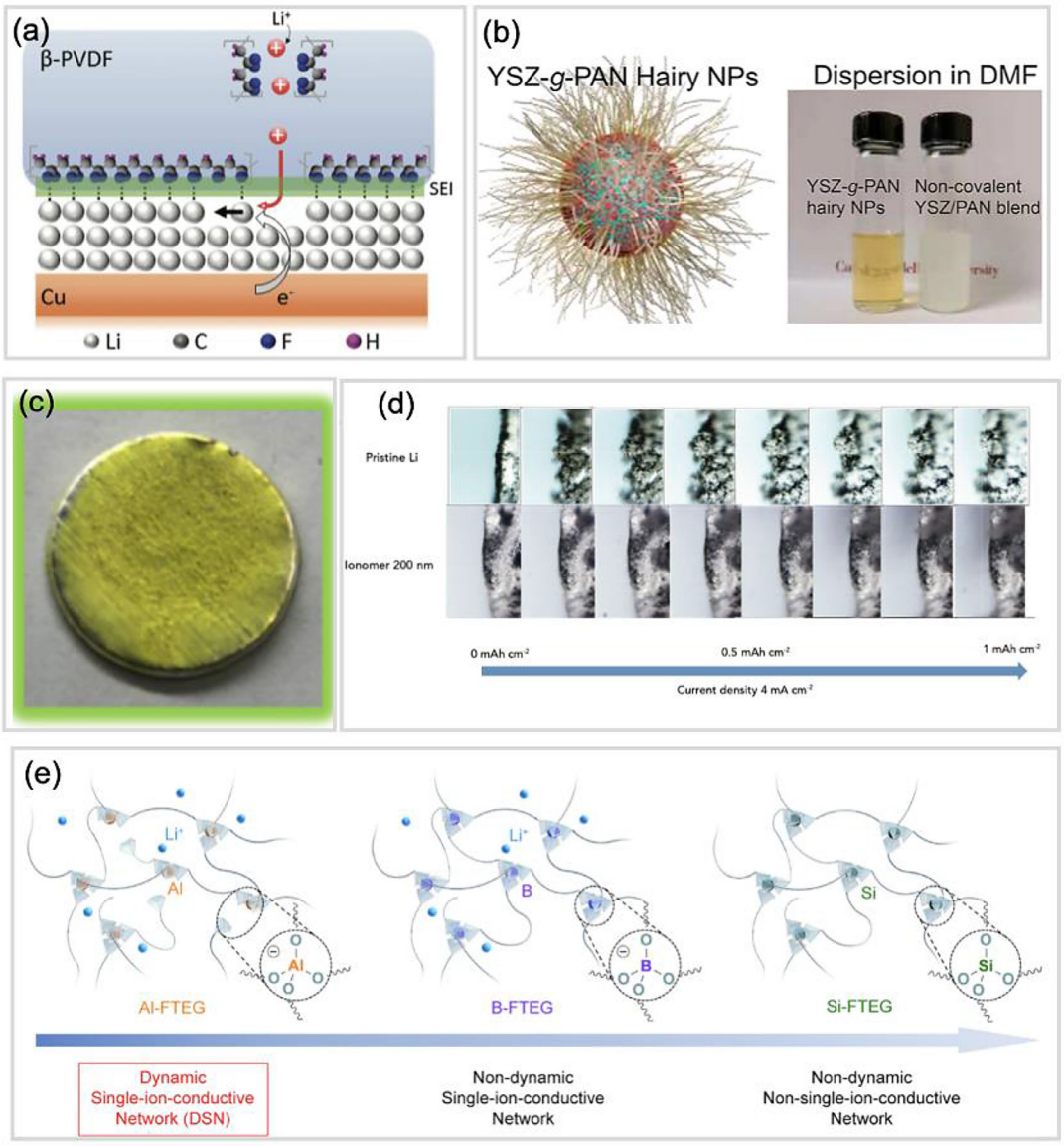

Fig. 10. (a). Schematic illustration of layer-by-layer deposition and preferential diffusion pathways for Li ions. [258], Copyright 2017. Reproduced with permission from Wiley-VCH. (b). Schematic of YSZ-*g*-PAN hybrids particle uniformly dispersed in organic solvent. [168], Copyright 2020. Reprinted with permission from Elsevier. (c). Lithium anode coated with PIM-1. [265], Copyright 2019. Reproduced with permission from American Chemical Society. (d) Snapshots of the lithium deposition in a custom-made optical visualization cell that uses pristine lithium and 200-nm-thick ionomer-coated lithium during the deposition of 1 mAh/cm^2 of lithium at a current density of 4 mA/cm^2. [268], Copyright 2017. Reprinted with permission from Cell Press. (e). Structure comparison of different types of crosslinked network as ASEIs containing or not bonds and single-ion conducting units. [269], Copyright 2019. Reprinted with permission from Cell Press.

F atoms in β-PVDF used as ASEI guided the transport of Li^+ and facilitated the interaction between electronegative C-F functional groups and Li, favoring a layer-by-layer Li deposition (Fig. 10a). A thin layer of β-phase PVDF ($\sim$4 μm) coated onto the surface of Cu current collectors resulted in stable Li deposition/stripping at high current density (5 mA/cm^2). In a Li/LFP cell, the β-phase PVDF ASEI on lithium anode enabled 94.3% capacity retention and stable CE of 99.85% at 0.5 C after 200 cycles [258].

Polymer ASEIs with high ionic conductivity. Highly conductive ASEIs diminish the interfacial resistance and spatial inhomogeneity, reducing the possibility of dendrite formation. Therefore, hybrid polymer/inorganic ASEIs are often used to enhance the ionic conductivites, as well as the transference number and mechanical robustness. Poly(vinyl alcohol) (PVA) was used as a soft glue combined with a Zn-MOF to fabricate a hybrid ASEI with high ionic conductivity and good flexibility to adjust to volume changes. PVA was spin coated and cemented into the surface of Zn-MOF, promoting the film formability and softness of the material. The Zn-MOF contained a large number of polar bonds (e.g. O-H and Zn-N), which could bind Li^+ and lead to fast Li^+ diffusion. Moreover, its porous structure hindered the migration of anions, increasing the uniformity of lithium flux, and its rigidity provided high mechanical strength to inhibit the dendrites growth. The ASEI had good electrolyte wettability, reducing the concentration gradients of ions at the surface. The ASEI-protected lithium metal anode achieved high Coulombic efficiency ($>$ 97.7%) over 250 cycles at a high current density of 3 mA/cm^2 [259]. Recently, a new class of polymer/inorganic hybrids ASEIs was made, which consisted of YSZ nanoparticles and PAN chains grafted from the YSZ surface [168]. The synthesis of YSZ-*g*-PAN exploited a universal approach to covalently anchor ATRP initiators onto the surface of metal oxides [260,261]. The grafted systems showed several advantages

over previously reported polymer-based ASEIs: i) improved dispersity of inorganics in the polymer matrix, enabling to obtain artificial SEI with uniform spatial composition by simple drop-casting (Fig. 10b); ii) the surface initiated (SI)-ATRP approach allowed precise control of PAN chain length and grafting density; iii) improved ionic conductivity ($> 1 \times 10^{-4}$ S/cm at r.t., two order of magnitudes higher than non-covalent blends with similar composition) and mechanical strength (7.56 GPa) due to the increased uniformity, reduced crystallinity and higher free volume; iv) the oxygen vacancy on the surface of YSZ acted as Lewis acid, partially trapping the anions, thus improving the lithium transference number. As a result, the lithium anode with the YSZ-*g*-PAN coating achieved long cycle life both in a symmetric cell ($>$ 2500 h at 3 mA/cm^2 and 3 mAh/cm^2) and in a full cell with a $LiNi_{0.8}Co_{0.15}Al_{0.05}O_2$ (NCA) cathode extracted from a commercial 18650 cell having high mass loadings (~28 mg/cm^2) [168].

Porous membranes can effectively manipulate the Li ion flux. Polyimides (PIs) have good high temperature performance and chemical resistance. Reactive-ion etching was used to develop a polymer ASEI based on a 3.5 μm PI coating possessing vertical nanochannels (pore size ~350 nm) with high aspect ratio. Due to the presence of nanochannels, the Li deposit is confined and eventual surface roughness could not be amplified because of the Li^+ flux confinement. Therefore, homogenous Li nuclei distribution and growth was achieved. At a current density of 3 mA/cm^2, the ASEI protected electrode showed CE of 88.6% over 140 cycles, while the CE of the unprotected electrode rapidly decayed in 50 cycles [262].

Polymer ASEI with enhanced t_{Li+}. Furthermore, the efficiency of Li^+ transport can be enhanced by nanoconfinment of the ion flux. It was calculated that when the pore radius is similar to the Debye screening length, the transport of cations is assisted by the electro-osmosis-driven hydrodynamic flow, caused by the interaction in capillaries between the diffuse double layer and the external field [263]. When the pore size and the Debye screening length is about the same order, the cation transference number approaches unity, therefore reducing losses caused by ion polarization. However, for the practical concentration of electrolyte used in a battery, the Debye screening length is $<$ 1 nm. Therefore, polymers of intrinsic microporosity (PIMs) are good candidates for use in batteries, since they are microporous materials containing a continuous network of interconnected intermolecular voids with less than 2 nm width [264]. PIM-1, a typical PIM, was employed as ASEI for lithium metal anode (Fig. 10c). When 1 μm-thick layer of PIM-1 with a porosity of 0.5~2 nm was coated onto a lithium metal anode, the transference number of the liquid electrolyte was increased from 0.2 to $>$ 0.7. Low interfacial resistance and dendrite suppression were obtained in a Li/Li symmetric cell that reached a cycle life of over 750 h with a capacity of 0.75 Ah. When paired with a high energy density sulfur cathode (4.9 mg/cm^2; 8.2 mAh/cm^2), ~24 μm of lithium was reversibly electrodeposited in each cycle at a C-rate of 0.2 [265]. The small pores of PIM-1 exhibited size-sieving ability, separating solvated Li ions and single Li ions, and allowing Li ions to pass the interphase layer while avoiding the contact between solvent molecules and lithium metal. This decreased the consumption of both lithium metal and electrolyte during cycling [266]. Recently, a diversity-oriented synthesis approach was employed to build a library of PIMs with shape-persistent free volume elements that served as solvation cages for Li ions. The synthetic strategy was based on the functionalization of bis(cathecol) monomers through multi-component Mannich reactions, followed by base-mediated step-growth polymerization. Structural and electrochemical characterization of the PIM library revealed that the Li^+ conductivity was enhanced by both the placement of specific classes of N- and O-based ion-coordinating functionality within the pore network, and in some cases by an ultramicroporous architecture capable of limiting the number of solvent molecules that can bound to Li^+. As a consequence, the concentration of Li^+ in certain PIMs increased via partitioning from the bulk electrolyte. The PIM with highest room temperature conductivity (2.06×10^{-4} S/cm) was employed as protective layer on Li metal in LMBs with NCM622 as cathode (1.44 mAh/cm^2). High capacity retention for over 400 cycles was observed even under a high current density of 5 mA/cm^2, showing largely improved performance in comparison to bare Li as well as Li coated with conventional PIM-1 [267].

An alternate approach to improve the transference number of ASEIs is by using single Li-ion conducting polymer coatings, with anions immobilized on the polymer backbone, similar to the case of SLIC polymer electrolytes (Section 2.5) [60,167] . Based on a linear stability analysis of lithium electrodeposition, [86] a lithiated perfluorinated ionomer was used as a coating layer with high transference number and high ionic conductivity, which synergistically contributed to suppressing dendrites [268]. The ionomer was deposited on Li metal by simple solution casting to form a conformal interface with conveniently controlled thickness by repeated casting or varying the solution concentration. When the thickness was decreased below 200 nm, the coating reached high ionic conductivity ($> 10^{-3}$ S/cm). The coating was then co-deposited with a nanoporous layer of Al_2O_3, to enhance the mechanical strength without decreasing the conductivity. At a current density of 4 mA/cm^2, the Li anode protected with a 200 nm-thick coating showed no evident dendrite growth, whereas a pristine lithium foil could not inhibit the dendrite growth (Fig. 10d). When paired with NCA cathode and tested at a high current density of 3 mA cm^{-2} and 3 mAh cm^{-2} capacity per cycle, the protected Li anode exhibited stable plating/stripping behavior for over 400 cycle with ~90% capacity retention.

Finally, a dynamic single-ion conductive network (DSN) was proposed as a multifunctional ASEI. The DSN consisted of tetrahedral $Al(OR)^{4-}$ aluminate anions as dynamic crosslinking centers, soft fluorinated chains (1H,1H,11H,11H-perfluoro-3,6,9-trioxaundecane-1,11-diol) (FTEG) as inert ligands and lithium ion as free counter ions. The DSN network exhibited viscoelasticity, single-ion transport and chemical inertness. The solution-processed DSN ASEI maintained low interfacial impedance and facilitated homogeneous Li electrodeposition. Integrated with a thin Li foil (42 μm thickness, ~8 mAh/cm^2) and a commercial NCM532 electrode (~95% active material, 2 mAh/cm^2 loading), the full cell also showed high capacity retention of ~85% and high average CE ($>$99.6%) after 160 cycles at a charge-discharge rate of C/2 [269]. Noticeably, the author demonstrated that the DSN networks showed better dendrite suppression performance than networks based on the same polymer backbone but without either single-ion feature or dynamic mechanical properties (Fig. 10e), highlighting the enhanced efficiency of multifunctional coatings.

3.2.3. Reactive polymer ASEIs

In addition to the conventional ex situ coating of a lithium metal surface, *in situ* formation of dense multifunctional protection layers using reactive precursors has become an effective approach for stabilizing lithium anodes. This strategy takes advantage of the highly reducing environment and the electrochemical process to generate compounds in the SEI that improves the anode stability. Such *in situ* formation process ensures homogeneity and can generate an ASEI with unique mechanical and electrochemical properties, by rational selection of the reactive components. The simplified manufacturing of the coating facilitates the cell processing. Therefore, reactive polymer ASEIs are discussed separately in this section. Largely, two categories of reactive polymeric ASEI could be identified: i) ASEI that forms from the reaction between a pre-polymer coating and lithium metal, which generates polymers or composites with improved mechanical and transport properties;

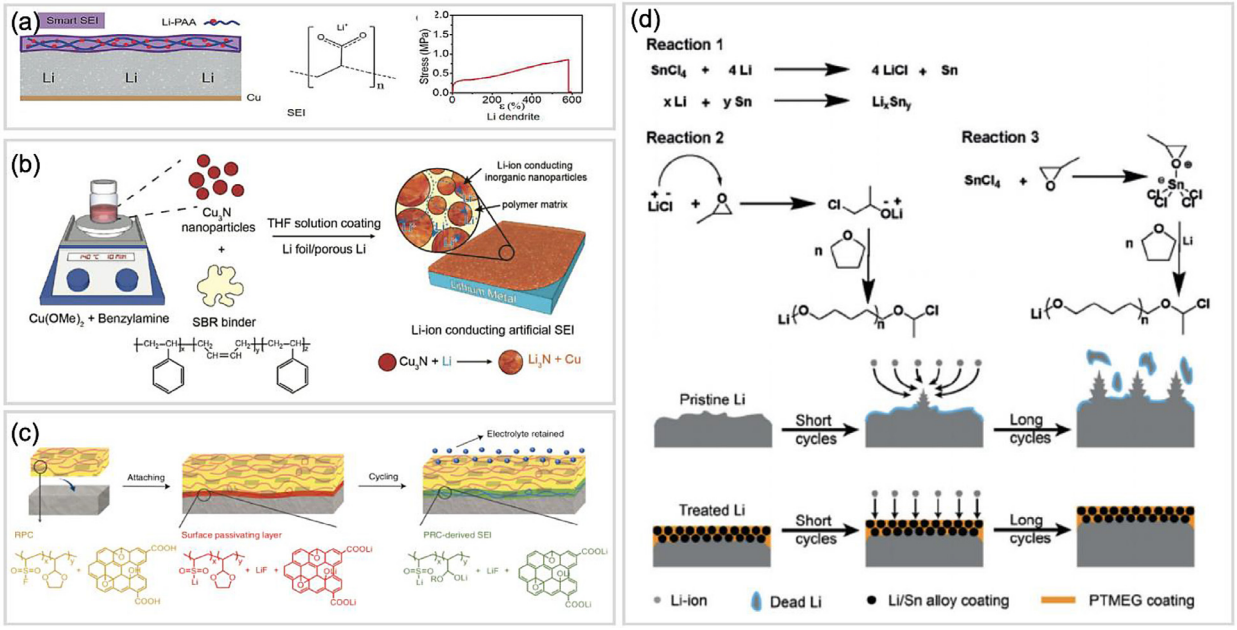

Fig. 11. (a) Schematic illustration of reactive Polymer ASEIs based on highly stretchable LiPAAs. [272], Copyright 2017. Reprinted with permission from Wiley-VCH; (b) Schematic illustration of the fabrication of the Cu_3N+SBR composite ASEI. [276], Copyright 2017. Reprinted with permission from Wiley-VCH; (c) Schematic illustration of formation of polycyclic ether/GO based reactive ASEI. [103], Copyright 2019. Reprinted with permission from Springer Nature; (d) Mechanism of forming polymer-alloy hybrids ASEI through *in situ* polymerization. [282], Copyright 2019. Reprinted with permission from Wiley-VCH.

ii) ASEI generated from a self-triggered *in situ* polymerization with enhanced conformability.

ASEI by reactive polymer coating with lithium metal. Reactive polymers can generate ASEI with robustness and flexibility. Lithium poly(acrylic acid) (LiPAA) is commonly employed as binder for electrode materials due to its great adhesiveness, mechanical stability and flexibility and single Li-ion conductivity. [270,271] When swollen by a liquid electrolyte, the LiPAA gel showed high stretchability (582 % strain), making LiPAA an ideal building block for an ASEI. By coating a layer of PAA onto the lithium surface, the polymer was directly lithiated to from LiPAA on site, obtaining a conformal ASEI with a thickness of 20 nm [272] (Fig. 11a). The LiPAA ASEI exhibited high stretchability and superior binding ability due to its high lithiophilicity. The stretchability helped withstand the volume change during lithium plating/stripping, while the compact and uniform structure prevented the exposure of lithium metal to the electrolyte. The cycle life of a symmetrical cell with LiPAA coated Li metal electrode was increased of more than 700 h compared to bare Li metal, under 0.5 mA/cm^2 current density. Similar to PAA, PVA is a low-cost and widely used synthetic polymer, with high thermal, mechanical, and chemical stabilities, and good film-forming properties. The hydroxyl reactive groups in PVA react with lithium salts and can participate in the SEI formation process, to form a robust Li-ion conductive layer. In both carbonate and ether-based electrolytes, a PVA protective layer (0.33 μm thickness) enabled a dendrite-free morphology for Li deposition and significantly stabilized the cycling performances in Li/Cu cells, which showed an average CE of 98.3% for over 630 cycles. The PVA ASEI on Li metal was tested in Li-sulfur, Li/LFP and Li/NCM622 full cells. Enhanced electrochemical performances in comparison to bare Li metal were achieved, even under lean electrolyte (7.5 μL/mAh) condition [273].

Reactive polymers were also used to generate ASEIs with both enhanced ionic conductivity and flexibility. Sulfur-rich reactive organic/inorganic hybrid SEIs were formed by exploiting the reaction between Li polysulfidophosphate (LiPSP) and poly(2-chloroethyl acrylate) (PCEA) prepared by free radical polymerization. LiPSP and a PCEA solution were mixed and drop casted together on the surface of lithium. LiPSP and PCEA underwent a nucleophilic substitution reaction that generated a crosslinked layer, along with inorganic lithium sulfides, obtaining a robust ASEI that can withstand electrode volume fluctuations. The crosslinking reaction generated LiCl, which enhanced the charge transfer kinetics of the SEI [274], together with the highly conductive Li_3PS_x formed during the reaction. The symmetric cycling performance showed average CE above 98.2% for over 130 cycles at a high current density of 4 mA/cm^2 and areal capacity of 4 mAh/cm^2. The full cell assembled with protected Li anode and LFP cathode (~2.4 mAh/cm^2) exhibited >89% capacity retention after 500 cycles, with high average CE of 99.9% [275]. An ASEI layer with high Li-ion conductivity, mechanical strength and flexibility was designed by mixing Cu_3N nanoparticles (sub-100 nm) in a styrene butadiene rubber (SBR). The Cu_3N NPs reacted with lithium metal to form Li_3N, one of the fastest Li-ion conductors with ionic conductivity of 10^{-3}-10^{-4} S/cm at r.t.. The protected electrode achieved a CE of 97.4% on over 100 cycles at an areal capacity of 1 mAh/cm^2 (Fig. 11b) [276]. Moreover, a stiff polymer with cyclic ether side chains, poly((*N*-2,2-dimethyl-1,3-dioxolane-4-methyl)-5-norbornene-*exo*-2,3-dicarboximide) was designed to prevent the reaction of carbonate electrolytes with Li metal, thanks to the strong affinity of the side chains for Li^+, while the polycyclic backbone ensured mechanical strength (Young's modulus of 0.37 GPa). The polymer was synthesized via ROMP and it formed a grafted skin layer (2 μm) on Li metal, due to the reaction of polycyclic ether units with lithium metal after electrochemical activation. The polycyclic ether components can also compete with and impair the reaction between Li metal and carbonate electrolyte, preventing electrolyte depletion during cycling. The ASEI regulated Li deposition and smoothed the surface morphology. In a Li/NCM532 full cell with grafted skin polymer ASEI, a capacity of 1.2 mAh/cm^2 was achieved and a cycle life of 400 cycles with 90% capacity retention [277].

LiF is regarded as one of the key components of a spontaneous SEI in a typical LIB with graphite anode. LiF is able to reduce the activation energy of Li^+ diffusion, promoting lithium

electrodeposition in the form of 2D planar structures instead of 3D dendrites [278]. On the other hand, reduced graphene oxide (rGO) has recently been identified as an effective building block for ASEIs, due to its i) increased lithiophilicity compared to GO thanks to its organic functional groups, ii) excellent mechanical strength to prevent dendrite growth, iii) dense packing that prevents side reactions between electrons and electrolytes [173,279,280]. Gao et al. recently demonstrated a molecular-level ASEI design using a reactive polymer composite (RPC), which effectively suppressed electrolyte consumption. The RPC consisted of a reactive poly(vinylsulfonyl fluoride-*ran*-2-vinyl-1,3-dioxolane) (P(SF-DOL)) and rGO nanosheets. The RPC-derived ASEI was formed in a two-step process, consisting of i) the anchoring of RPC to the lithium surface by reaction between lithium, sulfonyl fluoride groups and carboxylic acid groups from rGO nanosheets, to form LiF, $-SO_2-$Li salts and $-CO_2-$Li salts; ii) the reduction of DOL groups to form -O-Li salts during cycling. (Fig. 11c) The RPC-derived ASEI contained polymeric Li salts embedded with LiF nanoparticles and rGO nanosheets and was sufficiently dense to block electrolyte access to the lithium surface. The RPC-derived ASEI enabled highly efficient Li deposition and stable cycling of 4 V Li/NCM532 cells under lean electrolyte (7 μL/mAh), limited Li excess (1.9-fold) and high areal capacity (3.4 mAh/cm^2) [103].

ASEIs by *in situ* polymerizations. Polymer ASEIs could also be formed through *in situ* polymerizations triggered by electrolyte additives. An alloy-hybrid layer was constructed on Li metal through a facile process, whereby Li metal was immersed into a solution of $SnCl_4$ in THF. $SnCl_4$ was reduced by Li metal and formed Li/Sn alloys and LiCl. The LiCl in the ASEI provided fast Li ion transport at the interface and exhibited high exchange currents [168,281]. Both LiCl and $SnCl_4$ triggered the ring-opening polymerization of THF, and propylene oxide was introduced to facilitate the polymerization process. (Fig. 11d) The as fabricated poly(tetramethylene glycol)–Li/Sn alloy hybrid layer had strong affinity for Li ions, similarly to PEO, and improved moisture stability and hydrophobicity due to the higher content of alkyl chains. The hybrid layer exhibited remarkable performance in Li/Li, Li/S and Li/LFP cells, particularly under practical testing conditions with high cathode mass loading (17.4 mg/cm^2) and areal capacity (3 mAh/cm^2) [282].

3.3. Polymer-engineering of separators

Another strategy to achieve stable LMBs that employ traditional liquid electrolytes consists of engineering the structure of polymer separators. In current LIBs, the electrodes are electronically isolated by porous polymer separators infiltrated with liquid electrolyte. Typical separators are made of polyolefins, generally semi-crystalline polyethylene (PEt) and/or polypropylene (PP), with a membrane thickness of less than 25 μm and a porosity of around 40% [283]. The separator function is to enable the transport of lithium ions between the electrodes while preventing short circuits. The pore structures of the separator strongly affects both the electrolyte resistance and the current distributions at the electrodes [188].

To design separators with good electrolyte wettability and low electrolyte resistance, high thermal stability, and homogeneous pore structure, different strategies were explored, including i) coating the surface of traditional separators on both sides or exclusively on the anodic side to build an ASEI; ii) combining multiple separators, and iii) fabricating novel separators. Both organic and inorganic materials, as well as hybrid organic/inorganic materials were used to modify traditional separators [284,285].

Biobased cellulose nanofibers (CNF) were used to fabricate CNF/PE/CNF sandwiched separators by a facile lamination procedure [284]. The CNF layers had homogeneous pore distribution (size ~20 nm) and good thermal stability, therefore the sandwiched separator was stable up to over 200°C. Moreover, the small and uniform pore size enabled even Li deposition at relatively high current densities and longer stable cycling of LMBs compared to a PE separator. Chitin is another abundant natural polymer that was used to fabricate a nonwoven mat-type separator enabling greatly improved performances than polyolefin separators [286]. By using a centrifugal jet-spinning technique, the separator exhibited a hierarchical structure comprising microfibers and nanofibers, and a large number of functional groups with high Li-affinity.

Graphene and rGO can enhance the mechanical strength and conductivity of separators. Coating a PP separator with a polydopamine layer, followed by graphene nanosheets in a carboxymethylcellulose binder resulted in improved electrolyte wettability, conductivity and capacity for Li storage [287]. As a consequence, the cycling stability and Coulombic efficiency of LMBs were greatly enhanced. The high polarity of modified separators was crucial to ensure a rapid Li^+ flux. Similar properties were achieved by blade-coating GO nanosheets with grafted polyacrylamide (PAM) brushes on top of a PP separator. The dense PAM brushes were synthesized by first introducing ATRP initiating sites on GO sheets and then growing polymer chains by SI ATRP (Fig. 12a) [190,288]. The large quantity of C=O groups and N–H bonds improved adhesion and favored homogeneous distribution of Li ions, while the robust GO backbones increased the mechanical strength. Moreover, the stacking of functionalized GO nanosheets formed channels for rapid electrolyte diffusion, and dendrite-free morphology of Li electrodeposition was observed even under very high current densities [190].

Polymer/inorganic composite layers coated on PE or PP separators combine high flexibility and mechanical strength. The inorganic component can be either non-conductive or conductive. PP separators were decorated with a layer of PAA and nanosilicon that formed lithiated species, enhancing the conductivity [289]. The robust and flexible separator was able to suppress dendrites. On the other hand, coating PP with PVDF and LLZTO provided a three-dimensional highly conductive network for fast Li^+ transport [290]. Moreover, the material was able to partially trap anions, enhancing t_{Li+} and enabling even electrodeposition on the Li anode. Recently, conventional polyolefin separators were coated with a homogenous ink comprising a microporous polymer host, PIM-1, and tetralkylammonium fluoride [291]. The latter served as soluble precursor for the generation of LiF, which has low lithium volume ratio, via *in situ* cation metathesis during cycling of a cell assembled with the coated separator (Fig. 12b). The resulting nanostructured LiF@PIM-1 possessed minimally reconfigurable ion-conducting domains embedded in a soft polymer matrix, thus behaving as a “soft ceramic” with high transference number that originate from nanoconfinement. This material was capable of suppressing dendrites and enabling long-term stable cycling of LMBs under practical conditions using thin Li anodes (~30 μm) and high-voltage NMC622 cathodes (1.44 mAh cm^{-2}) at high current density (1 mA/cm^2).

3.4. Artificial SEI toward solid electrolyte

Solid electrolytes are prompt to overcome safety and ageing issues associated with conventional liquid electrolytes. Moreover, all-solid-state Li metal batteries can achieve much greater energy density than LIBs [79]. However, large interfacial resistance is typically established between the solid electrolyte and the electrodes, due to the insufficient solid-solid contact [292]. Interfacial instabilities lead to the formation of ionically insulating or electronically conducting decomposition products and eventual growth and penetration of dendrites through the solid electrolyte [293]. Hence, different strategies were proposed to improve the interfacial stability and contact between solid electrolytes and Li metal anodes. To enhance the cycle life of all-solid-state LMBs, several polymers

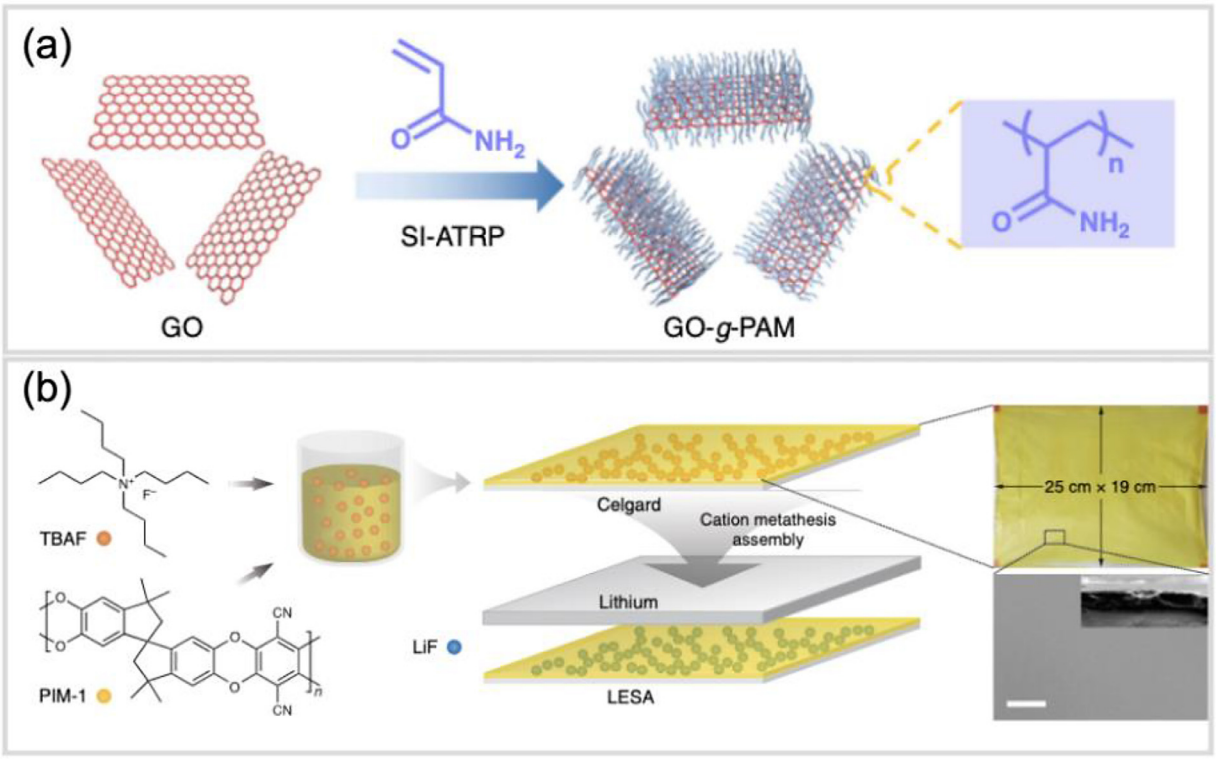

Fig. 12. (a) Schematic illustration of making GO-*g*-PAM molecular brushes by grafting PAM from GO surface via SI-ATRP. [190], Copyright 2019. Reprinted with permission from Springer Nature; (b) Schematic illustration of making PIM-1/LiF based solid-state coating on polyolefin separators. [291], Copyright 2020. Reprinted with permission from Springer Nature.

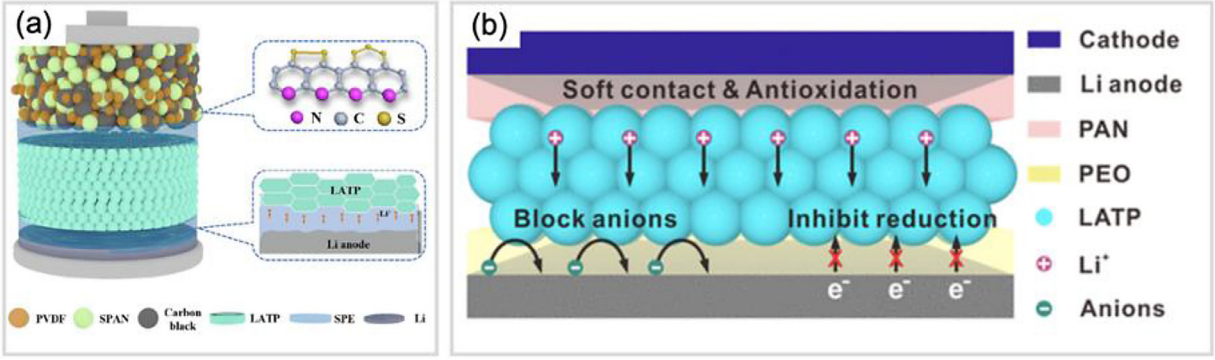

Fig. 13. Different strategies to improve the interfacial contact between ceramic solid electrolyte and electrodes: (a) sandwich-type electrolyte with LATP layer between two PEO/LiTFSI layers. [294], Copyright 2020. Reproduced with permission from Elsevier. (b) Illustrations of an all-solid-state LMB with the solid electrolyte LATP protected by DPCE. [297], Copyright 2019. Reproduced with permission from American Chemical Society.

were used as coatings applied either to the Li metal electrode or to the solid electrolyte. This latter approach was typically used to modify both the anode interface and cathode interface, to realize sandwiched electrolytes, multilayer structures, or Janus-type electrolytes.

Due to its high Li-ion conductivity and relative stability versus Li metal, PEO was often exploited to construct artificial interphases for all-solid–state LMBs, upon mixing with Li salts. PEO/LiTFSI (PEO (M_n = 600,000, EO/Li= 8/1) was deposited on the surface of the NASICON-type solid electrolyte $Li_{1.3}Al_{0.3}Ti_{1.7}(PO_4)_3$ (LATP) [294]. The as-fabricated sandwiched electrolyte SPE-LATP-SPE showed stable cycling performance in a Li/Li symmetric cell for over 200 h at 75°C. When employed in a full-cell with a sulfur-polyacrylonitrile (SPAN) composite cathode (Fig. 13a), high Coulombic efficiency and long-term cyclic stability were obtained, demonstrating that the PEO layer reduced the interfacial resistance with the electrodes and improved the stability. PEO/LiTFSI was also used to stabilize the interface between LLZO and Li metal [295]. The PEO/LiTFSI film (with thickness of 10 μm) was transfer-coated onto Li metal disks that were subsequently used for symmetric cycling tests with LLZO as solid-electrolyte. At 55°C and areal capacities of 0.025 mAh cm^{-2} and 0.1 mAh cm^{-2} the cycle life of the device was >500 cycles. Room temperature areas specific resistance (ASR) measurements showed a significant decrease in the interfacial resistance from 765.0 kΩ cm^2 of the bare electrode to 13.05 kΩ cm^2 of the PEO/LiTFSI-caoted Li metal. Furthermore, a Li metal electrode with PEO/LiTFSI artificial SEI layer was used with the composite solid electrolyte PVDF-HFP-LLZTO [296].The Li/Li symmetric cell was stably cycled for 600 h at a current density of 0.5 mA/cm^2 and a relatively low temperature of 40°C. All-solid-state

LMBs with PEO/LiTFSI-coated Li metal anode, the composite electrolyte and LCO or NCM111 cathodes retained CEs of 97% for 60 and 80 cycles, respectively, at 0.1 C and 40°C.

However, PEO-based polymers are generally poorly stable at high voltages, thus the use of solid-electrolytes sandwiched between PEO layers is limited to low-voltage cathode materials. To enable the use of solid-electrolytes with high-voltage cathodes, different polymer coatings were applied on the two sides of a ceramic electrolyte, forming a disparate-polymers protected ceramic electrolyte (DPCE), with PEO facing the anode side and PAN the cathode side (Fig. 13b) [297]. Both polymers ensured sufficient contact at the interfaces. Moreover, the stability of PEO under reductive potentials and the oxidative stability of PAN protected LATP from undesired redox processes. When the solid electrolyte with Janus interfaces was utilized in a full cell with Li metal anode and NCM622 cathode, 89% capacity retention was achieved after 120 cycles with high CE (> 99.5%) at 60°C.

In order to improve the ability of polymer interphases to mechanically suppress the growth of dendrites, a cross-linked polymer was employed to modify a LATP ceramic electrolyte [298]. The polymer network was constructed by using PMEA, which contained a polyacrylate backbone that provided electrochemical stability and structural integrity, while the PEO side segments facilitated the transport of Li ions. In Li|LFP all-solid-state batteries, the PMEA–LATP electrolyte enable to measure high CE of 99.8–100% over 640 cycles.

Hybrid inorganic/polymer artificial SEIs were also applied in all-solid-state LMBs, motivated by the improvement of mechanical properties offered by the inorganic nanoparticles, while simultaneously creating a smoother transition layer with increased compatibility with inorganic electrolytes [299]. SiO_2 particles were treated with $CH_3O–(CH_2CH_2O)_x–(CH_2)_3Si(OCH_2CH_3)_3$ (PEG-silane) via a silanization reaction to form a hybrid coating for LICGC ($Li_2O–Al_2O_3–SiO_2–P_2O_5–TiO_2–GeO_2$) solid electrolyte. The PEO-based polymer chains grafted onto the nanoparticles thanks to the abundance of silanol groups on SiO_2. The 200 nm hybrid layer showed good adhesion and wettability, and decreased the interfacial resistance. By using excess amount of PEG-silane, the free polymer contributed to inhibiting the corrosion of LICGC by Li metal.

PVDF-based ASEIs showed good capability of stabilizing the performance of all-solid-state LMBs. A sandwiched composite electrolyte PVDF/LLTO-PEO/PVDF was reported, in which the PVDF layer prevented the reaction between LLTO and Li metal, and effectively suppressed the dendrite growth [300]. $LiClO_4$ was mixed with PVDF to exploit the strong interaction between PVDF and ClO_4^-, which resulted in high Li transference number (t_{Li+} =0.74). The sandwiched electrolyte enabled high cycling stability of a Li/LCO full cell for over 100 cycles at 2C. Aiming to improve the conductivity of the coating, a plasticized polymer ASEI was prepared by adding small amount of carbonate-based liquid electrolyte in a PVDF-HFP polymer matrix [301]. The plasticized polymer layer showed good ionic conductivity (5×10^{-4} S/cm) and wide electrochemical stability window of 0–4.5 V vs Li^+/Li. Such plasticized polymer layer was employed as ASEI between Li metal and the ceramic electrolyte $Li_7La_{2.75}Ca_{0.25}Zr_{1.75}Nb_{0.25}O_{12}$ (LLCZNO) and paired with an LFP cathode. The full cell showed high capacity (140 mAh/g at 1C) and stable cycling performance for over 70 cycles at room temperature.

3.5. Summary

Section 3 discussed macromolecular approaches to stabilize the interface between lithium anode and electrolyte for both liquid electrolyte-based and solid electrolyte-based LMBs. Crucial aspects of an ASEI paired with conventional liquid electrolytes are its mechanical properties and lithium ion transport properties. These features could be tuned by either directly employing polymers with target properties as ASEIs, or by employing reactive polymers that generate an ASEI with desired characteristic *in situ*, by reacting with lithium metal before or during cycling. Both mechanically strong polymer ASEIs with relatively high shear modulus and soft polymer ASEIs with elasticity or viscoelasticity were effective in suppressing lithium dendrites. To enhance the shear modulus of polymer-based ASEIs, mechanically strong additives were introduced, including organic fillers (e.g. Kevlar fiber), and inorganic fillers (e.g. SiO_2, Al_2O_3, YSZ, rGO, etc). RDRP has been used to graft polymer chains from the fillers, leading to further enhanced mechanical strength owing to the improved membrane uniformity. Soft polymer ASEI stabilized the anode/electrolyte interface by adapting to the sharp protrusions of lithium dendrites. Among the soft polymers utilized as ASEIs are PDMS, LiPAA, SBR, and networks with dynamic linkages, such as urea bonds with high density of hydrogen bonds, and borate or aluminate anionic centers with self-healing properties. Noticeably, the elastic LiPAA ASEI was formed by reacting PAA with lithium metal *in situ*, thus achieving better surface coverage and contact.

Desirable electrical properties of an ASEI include high dielectric constants, high and uniform ionic conductivity, and high transference number. Thus, ionically conductive polymers were used as ASEIs such as PEO, PAN, or *in situ* formed polyalkylethers. To further enhance their ionic conductivity, highly conductive lithium salts (e.g. Li_3PS_4), Lewis acid type metal oxides (e.g. YSZ), or non-conductive fillers with abundant polar functional groups (e.g. MOFs) were introduced in the polymer matrices. Fillers forming uniformly distributed nanochannels or polymers with high dielectric constant, such as PVDF, allowed for homogeneizing the ion flux on Li metal. ASEIs with high t_{Li+} were achieved by either using SLIC polymers (e.g. sulfonate-based or TFSI-based polyanions) or nanoporous polymers with an overlapped Debye screening length (e.g. PIM-1).

Some polymers simultaneously possess desirable mechanical and electrical properties. For examples, elastic LiPAA and aluminate-based dynamic networks are SLICs with high t_{Li+}, and polymer films with YSZ NPs result in high t_{Li+} due to the positive charges on the YSZ surface. Finally, ASEIs with high chemical and electrochemical stability were designed by using polymers with high chemical stability (e.g. PI), hydrophobic polyalkylethers with long alkyl segments that were formed during cycling from additives in the electrolyte, and reactive polymers bearing pendant cyclic ether groups that competed with the consumption of liquid electrolyte during cycling.

An alternate approach to stabilize the interface between lithium metal anode and liquid electrolyte consists of coating a commercial separator with a layer of functional polymers. The pore sizes and distributions, electrolyte wettability, and thermal stabilities of separators strongly affect the interface resistance and current distributions within the electrodes. Coatings for separator include biobased polymers (e.g. chitin), graphene or GO with high mechanical strength, covalently grafted PAM with high affinity for Li^+, polymer/inorganic composite layers with enhanced mechanical properties and ionic conductivity, and “soft ceramics” with high transference number comprising a microporous layer (e.g. PIM-1) and LiF.

Polymer ASEIs for solid-state batteries serve for improving the physical interfacial contact between solid electrolyte and metallic lithium, while reducing side reactions during cycling. This is especially important for ceramic electrolytes that have rough surface and poor stability against lithium metal, albeit high conductivity and transference number. Widely adopted polymers include PEO, PAN, PVDF, etc, due to their high flexibility, high conductivity and

high resistance to electrochemical reduction in the anode environment.

4. Polymer/lithium composite anode

The cycling stability of LIBs is partly due to the 3D porous anode structure that allows the lithium intercalation to reversibly take place within the entire electrode. In comparison, the electrolyte and interface engineering strategies developed to stabilize LMBs and described in previous sections only improve the lithium electrodeposition at the anode surface. Therefore, an approach that has the potential to improve the stability of LMBs, eventually making LMBs more stable than LIBs, consists of transforming the 2D structure of a typical lithium foil into a 3D composite structure with extra functionalities. The 3D anode consists of a 3D host material and lithium metal and could provide the following advantages: i) translocating the charge-transfer process to the entire 3D structure, reducing the local current density; ii) mitigating volume changes during Li plating/stripping, adding dimensional stability and eventually reducing the cell overpotential. Therefore, a 3D anode can improve both stability and safety of LMBs [302,303]. Typical 3D host materials include porous carbons [175,304,305], ceramics and metal oxides [185,306,307], and metal alloys including metal-coated scaffolds. [308–310] The use of polymer materials as hosts for 3D polymer/lithium anode is relatively new, despite polymer materials are commonly used in functional nanocomposites for numerous applications, including application as host for silicon anodes [311]. Polymer materials as 3D host for composite Li anodes are highly promising as i) polymers can be designed with abundance of functional groups to guide lithium transport; ii) they are lightweight, which is beneficial to the LMB energy density; iii) thermoplastics can be processed in a molten state at a temperature close or below the melting point of lithium; iv) flexible/flowable polymers improve the surface contact when pairing the composite anode with solid electrolytes. A few polymer/lithium composite anodes were reported in recent years for both liquid and solid electrolytes, showing impressive performances.

4.1. Polymer/lithium composite anode with liquid anode

Due to the abundance of lithiophilic functional groups, such as -OH, -COO-, -C≡N groups, porous polymer membranes can serve as host to form composite anodes whereby polymer functionalities guide the Li deposition. This strategy has the potential to be applied to “anode-free” LMBs, where lithium comes from a lithiated cathode, maximizing the cell energy density. A porous 3D oxidized PAN network was deposited on a Cu current collector. The network was created by electrospinning of a PAN/(polyvinylpyrrolidone) PVP mixture solution, followed by a thermal stabilization process to oxidize PAN and remove PVP. The latter contributed to modulating the fiber morphology to preserve the fiber uniformity during the thermal stabilization step, where PAN underwent a cyclization reaction to form a ladder structure with polar functional groups (C=N, C-N, C=O, O-H) [265]. These groups served as anchoring points to prevent Li ions from moving towards hot-spots, retarding the accelerated lithium plating, and thus reducing the dendrites formation (Fig. 14a). The composite anode enabled a CE of 97.4% over 120 cycles in an ether-based electrolyte at a current density of 3 mA/cm^2, for a total of 1 mAh/cm^2 of plated lithium per cycle [312].

A 3D crosslinked polyethylenimine (PEI) sponge with Li^+-affinity was developed and used as a lithium metal host by a combination of self-concentrating and Li^+-pumping features. The strong Li^+-affinity of the sponge concentrated Li ions in the internal electrode structure rather than in the bulk solution. Meanwhile, the electric double layer promoted electro-osmosis during Li plating/stripping, enhancing the ion-transport within the microporous structure (Fig. 14b). Such design reduced the concentration polarization, therefore uniform Li^+ distribution and dendrite-free Li plating/stripping at high current and deposition capacity (3.8 mAh/cm^2) was achieved, with 99.78% average CE and a practical negative to positive electrode capacity ratio (N/P) of 2 [313].

Liang et al, developed a simple rolling-cutting method to prepare nanoporous polyethylene (PEt)/lithium composite anode. A thin layer of polymer separator was placed tightly on top of lithium foil, which was then manually rolled into a cylinder and cut into round disks using a sharp blade, similar to the preparation of the food sushi (Fig. 14c). With such design, the porous separator could be embedded into the lithium matrix, forming alternating rings of lithium and ionically conducting polymer separator once wetted by the electrolyte. The cross-sectional area of the composite disk could be tuned by the rolling length and the block length of the lithium could be tuned by varying the thickness of initial lithium foil. Such composite anode could achieve a balance between reduced mossy lithium and increased side reactions – i) the 3D structure could reduce the actual areal current density and the chance of developing mossy lithium; ii) due to the use of micron-scale polymer separators and lithium foils, the enhanced surface area is lower than in the case of nanoscale porous host, thus reducing the extent of side reactions and formation of SEI between electrolyte and lithium. As a result, the mesoscale composite anode could be cycled for 200 cycles with low polarization under a high current density up to 5 mA/cm^2 [314].

4.2. Polymer/lithium composite anode with solid electrolyte

Polymer/lithium composite anodes can also improve the performance of LMBs with solid-state electrolytes. The high surface roughness of both conventional Li metal anodes and solid electrolytes can lead to high interfacial resistance, low areal capacity, and poor power output. Although coating Li metal with an inorganic layer, e.g. silicone, aluminum oxide, or zinc oxide, can increase the surface wettability to a certain extent, the rigidity of the layer can result in mechanical failures upon repeated volume changes at the anode. Therefore, the use of polymer materials as wetting agents to improve the surface contact is critical to improve the compatibility of Li metal anodes with solid electrolytes.

Liu et al. created a tri-layer architecture composed of molten lithium metal, layered rGO flakes and a flowable PEG interlayer (Fig. 14d). By contacting a densely packed GO film with molten lithium, a “spark reaction” happened that stretched the gaps between GO layers. The molten lithium was sucked into the interlayers via enhanced capillary forces. The remaining surface functionalities of rGO conferred lithiophilicity to the obtained composite anode. A flowable PEG/LiTFSI electrolyte was then thermally infused into the gaps of the Li/rGO composite. An all-solid-state LMB was constructed with the tri-layer anode, PEG/silica composite electrolyte, and LFP as cathode with high–mass loading. Satisfactory specific capacity (110 mAh/g) was obtained even at a rate of 5 C at 80°C, and a capacity retention of 93.6% was measured after 300 cycles at a current density of 3 mA/cm^2 [315].

Garnet-type electrolytes based on LLZO have high ionic conductivity and very high electrochemical stability against Li metal, however the insufficient interfacial contact with Li metal prevents their use under practical current densities [316]. Our group employed an *in-situ* emulsification approach to create uniformly dispersed lithium microparticles (Li MPs) in an electrically and ionically conductive polymeric media made of PEG, LiTFSI and conductive carbon (Fig. 14e) [21,317]. The resulting semiliquid lithium metal anode (SLMA) had a lithium content up to 40 vol%, with a theoretical

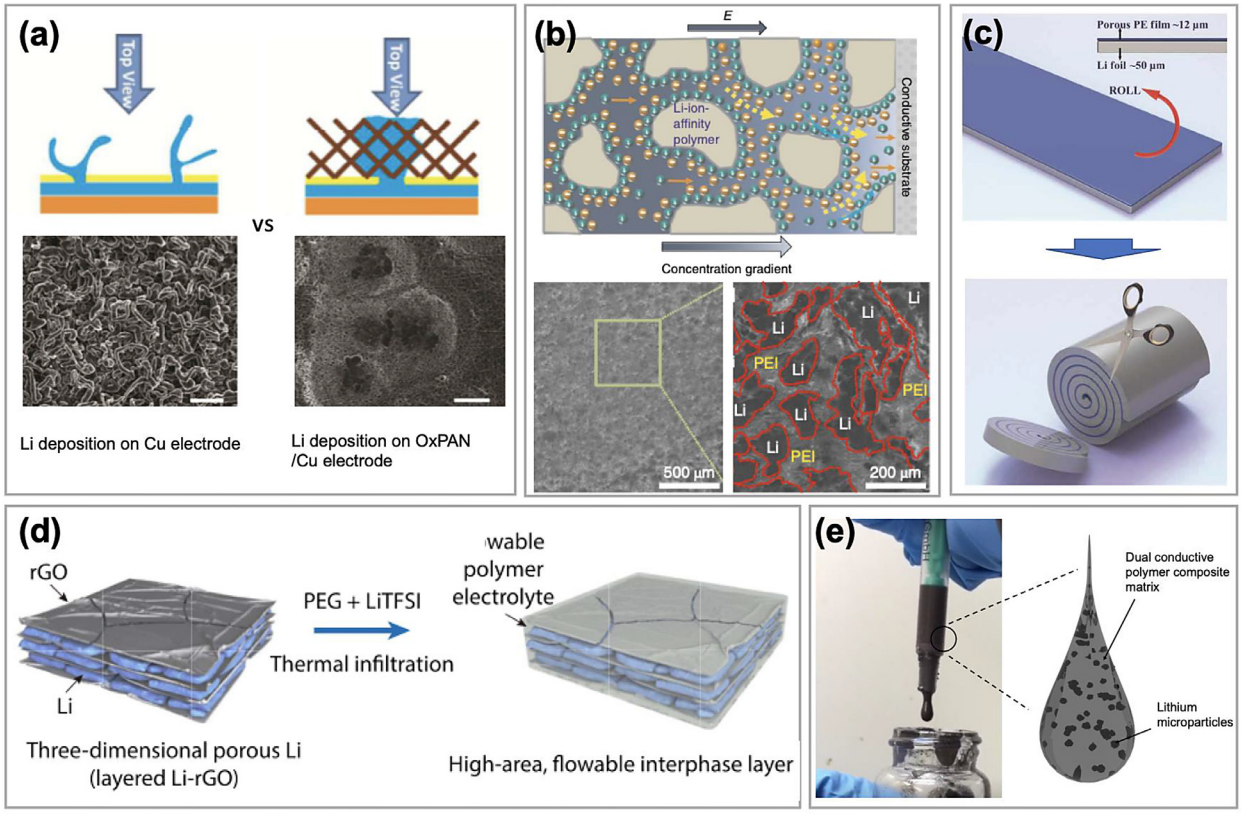

Fig. 14. (a) SEM images (scale bars of 20 μm) of the morphology of deposited lithium on a bare Cu current collector vs an oxidized PAN fiber network on Cu. The Li deposition was performed at a current density of 3 mA/cm^2 for a total deposited Li of 3 mAh/cm^2. [312], Copyright 2015. Reprinted with permission from American Chemical Society. (b) Up: illustration of electrokinetic phenomena in a 3D PEI sponge under an electric field. Cyan arrows represent electrokinetic surface conduction, yellow dashed arrows represent electro-osmosis and orange arrows represent the cations movement. Bottom: SEM images of surface morphology of the composite anode after Li deposition at a deposition capacity of 2 mAh/cm^2 and current density of 2 mA/cm^2. [313], Copyright 2018. Reprinted with permission from Springer Nature. (c) Illustration of fabrication of the PEt/Li composite anode through a rolling-cutting method. [314], Copyright 2019. Reprinted with permission from Springer Nature. (d) Picture of flowable semi-liquid lithium metal anode. [315], Copyright 2019. Reproduced with permission from AAAS. (e) Schematics illustrating the fabrication process of a semi-liquid lithium metal anode. [21], Copyright 2019. Reprinted with permission from Cell Press.

volumetric energy density of 800 mAh/cm^3, and exhibited liquid-like mechanical response even at room temperature. The SLMA enabled to cycle a symmetric cell with LLZO electrolyte for ~400 hours at a current density of 1 mA/cm^2 (1 h at each step) without observing polarization. Such phase–reverse design, i.e. from solid electrode and liquid electrolyte to liquid-like electrode and solid electrolyte, and the role of polymer materials in composite electrode preparation represent key steps in the development of safe LMBs [21]. Moreover, the Li MPs employed for SLMA could be extracted via a solvent-processed approach. The extracted Li powder was easily processed in a composite anode by blending with a conductive filler and polymer binders, thus through a manufacturing approach that resembles the traditional anode preparation approach in the LIB industry [317].

4.3. Summary

Section 4 discussed functional polymers that were employed as host materials for making polymer/lithium composite anodes paired with either liquid electrolytes or solid electrolytes. Porous polymer frameworks (e.g. PAN, PEI) with lithiophilic polar functionalities were used as guiding hosts, leading to homogeneous lithium deposition in an anode-free set up. Polymers with high electrolyte wettability, such as porous PEt membranes, were employed to fabricate a 3D structure with lithium metal, improving the surface contact between lithium metal and electrolyte, and lowering the local current density. Soft ionically conductive polymers, such as PEO, were used to create semi-liquid lithium metal anodes with enhanced ionic conductivity, that showed excellent performance in solid-state batteries.

5. Polymers for metal oxide cathodes

When considering LMBs at the cell-level, two categories of cathode materials are available: i) lithiated layered metal oxides, which are also adopted for LIBs, or ii) non-lithiated high-energy-density cathode materials such as sulfur or oxygen. Adopting layered metal oxides-based cathodes for LMBs has the advantage that the original production infrastructure inherited from the LIB industry can be preserved for LMBs production. Meanwhile, a LMB using similar electrolyte and cathode materials as a LIB can greatly increase pack-level energy density [318].

LCO was used in the first generation of LIBs commercialized by SONY, and still holds an edge over other cathode materials that have more rigid requirements for the voltage platform. However, the high amount of cobalt in LCO has urged to seek for a replacement of higher-capacity cathode with lower cobalt content. Promising lower-cost candidates are the nickel-rich NCM811 or a lithium-rich cathode such as $Li_{1.2}Ni_{0.2}Mn_{0.6}O_2$ (LNMO).

Polymers are widely used to improve the performance of metal oxide cathodes. The most common use of polymer materials is as cathode binders, responsible for integrating the active materials and conductive filler onto the current collector. Thus, the binder greatly affects the mechanic integrity of the electrode, its resistance and long-term stability. In addition, polymer coatings are often introduced in the cathode to minimize side reactions at the

cathode electrolyte interphase (CEI) and reduce the interfacial resistance. The following subsections present several applications of polymers as binders and artificial CEIs in LMB cathodes.

5.1. Polymer binders for metal oxide cathodes

Polymer binders are mixed with active materials and conductive fillers, such as carbon black (CB), and serve to integrate these components together, providing mechanical stability and promoting the adhesion of the electrode materials to the current collector. The binder affects various properties of the cathode, including dispersion and distribution of active materials and CB, electronic and ionic conductivity, porosity, and mechanical properties. Tremendous efforts were put into the development of effective binders, and the most reported materials include PVDF, poly(tetrafluoroethylene) (PTFE), carboxymethyl cellulose (CMC) [319–322], PEO [322,323], SBR [324], PAA [325,326], and polyacrylic rubber latex (LA132) and its derivatives [327]. Moreover, blends of two or more binders were employed to further increase the overall performance.

PVDF is the most widely used binder for metal-oxide cathodes in commercial LIBs, originally employed in the first lithium-ion cells commercialized by SONY. PVDF offers several advantages as binder for cathodes: i) electrochemical and chemical stability; ii) good bonding strength; iii) good mechanical strength. These advantages enable overall good electrode performance. However, there are several drawbacks associated with PVDF: i) in the cell manufacturing processes, N-methyl-2-pyrrolidone (NMPy) is generally used as a solvent to dissolve PVDF. This entails high cost, safety and environmental issues, and the critical need to control the relative humidity during the process (< 2%); ii) PVDF has low flexibility, which causes mechanical failure in the active materials upon volume changes during cycling, therefore deteriorating the cycle life of the battery; iii) PVDF degradation products contain unsaturated fluorinated compound (C=CF–) that can be hazardous to the health and environment [319].

In order to find a replacement for PVDF, other binders were investigated. CMC showed good performance as both a dispersing agent and thickener, capable of stabilizing the slurry and increasing the viscosity without substantially changing other properties. By applying CMC to an LFP cathode, CMC was able to improve the dispersion properties, while maintaining the long-term dispersing efficiency of LFP, due to the enhanced interaction with active material particles and adsorption onto these particles [328]. When applying CMC to LFP, the LMB displayed good performance for 1000 cycles, with an overall capacity fading of only 0.025% per cycle, a performance very close to PVDF-based electrodes [319]. CMC could also be used for a high voltage cathode (Li_2MnO_3–$LiMO_2$), up to at least 4.8 V [321]. The CMC-based electrodes showed superior cycling stability with less than 0.1% capacity fading per cycle, while a similar PVDF-based electrode showed 0.2% capacity fading per cycle. On the other hand, CMC also showed good thickening effect. In a comparison with hydroxypropylmethyl celluse (HPMC), an electrode slurry with HPMC displayed liquid-like behavior with poor electronic wiring, while the CMC-based electrode slurry displayed a solid-like behavior due to the buildup of a network bridged by CMC chains [322,329]. Finally, the use of CMC allows to prepare more compact cathodes, compared to PVDF.

In addition to the mechanical properties, binders also affect the electronic and ionic conductivity of the electrode. Guys et al. systematically investigated electronic transport properties of composite electrodes based on $Li_{1.2}V_3O_8$, CB, and PEO [330]. The measured conductivity followed a unique relationship, independent on the binder combination and the active materials presence, according to the relation: $\log\sigma = \log\sigma_c - b * \frac{\phi_{binder}}{\phi_c}$, where $\sigma_c$is the measured electronic conductivity of active materials, ϕ_c is the critical volume fraction for percolation of active materials and ϕ_{binder} is the binder volume fraction. The result suggested that the electronic transport happened via a tunneling mechanism through the insulating polymer layers in between conducting particles. Choi et al. [331] proposed that the binder helps increasing the amount of liquid electrolyte uptake into the electrode and the electrode ionic conductivity.

Combining different polymers together is an efficient way to maximize the functionality of binder materials. For example, ammonium polyacrylic acid (PAA-NH_4) and LA132 were combined as a binder system, in which PAA-NH_4 acted as dispersant in aqueous solution to help increasing the absorption of LA132 binder onto the cathode materials surface [332]. Scanning electron microscope analysis suggested that a LCO sheet prepared with LA132, in the absence of PAA-NH_4, had significant powder agglomeration and binder accumulation around the powder. These undesired coagulations were diminished by increasing the PAA-NH_4 content. Thus, the addition of PAA-NH_4 in the range of 0.01–0.02 wt% improved the LCO electrode capacity, rate capability and stability after cycling. Higher loadings of PAA–NH_4 could decrease the adhesion strength, electronic conduction, and overall electrochemical properties of LCO.

5.2. Polymer CEI for metal oxide cathodes

Layered metal oxides cathode materials include LCO, NCM ($LiNi_xCo_yMn_zO_2$ with x+y+z=1), and NCA. These materials have been widely used in commercial LIBs. Other promising metal-oxide based cathode materials such as Li-rich, cation-disordered rock-salt cathodes (e.g. $LiNi_{0.5}Mn_{1.5}O_4$ spinel cathode) [333], are able to deliver high energy density. For all these cathodes, one common issue is the occurrence of side reactions at the interface between cathode and electrolyte and the dissolution of active materials into electrolytes, which degrade the performance of the cathode in term of cycling stability and resistance. One effective strategy to tackle this problem is to apply a polymer coating as artificial CEIs on the particle surface of cathode active materials. It should be noticed that such polymer coatings on the cathode cover the surface of each secondary particle of active materials, while polymer-based coatings on Li metal anode (polymer ASEI, Section 3) typically cover the whole electrode surface.

Inorganic materials, such as Al_2O_3 and TiO_2, were used as coating for cathode active materials. However, polymer coatings offer several advantages compared to inorganics, such as facile control of coating thickness and homogeneity, and improvement of the electronic conductivity of the cathode. These benefits add to the general advantages of cathode active material coating, which include: i) mitigating side reactions between electrolyte and active materials; ii) improving the long-term stability of the active materials; iii) increasing the overall electrode conductivity. To be effective, polymer coatings should exhibit high ionic/electronic conductivity, chemical/electrochemical stability, continuous surface coverage, and mechanical flexibility. Common polymers employed as CEI coatings include poly(3,4-ethylenedioxythiophene) (PEDOT) [334–336,338,345], polyaniline (PANI) [337], carbonized PAN [343], polypyrrole (PPy) [344], poly(ethylene glycol diacrylate) (PEGDA) [342], polyimide (PI) [340,341], poly(N-vinylpyrrolidone) (PVP) [337] (Table 1). These polymers were selected primarily for their intrinsic electronic/ionic conductive properties that enhance the electrode conductivity. Additionally, these materials can be synthesized at low temperatures with simple procedures. One common approach to overcome the insufficient performance improvement achieved by using a single polymer coating consists of implementing a dual-phase coating that combines two polymers with complementary characteristics, thus meeting all requirements for effective coatings. However, some issues remain largely un-

Table 1
Polymers used as artificial CEIs for various layered metal oxide cathodes in LMBs.

Coating polymer	Active materials	Coating method	Thickness (nm)	Cycling voltage	Capacity retention/cycles/rate (Capacity retention without polymer CEI)	Ref.
PEDOT	$LiNi_{0.85}Co_{0.1}Mn_{0.05}O_2$	Solvent-free oCVD	20	2.7-4.3V	91%/100/0.1 C/ (54%)	[334]
PEDOT	$LiMn_2O_4$	Solvent-free oCVD	20	3.5-4.3V	84%/100/1 C (73%)	[335]
PEDOT-*co*-PEO	$LiNi_{0.6}Co_{0.2}Mn_{0.2}O_2$	Surfactant-free wet coating	11-18	2.8-4.3V	93.9%/100/0.5 C (89.3%)	[336]
PVP+ PANI	$LiNi_{0.8}Co_{0.1}Mn_{0.1}O_2$	Surfactant-induced wet coating	5-7	2.7-4.3V	88.7%/100/0.4 C (66.3%)	[337]
PEDOT:PSS	$Li_{1.2}Ni_{0.2}Mn_{0.6}O_2$	Surfactant-free wet coating	10-14	2.0-4.8V	51.6%/100/0.3 C (30%)	[338]
PEDOT	$LiNi_{0.5}Mn_{1.5}O_4$	*in situ* polymerization	< 10	3.5-4.9 V	90%/100/1 C (60%)	[339]
PI/PVP interpenetrating network	$LiCoO_2$	*Wet coating followed by in situ* polymerization	~5	3.0-4.4V	87%/80/0.5 C (38%)	[340]
PI	$LiCoO_2$	*in situ* polymerization	~10	3.0-4.4V	85%/50/0.5 C (75%)	[341]
PEGDA	$LiCoO_2$	*in situ* polymerization	~20	3.0-4.4V	88%/30/0.5 C (80%)	[342]
PAN	$LiCoO_2$	Wet coating followed by *in situ* crosslinking	~40	3.0-4.5V	95%//60/0.7 C (87%)	[343]
PPy	$LiCoO_2$	*in situ* polymerization	~20	3.0-4.5V	94.3%/170/0.2 C (83.5%)	[344]

solved: i) most coating methods do not offer delicate control over the coating thickness for both primary and secondary particles, resulting in coating inhomogeneity; ii) at high voltages (>4.8 V) many polymers exhibit poor oxidative stability.

Early works on polymer coating stemmed from the need of improving the conductivity of LFP cathodes. In 2007, a PPy/ferrocene polymer coating was first applied to LFP, obtaining greatly improved discharge capacity and rate capability in comparison to the control group using CB [346]. In the past 20 years, coating materials were greatly extended to other conductive polymers, and the purpose shifted from simply enhancing the conductivity of cathodes, to simultaneously mitigating side reactions at the cathode electrolyte interphase to improve the device long-term stability. PPy-coated LCO was prepared in the presence of sodium p-toluenesulfonate as dopant [344]. The capacity retention of the cathode increased from 52.4% without coating to 80.1% with coating. The long-term stability of the PPy-coated LCO was attributed to the continuous and thin PPy film that protected the cathode from the attack of HF, which originated from the decomposition of $LiPF_6$, especially under high temperature. Moreover, the coating suppressed the dissolution of Co into the electrolyte. PEDOT: poly(styrenesulfonate) (PSS) was applied to NCM111, and the morphology and performance were thoroughly investigated [347]. Several factors played a relevant role in the performance enhancement: i) the conducting polymer protected the transition metals from HF attack and/or undesired redox reactions with the electrolyte, suppressing the formation of LiF and Li_2CO_3, thereby offering better Li^+ diffusion pathways; ii) the coating helped the layer structured cathode maintaining the initial local atomic environment within the bulk electrode, which resulted in a lower voltage decay in the galvanostatic profile; iii) the coating suppressed the transformation of the cathode from a layered structure into a spinel/rocksalt structure, which typically creates a series of phase mismatches on charge–discharge cycles and is an inherent problem of layered oxide electrodes.

The ability of polymer coatings to mitigate side reactions at the interface is particularly important for cathodes that are operated under relatively high voltages, causing more side reactions to occur at the interface. PPy was applied onto $LiNi_{0.5}Mn_{1.5}O_4$ and the cathode was cycled in the voltage range between 3.5 V and 4.9 V [348]. When comparing with the cathode without coating, the coated cathode showed drastically improved long-term cycling stability (91% vs. 76.7% capacity retention after 300 cycles).

The difficulty in developing a polymer that satisfies all requirements of a good cathode coating prompt the use of multiple polymers as coating layers. PEDOT is known to have high electronic conductivity and good electrochemical stability (up to 4.6 V), but relatively low ionic conductivity. Therefore, PEDOT was combined with PEG that has high ionic conductivity [336]. The dual-conductive polymer coating showed superior performance than the sole PEDOT. The surface-modified NCM622 cathode using PEDOT-co-PEG showed higher discharge capacity (166.0 mAh/g) at 5C rate than the pristine cathode (145.8 mAh/g) and a PEDOT-coated cathode (159.3 mAh/g). The enhanced high-rate performance was attribute to the good mix of ionic and electronic conduction. Composites of lithium-rich $Li_{1.2}Ni_{0.2}Mn_{0.6}O_2$ and PEDOT:PSS were prepared via coprecipitation followed by a wet coating method [338]. The thicknesses of the polymer coating ranged between 5 and 20 nm. A composite with an optimal 3 wt% coating exhibited good rate capability and cycling properties, with excellent initial discharge capacity of 286.5 mAh/g at 0.1C and stable discharge capacity of 146.9 mAh/g at 1C for 100 cycles.

One important issue of polymer coatings is eventual thickness inhomogeneity, due to poor control over the synthetic conditions. This issue was typically addressed by using better surfactants or advanced synthetic routes. Uniform coatings of conductive PANI on the surface of NCM811 were obtained by pretreating NCM811 particles with PVP. Owing to the bonding tendency between the pyrrolidone rings of PVP and –NH– groups of PANI (Fig. 15a), the PANI layer could be uniformly anchored onto the surface of NCM811, with a thickness of 5-7 nm [337]. The hydrophobic surfactant cetyltrimethyl ammonium bromide (CTAB) was mixed with PEDOT in aqueous solution to provide a driving force to guarantee a uniform and conductive layer during the surface coating process [339]. While the use of a surfactant can provide good control over the homogeneity of the coating on secondary particles, it is harder to finely control the coating thickness over both primary and secondary particles. A protective and conductive PEDOT skin was built on a layered oxide cathode via oxidative chemical vapor deposition (oCVD), rather than by using a more conventional wet chemistry process. In the solvent-free process, $VOCl_3$ oxidizing vapors and the EDOT monomer were simultaneously introduced into a rotary reactor, and then adsorbed onto the NCM111 particles surface (Fig. 15b). Then, the film polymerized via oxidative step-growth polymerization. This method enabled to successfully create a PEDOT skin with uniform thickness on both secondary and primary particles of the layered oxide cathode materials (Fig. 15c). At 0.1 C rate, the capacity retention over 50 cycles was improved from 67.6% for bare NCM to 76.7%, 85.2%, 96.6% and 95.8% for the materials prepared with 20, 40, 60 and 80 minutes of oCVD, re-

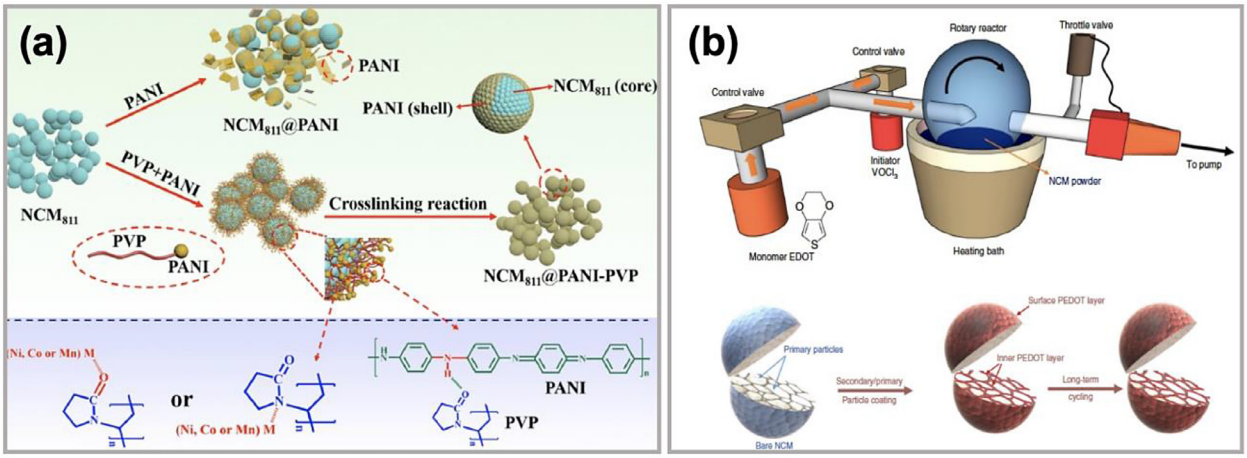

Fig. 15. (a) Schematic illustration of the preparation of NCM811@PANI−PVP, and possible reaction among NCM811, PVP, and PANI. [337]. Copyright 2019, Reproduced with permission from American Chemical Society. (b) A schematic diagram of the experimental oCVD setup for the in situ solvent-free polymerization on NCM secondary/primary particles surface, and illustration of the structural stability of both secondary/primary particles coating and secondary particles coating after long-term cycling [334]. Copyright 2019, Reproduced with permission from Springer Nature.

spectively. At the higher rate of 1 C, a more remarkable cycling stability enhancement was observed, from 47.7% for bare NCM after 200 cycles, to 79.1, 83.0, 91.1 and 89.5% for the coated cathodes with increasing preparation time. It is noteworthy that the capacity enhancement was achieved in a carbonate-based electrolyte without additives and with a high cut-off voltage (4.6 V). This exceptional cycling stability resulted from the ability of PEDOT skin to: i) suppress the undesired layered-to-spinel/rock-salt phase transformation; ii) mitigate intergranular and intragranular mechanical cracking; iii) stabilize the cathode electrolyte interface [334]. oCVD was also used to apply coatings on cathodes with higher energy density, such as layered Ni-rich $LiNi_{0.85}Mn_{0.05}Co_{0.1}O_2$ and Li-rich $Li_{1.2}Mn_{0.54}Ni_{0.13}Co_{0.13}O_2$, and demonstrated good performances [334].

5.3. Summary

Section 5 presented functional polymers applied as binders or artificial CEI coatings in LMBs with layered metal oxide cathodes. An effective binder increases the dispersion and distribution of active materials and conductive agents in the cathode, thus affecting its electronic and ionic conductivity and mechanical integrity. PVDF and PTFE are two of the most widely applied binder materials, due to their excellent electrochemical and chemical stability and bonding strength. However, the mechanical stiffness, fluorinated degradation products, and the use of organic solvents for processing entails for the development of new binder materials with optimal thickening and dispersing ability, good ionic conductivity, high electrolyte uptake and amenable of being processed in aqueous solutions. Such binder materials include CMC, PEO, PAA, and polyacrylic rubber latex. In addition, combinations of multiple binders can enhance the overall performances. Polymer CEIs help reduce interfacial resistance and side reactions, therefore improving the long-term stability of the active materials in the cathode. To be effective artificial CEIs, polymers should have good ionic/electronic conductivity, high chemical/electrochemical stability, and excellent surface coating ability and mechanical properties. Among the reported polymer CEIs are highly durable polymers (e.g. PI), ionically conductive polymers (e.g. PEO-based polymers) and electronically conductive polymers (e.g. PEDOT, PANI, PPy, carbonized PAN). In addition, physical blend of multiple polymers (e.g. PVP+PANI, PI+PVP) and block copolymers (PEDOT-*co*-PEO) were used to exploit their multiple functionality. Typical coating methods include surfactant-free wet coating, *in situ* solution polymerization/crosslinking, and solvent-free oxidative polymerization.

6. Polymers for sulfur cathode in Li-S batteries

Commercial cathode materials for LIBs are expected to soon reach their maximum capacity due to the limited number of crystallographic sites naturally available in these materials for the insertion and extraction of lithium ions. Li-sulfur is one of the most promising next-generation battery chemistries, providing a theoretical capacity of 1672 mAh/g. Key problems with Li-S batteries include: i) the formation of intermediate products (i.e. lithium polysulfides Li_2S_x) during cycling along with their formidable structural and morphological changes, which can lead to unstable electrochemical contact within the sulfur electrode; ii) Li_2S_x intermediates tend to dissolve in the electrolyte and shuttle between the anode and cathode during cycling, reacting with both the lithium metal anode and the sulfur cathode (i.e. the shuttle effect); iii) the high resistance of sulfur (σ ~10−30 S/cm) and of polysulfide intermediates, due to their insulating nature that can cause large polarization, reducing the energy efficiency of the battery and the utilization efficiency of active materials. Polymers were applied in the cathode of Li-S batteries as protective polymer coatings on sulfur particles, composite frameworks or binders. This section summarizes the opportunities provided by polymer materials in addressing the challenges of Li-S batteries. Three main approaches adopted in the implementation of polymer materials into S cathodes are presented: i) conductive polymer/sulfur composite, ii) organosulfide polymer composites, and iii) polymer binders.

6.1. Conductive polymer/sulfur composite cathodes

For the cathode in a Li-S battery, compositing conductive polymer provides the following advantages: i) it confines the sulfur active material, suppresses the shuttle effect and buffers the volume expansion of the cathode, increasing the utilization of active material and the stability; ii) it improves the electronic conductivity of the electrode and the sluggish kinetics caused by the insulating nature of S. The materials used as coatings range from inorganic ceramic oxides, to organic polymer materials and hybrid polymer/inorganic materials. The choice of conductive polymers include PPy, PANI, PEDOT [371], and poly(N-vinylcarbazole) (PVK) [372], etc. Factors affecting the performance of such composite cathode include electronic conductivity, electrochemical sta-

Table 2
Examples of conductive polymer/sulfur composite cathodes.

Materials	Composite Structure	Sulfur content (wt%)[a]	Sulfur mass loading (mg/cm^2)	Cycling performance (mAh g^{-1}/cycles/rate/voltage window)	Ref.
PPy/S/CB/PVDF	Layered	50	N/A	700/20/50mAg^{-1}/1.5-3.0 V	[349]
PPy/S/CB/PTFE	Tubular	37.3	4	525/2001 C/1.7-2.8 V	[350]
PPy/S/CB/PVDF	Core-shell	49	1.2-1.5	690/200/0.2 C/1.5-3.0 V	[351]
PPy/S/CB/PVDF	Tubular	~48	4	428/50/1 C/1.5-3.0 V	[352]
PPy/S/CB/PVDF	Core-shell	~46.2	N/A	400/50/1 C/1.5-2.8 V	[353]
PPy/MnO_2/S/CB	Core-shell	66	3	900/150/1 C/1.7-3.0 V	[354]
PPy/MnO_2/S/CB/PVDF	Tubular	52.5	2	550/500/1 C/1.5-3.0 V	[355]
PPy/S/graphene/CB/PVDF	Layered	52	1-3	698/500/0.5 C/1.7-2.8 V	[356]
PPy/S/PCN-224/CB/PVDF	Core-shell	60	0.8~1.4	670/200/10 C/1.8-2.7 V	[357]
PANI/S/C/CB/PTFE	Core-shell	30.59	0.9-1.2	405/200/10 C/1.0-3.0 V	[358]
PANI/S/CB/Sodium Alginate	Yolk-shell	46.4	N/A	628/200/0.5 C/1.5-3.0 V	[359]
PANI/S/Curved Graphene/CB/PVDF	Tubular	44	0.6-1.2	851/200/0.2 C/1.5-2.8 V	[360]
PANI/S/N-doped graphene/CB/PVDF	layered	42	N/A	693/100/0.5 C/1.4-3.0 V	[361]
PANI/S/CNT/PSS	Layered	67.5	1.85	818/600/0.3 C/1.0-3.0 V	[362]
PANI/S/C-NF	Tubular	67.1	2	711/300/0.2 C/1.7-2.8 V	[363]
PANI/S/CB/PVDF	Nanoporous	52	3.01	750/200/0.3 C/1.0-3 V	[364]
PEDOT:PSS/S/CB/PVDF	Layered	72	N/A	672/200/1 C/1.5-3.0 V	[365]
PEDOT/S/MnO_2/CB/PVDF	Core-shell	65.25	N/A	545/200/0.5 C/1.5-2.8 V	[366]
PEDOT/S/C-NT	Core-shell	49	1.1~1.47	532/200.0.5 C/1.5-3.0 V	[367]
PEDOT:PSS/S/rGO	Layered	56.4	2~3	~750/500/1 C/1.5-2.8 V	[368]
PEDOT/S/bacteria-derived carbon/graphene	Core-shell	63.3	N/A	482.1/1000/5 C/1.6-2.8 V	[369]
PEDOT/S/Prussian blue nanocube	Core-shell	66	N/A	544/200/5 C/1.8-2.8	[370]
PEDOT/S/CB/PVDF	Core-shell hollow sphere	54.6	1.5	860/300/0.2 C/1.7-2.6 V	[371]
PVK/S/CB/PVDF	Core-shell hollow sphere	49.56	1	687.7/200/0.5 C/1.0-3.0 V	[372]

[a] Including weight of conductive fillers and binders

bility windows, easiness and cost of synthesis, etc. Moreover, these polymers can form composite of different structures, such as planar [373], core-shell [353], yolk-shell [359], tubular [350], thus affecting the efficiency of coated cathode (Table 2).

PPy-based composite cathode. PPy is one of the most commonly used electronically conductive polymers for Li-S batteries. PPy can be polymerized by chemical oxidation [374], electrochemical polymerization [375], and emulsion polymerization [376]. Its good electronic conductivity provides the active material with additional conductive paths and the hydrogen bonds in PPy contribute to the interaction between sulfur molecules and polymer chains, thereby enhancing the cathode stability. A simple blend of PPy and sulfur (50 wt%) could deliver an initial discharge capacity of 1280 mAh/g and ~700mAh/g after 20 cycles at a current density of 50 mA/g [349]. More advanced structures could further improve the cycling performance. Core-shell structured PPy/S composite cathodes were prepared by adding sulfur to an aqueous solution containing decyltrimethylammonium bromide (DeTAB), a cationic surfactant that promoted the formation of nanosized spherical PPy. With this approach, PPy nanoparticles nucleated onto S particles and formed PPy shells. The core-shell structure of conductive PPy coating enabled fast and efficient transport of lithium ions and charge transfer within the electrodes. The composite delivered a capacity of ~700 mAh/g at the first cycle and 400 mAh/g after 50 cycle, under 1 C rate [353]. With PPy coated sulfur particles, an *in situ* reaction with potassium permanganate ($KMnO_4$) causes the formation of an interior thin layer of MnO_2 between the sulfur particles and the PPy outer layer, which can also generate thiosulfate groups by reacting with lithium polysulfide. The thiosulfate groups formed on the surface of MnO_2 were able to anchor long-chain polysulfides, significantly minimizing the shuttle effect. The multilayer core-shell composite enabled to use a binder-free cathode with a Coulombic efficiency as high as 98% and the self-discharge after 168 hours could be reduced from 34% to less than 9% [354]. The PPy/sulfur core-shell structure could also be created by a melting-diffusion strategy. Ultrathin wrinkled PPy hollow nanospheres were prepared via *in situ* polymerization of pyrrole, with Fe_3O_4 nanospheres as hard template. Composite PPy/sulfur cathode was made by infiltrating sulfur into the PPy nanosphere at 155 °C. Due to the synergistic effect of the ability of PPy to chemically bind to intermediate products and the high elasticity of the PPy sphere-shell structure that efficiently accommodated volume expansions, the composite cathode delivered an initial discharge capacity as high as 1500.5 mAh/g at 0.1C, and 690 mAh/g after 200 cycles [351]. Well-defined coaxial tubular sulfur/PPy composites were fabricated via a one-pot *in situ* disproportionation reaction method, resulting in thin layers of sulfur wrapping around PPy nanotubes. In these composites, the PPy nanotubes acted as a hollow conductive backbone that effectively facilitated the diffusion of electrolyte, and the ion and electron transport. The composite cathode with 53.3 wt% sulfur loading exhibited high initial discharge specific capacity of 1117 mAh/g with a remarkable cycling stability, retaining 692 mAh/g and 525 mAh/g capacity, after 200 cycles at a current density of 0.2C and 1C, respectively [350]. In a reverse tubular design, PPy was constructed outside tubular sulfur with MnO_2 as the intermediate layer. MnO_2 suppressed the shuttling effect while the PPy served as conducting framework. A stable CE of ~98.6% and a capacity decay rate of 0.07% per cycle within 500 cycles at 1C were achieved for S/PPy-MnO2 ternary electrodes with 70 wt%S and 5wt % MnO_2 [355].

Introducing a second porous host in addition to the conductive PPy is another viable option to achieve high-performance Li-S batteries. For example, PPy was coated around the surface of a sulfur/graphene aerogel composite via a vapor-phase deposition approach. The micropores and mesopores of the graphene aerogel provided high surface area, allowing to host high amount of sul-

fur and polysulfides, while preserving high internal conductivity. The use of vapor-phase deposition allowed for the monomer vapor to diffuse into otherwise inaccessible small pores, thus maximizing the effect of PPy polymer coating. Such PPy@S/graphene aerogel composite cathode delivered a specific capacity of 1167 and 409.1 mAh/g at 0.2 and 5 C, respectively, while maintaining a capacity of 698 mAh/g at 0.5 C after 500 cycles [356]. In addition, MOFs were employed as sulfur hosts. MOFs have high surface area and tunable polarity, allowing for fast ion diffusions and suppression of the shuttling effect. However, the limited electron transfer with MOFs limit their uses as electrode frameworks. By coating PPy around sulfur-hosted MOF frameworks, high ion and electron diffusion could be achieved. PCN-224 was chosen as a MOF framework, and the S/PCN-224 composite was prepared by a melt diffusion method. A PPy-coated S/PCN-224 composite cathode delivered an ultrahigh capacity of 670 and 440 mAh/g at 10C after 200 and1000 cycles, respectively [357].

PANI-based composite cathode. PANI was also extensively used as coating material for cathodes in Li-S battery due to its excellent electrochemical stability and conductivity. PANI can be synthesized by oxidation polymerization [377], interfacial polymerization [378], electrochemical polymerization [379], etc. A study into the effect of PANI coating on the sulfur cathode showed that the PANI-S composite containing 15 wt% of PANI delivered a capacity of 1134.01 mAh/g at the first discharge during cycling at 0.2 mA/cm^2. The capacity was much higher than that of bare sulfur, due to the enhanced conductivity of the cathode [380]. Similar to PPy, different design structures of PANI further improved the electrode performance. PANI-coated sulfur/CB (S/C) composites with core-shell structure were made via either ball-milling or thermal treatment of CB and sublimed sulfur, followed by in-situ oxidative polymerization of aniline in the presence of the S/C composite and ammonium persulfate. The cathode composite with 43.7 wt% sulfur showed excellent rate-capability with a maximum discharge capacity of 635.5 mAh/g under 10C rate. The improved performance was ascribed to the synergistic effect on the electrical conductivity from both the conductive CB in the matrix and the PANI on the surface [358]. While the core-shell structure can greatly enhance the rate capability of a S cathode, its ability to alleviate the volume expansion and enhance long-term cycling stability is limited. To solve this, S−PANI yolk−shell nanoarchitectures were synthesized via heating treatment of the core−shell composite. The capacity of Li-S batteries using yolk−shell S−PANI could be stabilized at 765 mAh/g at 0.2 C, while 635 mAh/g capacity was reached when using a core-shell structure. The advantage of the yolk−shell structure lies in the presence of internal void space to accommodate the volumetric expansion of sulfur during cycling, thus preserving the structural integrity of the shell while minimizing polysulfide dissolution [359]. PANI was also employed to form composites with conductive carbons of high surface areas, such as graphene [360,361], carbon nanotubes (CNTs) [362], and carbon nanofibers (C-NFs) [363], to form tertiary-phase composite cathodes with improved cycling performances (Table 2).

Another strategy to combine the advantages of different conductive polymers consists of designing and using copolymers. Qiu et al. copolymerized pyrrole with aniline to obtain P(Py-*co*-ANI) copolymer nanofibers, which were then used as coating materials for S cathodes. The copolymer coated cathode delivered a high initial discharge capacity of 1285 mAh/g, which remained at 866 mAh/g after 40 cycles. The enhanced performance if compared to PPy or PANI homopolymers suggested that combining the advantages of different polymers is a promising coating strategy [381].

PEDOT-based composite cathode. PEDOT possesses many advantages over other conductive polymers, such as high stability, moderate bandgap, and optical transparency. However, PEDOT has limited solubility in most solvents, and therefore it is often used together with polystyrene sulfonate to improve the solubility by forming PEDOT:PSS. PEDOT can be synthesized by oxidative polymerization or electrochemical polymerization [382,383]. An hydrothermal approach was adopted to uniformly mix PEDOT:PSS with sulfur microparticles, forming a simple PEDOT:PSS/sulfur nanocomposite with 90 wt% sulfur. Mixed with CB and PVDF, the composite cathode exhibited a initial discharge capacity of 897 mAh/g at 1 C and a capacity retention of 75% after 200 cycles [365]. S@PEDOT/MnO_2 dual-shell structure was made by coating sulfur nanoparticles with PEDOT through *in situ* polymerization, followed by *in situ* reduction of $KMnO_4$ on the PEDOT surface. The MnO_2 nanoshell functionalized on PEDOT provided a high active contact area to enhance the wettability of the electrode materials with electrolytes, and further interlink the polymer chains to improve the conductivity and stability of the composite. A composite cathode based on S@PEDOT/MnO_2 dual-shell structure exhibited an improved capacity of 545 mAh/g after 200 cycles at 0.5 C [366]. Similar to PPy and PANI, PEDOT was also used to coat sulfur composites with conductive hosts, such as C-NT [367], rGO [368], bacteria-derived N,P-doped carbon [369], or Prussian blue analogues [370], and demonstrated improved cycling performances.

Comparison of PPy, PANI and PEDOT. In order to understand the role and difference of PPy, PANI and PEDOT in a composite sulfur cathode, Li et al. investigated the performance of hollow sulfur spheres coated with the three conductive polymers. It was found that the conductivity greatly affected the rate performance of the electrode. The conductivity of the three polymers decreased in the order PEDOT > PPy > PANI. Ab initio simulations indicated that the binding energy between heteroatoms in the polymer and Li_xS decreased in the order PEDOT (1.22 eV) > PANI (0.67 eV) > PPY (0.64 eV), suggesting that PEDOT is the most efficient at reducing the diffusion of polysulfide, in addition to providing physical confinement. Long-term cycling test results showed that after 100 cycles of charge/discharge, a reversible capacity of 740, 885, and 1004 mAh/g was obtained for PANI-S, PPy-S, and PEDOT-S (capacity retention of 65%, 74%, and 86%), respectively [371].

6.2. Organosulfide polymer cathodes for Li-S batteries

The non-covalent composite/coating strategy discussed in the previous section implied physical incorporation of polymers directly into the sulfur cathode. While this strategy ensures good contact between coating and active materials during synthesis, the contact typically worsen during cycling due to the volume change of the materials. Therefore, a different strategy was explored consisting of the copolymerization of linear polysulfur with polymerizable linkers to form organosulfide polymers that resulted in improved electrochemical performances of Li-S batteries. Typically, functional polymers were anchored to sulfur with strong chemical bonds by heating at ~200°C, where radical insertion of ring opened sulfur diradical sulfur within polymers takes place to form stable heteroatom/S bonds [384]. During the discharge process, Li_2S and short insoluble lithium polysulfide were generated and formed carbon conjugated bonds, rather than longer lithium polysulfides upon continuous breakdown of C–S bonds. The final discharge product was a mixture of the conjugated polymer backbone and Li_2S. In the charging step, the conjugated polymer backbone trapped Li_2S with delocalized radical cations and led to the growth of cyclic sulfur. The absence of long chain lithium polysulfides during cycling contributed to long-term stability of the sulfur cathodes, minimizing the shuttle effect.

When compared to non-covalent cathode composites, organosulfide frameworks have the following benefits: i) lower synthetic temperature and simpler synthetic methods; ii) providing a confining effect for S and intermediate products during cycling

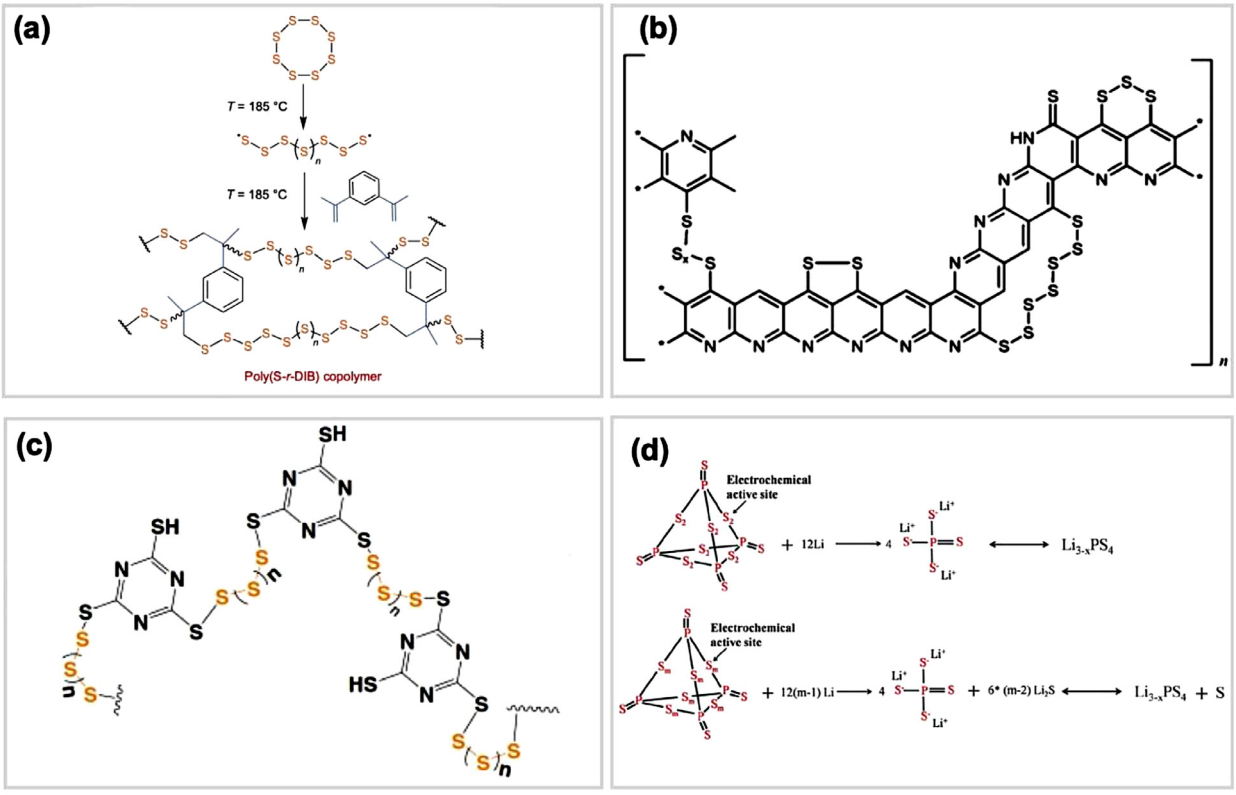

Fig. 16. (a) Synthetic scheme of copolymerization of S8 with DIB to form organosulfide polymer composite [386]. Copyright 2013, Reproduced with permission from Springer Nature. (b) Proposed structure of SPAN, containing all relevant functional groups ($0 < x < 6$; $y = 1,2$) [387]. Copyright 2011, Reproduced with permission from American Chemical Society. (c) Proposed structure of three-dimensionally interconnected sulfur-rich polymers [388]. Copyright 2015, Reproduced with permission from Springer Nature.(d) Schematic of the electrochemical active sites of P_4S_{16}, and P_4S_{4+6m} (m>3) [389] and their corresponding electrochemical reaction. Copyright 2017, Reproduced with permission from Wiley-VCH.

by interchain or intrachain bonding; iii) alleviating the volume change of the cathode during cycling due to the soft nature of the polymer with good resilience. In general, organosulfide polymer composites include unsaturated hydrocarbon-derived organosulfide, nitrile-derived organosulfide, thiol-derived organosulfide, and phosphorous-derived organosulfide [385].

In 2013, Cheng, et al. reported the direct copolymerization of molten liquid sulfur with 1,3-diisopropenylbenzene (DIB) through radical polymerization (inverse vulcanization) to form poly(S-*co*-DIB) (Fig. 16a) [386,390]. Such polymer exhibited an initial specific discharge capacity of 1100 mAh/g and a long-term cycling performance of 823 mAh/g at 100 cycles at a rate of C/10, which is superior to pure S_8 and represented the highest value for polymer-based sulfur cathodes reported to date. A similar approach was used to copolymerize S_8 with an ionic liquid based crosslinker,1-vinyl-3-al-lylimidazolium bromide (DVIMBr), to form poly(S-*co*-DVIMBr) [391]. The introduction of imidazolium-based ion pairs served to further anchor intermediate polysulfide while improving the ionic conductivity within the electrode. The Li–S cell with poly(S-co-DVIMBr) cathode showed high capacity retention of 90.22 % over 900 cycles.

PAN is the most commonly used nitrile source to form nitrile-derived organosulfur polymers. These materials were generally prepared by heating a mixture of sulfur and PAN powders at elevated temperatures of around 280-450°C under inert gas for 6 h, to form unsaturated chains with conjugated electrons. During the process, sulfur triggers the dehydrogenation of PAN, in which the CN group is cyclized and generates a thermally stable heterocyclic compound with embedded sulfur. Although both sulfur and PAN are non-conductive materials, the as-formed S/PAN material exhibited a high electrical conductivity of 10^4 S/cm, which increased the utilization efficiency of sulfur active materials. Moreover, the formation of the framework structure contributed to achieving higher sulfur loading. Noticeably, polymerization of PAN could be well controlled by RDRP [392–394], resulting in porous polymer and nanocarbons with promising electrochemical properties when doped with hetero atoms [265,395,396].

Sulfur−polyacrylonitrile composite (SPAN) was first applied as a cathode in a Li-S battery by Wang et al. in 2003 and delivered a specific capacity of 1000 mAh/g, using a 65 wt% sulfur content [397]. The author proposed that at 300 °C the highly-polarized -CN groups cyclized and formed a compound with intercalated sulfur. Subsequent structural analysis of SPAN suggested that in all composites sulfur was covalently bound exclusively to carbon, and the short -S_x- chains were covalently linked to the dehydrogenated and cyclized PAN backbone [387,398]. Moreover, N−C−S fragments from 2-pyridylthiolates were identified, as well as S_x ($x \geq 2$) and thioamide fragments (Fig. 16b). Wei et al. [399] reported a facile approach to create a family of SPAN nanocomposites in which sulfur was maintained as S_3/S_2 during all stages of the redox process. The composite preparation exploited specific interactions between the nitrile groups on the polymer backbone and sulfur to promote ring formation and dehydrogenation. By entrapping relatively small molecular sulfur species in the cathode through covalent bonding and physical confinement in a polymer host, the cathode materials exhibited excellent long-term stability, due to the elimination of polysulfide dissolution and shuttling between lithium anode and sulfur cathode. The Li-S battery delivered ~1000 mAh/g capacity even after cycling for over 1000 cycles at 0.4 C (1 C = 1675 mA/g). The capacity degradation/fade upon repeated

cycles of charge/discharge was only 0.027% per cycle. Heteroatom doped sulfur-rich copolymers can improve the electron conductivity of sulfur, enhance the adsorption of sulfur to the carbon host and facilitate the formation of low-order lithium polysulfides. Different heteroatom doping brings different effects on the composite properties through different mechanisms. Selenium (Se)-doped SPAN cathode showed excellent electrochemical performance, such as high reversible capacity of 1300 mAh/g at 0.2 A/g rate, and less than 15% capacity fading after 800 cycles [400]. The good performance was explained by the high lithium ion diffusion coefficient and relatively low polarization due to the chemical similarity of Se with sulfur, but higher electronic conductivity. This further resulted in rapid conversion of polysulfide intermediates and fast reaction kinetics, which in turn prevented the dissolution of polysulfide intermediates in the electrolyte.

Thiol-derived organosulfide polymers are a favorable alternative for synthesizing sulfur-enriched copolymers. The typical synthesis involved the ring-opening polymerization of sulfur and thiol-containing polymers at elevated temperatures (>180°C). Trithiocyanuric acid crystals were employed as soft template for the ROP along the thiol surfaces to create 3D interconnected sulfur-rich phases, as shown in Fig. 16c [388]. This unique strategy offered better control over the shape and morphology when compared with other reported vulcanized polymers. The cathode had relatively high sulfur mass loading (> 60%), and displayed a discharge capacity of 945 mAh/g after 100 cycles at 0.2C with high-capacity retention of 92%. The materials showed excellent rate capability: 872 mAh/g at 1C, 803 mAh/g at 3C and 730 mAh/g at 5 C. The superior rate capability was ascribed to the ordered Li-ion coordination sites of organic crystals, allowing the seamless transport of Li-ion into the active materials.

For organosulfide polymers, increasing the sulfur loading can have risks: i) it can decrease the electronic conductivity and efficiency in active material utilization; ii) it can decrease the long-term stability as some free sulfur can be present, instead of being chemically bound to or physically confined into the framework. To tackle the issues associated with increased sulfur loading, an orthogonal synthetic approach was employed for the preparation of sulfur-impregnated benzoxazine polymers [401]. The polymerization of benzoxazine was performed via ROP, while sulfur was incorporated independently via a vulcanization reaction, utilizing the thiol functionality of benzoxazine. Thus, sulfuric chains were covalently linked to the polymer matrix through the thiol groups. This approach enabled to achieve a sulfur loading of ~72 wt% along with a homogeneous distribution of sulfur within the polymer composite. The electrode showed superior long-term cycling performance, with 92.7% capacity retention after 1000 cycles. This work indicated that appropriate monomer and composite design can provide increased and practical sulfur loading while maintaining high performance.

Sulfur-rich phosphorus sulfide molecules (P_4S_{10+n}) were synthesized through the reaction between sulfur and P_4S_{10} (Fig. 16d) at elevated temperature, whereby small polysulfide diradicals react to form of P_2S_5 [389]. When used as cathode materials, initial discharge capacity of 1223 mAh/g was achieved at 100 mA/g, which stabilized at approximately 720 mAh/g after 100 cycles. This new class of P-S molecules pave the way to novel S composite cathodes with high energy density and high stability at room temperature.

Despite the good reported performances, organosulfide polymer composites leave room for further improvement. The sulfur loading required for practical application, > 4 mg/cm^2, remains to be achieved without penalizing other properties, such as conductivity. Another challenge is improving the long-term cycling stability hampered by interactions between polysulfides and the polymer matrix. More efforts are necessary to: i) improve the synthesis of organosulfur copolymers by proper selection of monomers with functional groups and better design of the structure/framework; ii) introduce heteroatoms into copolymers in order to improve the conductivity and number of sulfur anchor sites for higher loading.

6.3. Polymer binders for Li-S batteries

Polymers are commonly used as binders for Li-S battery. In this type of battery chemistry, the binder should buffer the volume expansion of electrode materials and limit the shuttle effect of intermediate products during cycling, in addition to the typical roles of binders in LIBs. Hence, polymer binders play a crucial role in regulating the Li-S cell performance, especially the cycle life. Additionally, binders should be i) insoluble in the electrolyte to maintain the structural integrity of the cathode, but they should swell in the electrolyte solution to promote the transport of Li ions to the electroactive material during charge/discharge; ii) both chemically and electrochemically stable during cell operation, within the potential window. Examples of polymer binders employed for improving the performance of Li-S batteries are reported in Table 3. The use of polymer binders in sulfur cathodes generally follows two approaches: i) using crosslinked networks as binders able to integrate the electrode materials, in order to increase the sulfur loading to meet the requirement for practical application (> 4 mg/cm^2); ii) using multi-functional binders. High S loading normally results in thicker electrodes, which can raise kinetics issues in mass transport and rate capability. In contrast, multi-functional binders serve as ionic/electronic conductors to improve the kinetics. Finally, efforts are devoted to developing eco-friendly and cost-efficient binders, in particular water-based binders.

On the basis of the solvent used, there are three types of binders: organic-solvent-based [402–408,413,414], water-based [409–411,415–418], and ionic-liquid-based [412] binders. Within organic-solvent-based binders, PVDF is the most widely used polymers for traditional metal oxide cathodes. However, applying PVDF to sulfur cathodes have a detrimental effect on device performance for two main reasons: i) when PVDF is dissolved in NMPy it can infiltrate the pores and dramatically reduce the surface area and pore volume available to the electrolyte during operation, therefore decreasing the utilization of active materials [404]; ii) PVDF lacks functional groups capable of binding to polysulfides. In contrast, water-based binders are advantageous in terms of cost, safety and environmental-friendliness. Moreover, water-based binders generally contain a large number of polar groups that increase the affinity for polysulfides. Commercially available water-based binders were investigated in Li-S batteries, including PEO, CMC, LA132, PAA, cyclodextrin, alginate, gum, and their derivatives [409–411,415–418].

Employing electron-rich functional groups is critical for suppressing the polysulfide shuttle-effect. PSS containing sulfonic acid groups helped confining the active materials during cycling, thanks to the strong electronegativity of the functional groups [413]. The capacity retention for the cell with PSS binder was 74.4% at 200 mA/g after 100 cycles, while 46.9% capacity was retained using a PVDF binder. An amino functional group-based binder was synthesized by reacting hexamethylene diisocyanate with PEI [419]. The composite materials possessed abundant amine groups and exhibited a hyperbranched network structure, which provided strong affinity to polysulfide intermediates. This unique feature contributed to the remarkably improved cycling performance with a capacity retention of 91.3% over 600 cycles at 2 C. A binder with strong hydrophilic character was obtained by crosslinking of poly(ethylene glycol) diglycidyl ether (PEGDGE) with PEI [407]. The Li-S battery using this binder showed superior long-term cycling performance with a discharge capacity of 430 mAh/g after 400 cycles under 1.5C. *In situ* micro-Raman characterizations suggested that the material effectively suppressed the dissolution of polysul-

Table 3
Examples of polymer binders employed in sulfur cathodes.

Processing solvent	Polymers	Binder (wt%)	Sulfur content (wt%)[a]	Sulfur mass loading (mg/cm^2)	Cycling performance (mAh g^{-1}/cycles/rate/voltage window)	Ref.
organic	Maleate-PEO	10	80	12	488/100/0.2 C/1.7-2.8 V	[402]
organic	Polyacrylate latex (PAL)	10	58.32	1.5	800/100/0.1 C/1.8 V-2.8 V	[403]
organic	PVDF	15	70.6	1	800/80/0.1 C/1.8 V- 2.6 V	[404]
organic	PAA + rGO	10	~60	0.8	635/100/0.5 C/1.7 V-3.0 V	[405]
organic	Crosslinked CMC	10	77	5.2-14.9	~1100/100/0.5 C/1.9-2.8 V	[406]
organic	Glycidol-modified PEI	10	48	1.2~1.5	430/400/1.5 C/1.5-3.0 V	[407]
Aqueous	Polysaccharide+glyco-proteins	20	44	4.8	841/500/0.2 C/1.8-2.6 V	[408]
Aqueous	DAA+SBMA+ PEGMA	8	56	9.7	674.2/350/0.5 C/1.7-2.8 V	[409]
Aqueous	PEO+ PVP	10	~50	0.5-0.8	800/200/1 C/1.8-2.6 V	[410]
Aqueous	CMC+SBR	10	~60	N/A	580/60/0.3 C/1.0-3.0 V	[411]
Ionic liquid	PAA+ PVDF	10	~80	2.7	590/100/0.3 C/1.7-2.7 V	[412]

[a] including weight of conductive fillers and binders

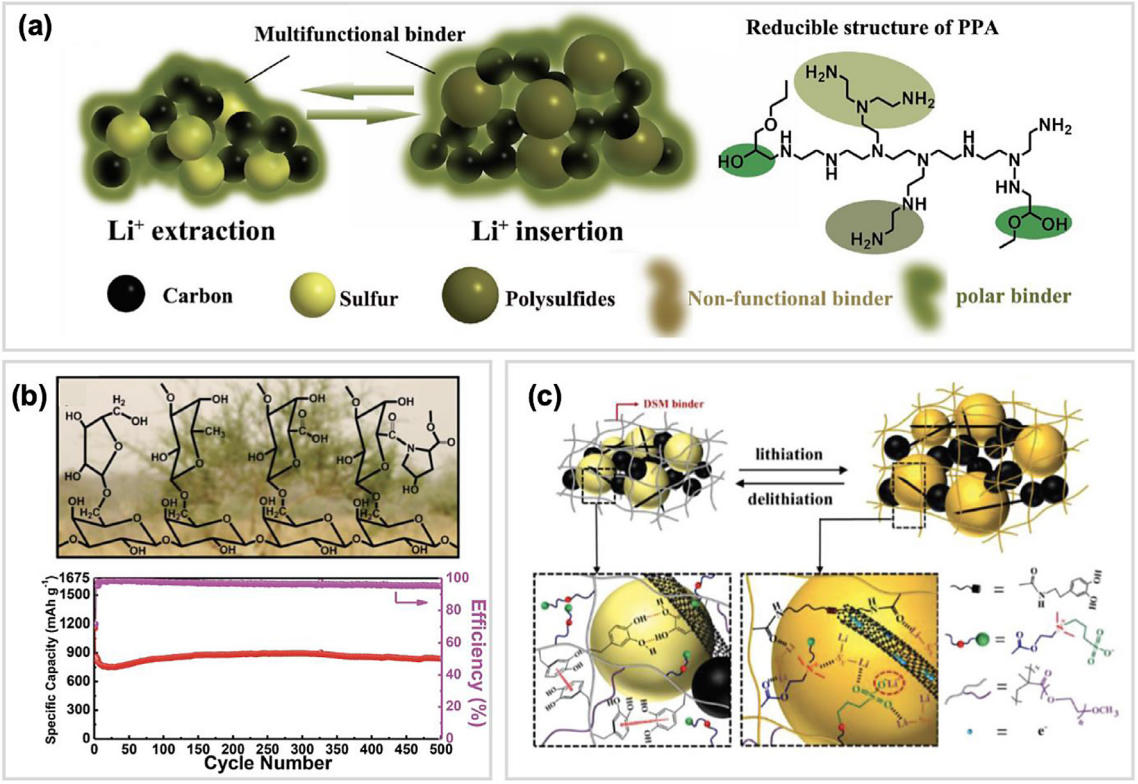

Fig. 17. (a) Schematics of the binder with abundant amino and amide groups and its reducible molecular structure [407]. Copyright 2018, Reproduced with permission from Wiley-VCH. (b) Proposed chemical structure of Gum Arabic [408] and long-term test when used in Li-S battery. Copyright 2015, Reproduced with permission from Wiley-VCH (c) Illustration of the interactions inside the 3D network binder. [409]. Copyright 2019, Reproduced with permission from Wiley-VCH

fides because only a weak mid-chain Li_2S_4 Raman signal was detected. Moreover, the binder exhibited abundant Li-N, Li-O, and S-O bonds (Fig. 17a), leading to significant improvements in capacity retention.

Other works focused on improving the binder electronic/ionic conductivity. Binders with high conductivity can: i) integrate the electrode together, ii) confine the shuttle effect of intermediate products, and iii) provide electronic/ionic conductive path/matrix. Polypyrrole-polyurethane (PPyPU) nanocomposites were synthesized by *in situ* emulsion polymerization of Py within a polyurethane continuous phase [414]. PPy suffers from a brittle nature, therefore the addition of elastomeric polyurethane contributed to creating a flexible electrode formulation. The benefits of this nanocomposite for flexible energy storage were two folds. First, the highly conjugated PPy nanoparticles formed an electrically percolating network within the PU matrix. Second, the elastomeric PU matrix accommodated the severe volume expansion of sulfur that can compromise the structural integrity of electrodes during cycling and negatively impact the long-term cycling performance. The sulfur cathode with PPyPU binder showed no evident capacity fade for 100 cycle. Moreover, the robust cathode remained operational after 50 bend/rolling cycles, indicating possible usage in wearable devices.

To meet practical application requirements, cathodes must have high sulfur loading. However, this causes high polarization, polysulfide redistribution and insufficient electronic conductivity inside the thick electrode. These challenges can be alleviated by appropriate binder design. Cross-linked CMC binders facilitated the formation of a hierarchical structure in the form of micro-particles and assisted the interparticle physical binding and electrical con-

nection [406]. By employing this binder, a sulfur mass loading up to 14.9 mg/cm^2 was obtained and the cathode showed very stable cycling over 80 cycles. A bifunctional binder with a linear PEI chain and maleate-capped ends provided flexibility within a high-loading cathode (sulfur loading of 12 mg/cm^2 and high sulfur content of 80 wt%) [402]. The maleate ends improved the polysulfide trapping ability by forming carbon−sulfur bonds. After cycling at 0.2 C for 200 cycles, the cathode showed 200 mAh/g higher capacity than the cathode made with PVDF binder.

The use of a blend binder system that combines two or more polymer generally enabled superior performance than the individual components, by combining the advantages of each polymer. For example, a mixture of SBR and CMC was used, aiming at exploiting the high flexibility and strong binding force of SBR, and the effective dispersion and thickening ability of CMC in aqueous suspensions, due to its two functional groups, i.e. carboxylate and hydroxyl groups [411]. The mixture binder resulted in high specific capacity of 580 mAh/g after 60 cycles, surpassing the performance of a PVDF binder (370 mAh/g). In blend binders, the optimization of the weight ratio of different components is necessary, as the composition affects the sulfur loading, mixing, rate capability, and cycling limits. For example, Lacey et al. [410] investigated the effect of various ratios (1:1, 7:3, 9:1) of PEO to PVP when applying their mixture as binder in sulfur cathodes. This binder system combined the complementary benefits of faster reactions of polysulfides and enhanced capacity attributed to PEO and improved capacity retention due to PVP. The mixtures with higher PEO content showed better rate capacity and long-term cycling stability, while the mixtures with higher PVP content generally showed higher capacity. Therefore, the composition of blend binder system should be carefully tuned depending on the properties of individual components and the desired performance.

In addition to conventionally used polymers, novel synthetic polymers with complex functionalities and architectures offer the possibility of achieving both high interaction with active materials and high sulfur loading. Gum Arabic (GA) was employed as low cost, nontoxic, and sustainable natural polymer derived from Acacia Senegal [408]. GA is a complex mixture of polysaccharides and glycoproteins, which provide abundant hydroxyl groups and long polymer chains (Fig. 17b). These structural features offered i) high binding strength enhancing the mechanical stability, ii) suitable ductility to buffer the volume change of sulfur and iii) ability to mitigate the shuttling effect of the polysulfides due to the confinement effect of functional groups. Therefore, the sulfur cathode using GA as binder showed: i) high sulfur loading, (75 wt%); ii) high capacity (initial capacity of 1386 mA/h); iii) high stability, 841 mAh/g capacity after 500 cycles. Bioinspired water-soluble 3D network binders were synthesized by one-step free radical polymerization of N-(3, 4-dihydroxyphenethyl) acrylamide (DAA), 2-methacryloyloxy ethyl dimethyl-3-sulfopropyl ammonium hydroxide (SBMA), and PEGMA (Fig. 17c) [409]. The presence of O atoms and N^+ sites provided anchoring sites for lithium polysulfides during cycling by forming Li-O and N^+- S_x^{2-} bonds, alleviating the shuttle effect. In addition, the abundant negatively charged sulfonate sites contributed to high electronic and ionic conductivities. As a result, a Li-S battery with 6 wt% binder in the cathode exhibited outstanding cycling performance for over 350 cycles at 1 C, with ultralow capacity fade rate of 0.005% per cycle. By introducing a quaternary ammonium cation into a β-cyclodextrin polymer, a new multifunctional aqueous polycation binder (β-CDp-N^+) for the sulfur cathode was prepared [415]. The unique hyperbranched network structure of the β-CDp-N^+ helped enduring the mechanical stress from large volume changes of sulfur particles during charge/discharge. The numerous hydroxyl and ether groups and quaternary ammonium cations contributed to enhancing the interactions between active materials, conductive additives and immobilizing polysulfides. Even with high sulfur loading of 5.5 mg/cm^2, the cathode with the hyperbranched binder delivered an areal capacity of 4.4 mAh/cm^2 at 50 mA/g after 45 cycles, which was much higher than that achieved using the cathode with a conventional PVDF binder (0.9 mAh/cm^2).

6.4. Summary

Section 6 discussed the applications of functional polymers in S cathodes, which include: i) conductive polymer/sulfur composite cathodes, ii) organosulfide composite cathodes, and iii) polymer binders. Compositing electronically conductive polymers with sulfur has the benefits of reducing the interface resistance while confining polysulfide intermediates. Electronic conductivity, mechanical properties, electrochemical stability and bonding energy between the polymer and polysulfides are critical in the selection of conductive polymers. Commonly adopted conductive polymers include PPy, PANI, PEDOT, and PVK. Composite cathodes can be made by *in situ* polymerization of monomers on the surface of sulfur particles or by melt-infusing sulfur into existing porous polymer hosts. MnO_2 was employed as extra functional layer, to anchor long-chain polysulfides by reacting with sulfur to generate thiosulfates. Conductive porous carbons (e.g. graphene, CNT, C-NF) and porous MOFs were employed as a second host to improve sulfur uptake and bulk conductivity. The composites can be constructed with different structures, including layered, tubular, and core-shell structures.

Sulfur can also be copolymerized with functional polymers to form organosulfide polymer cathodes. Compared to non-covalent composites of sulfur and polymers, organosulfide cathodes have the advantage of confining intermediates through interchain and intrachain interactions. Organosulfide polymer cathodes can be formed with various functional polymers to obtain unsaturated hydrocarbon-derived organosulfide polymers, nitrile-derived organosulfide polymers, thiol-derived organosulfide polymers, phosphorous-derived organosulfide, etc.

In Li-S batteries, polymer binders buffer the volume expansion of the cathode and limit the shuttle effect of intermediate products, in addition to performing the typical tasks of binders in LIBs. Polymers with electron-rich functionalities containing heteroatoms as O, N, halogen (e.g. PSS, PEI, PEO, etc) were generally employed to suppress the shuttle effect. Conductive polymers functionalized with mechanically strong polymer segments (e.g. PPy-*co*-PU) were used to improve the electronic conductivity without decreasing the mechanical integrity. Polymer binders with complex architectures (e.g. crosslinked, hyperbranched) and functionalities having high electronegativity were employed to improve the sulfur loading. In order to simultaneously achieve suppression of shuttle effect and high sulfur loading, binders based on polymer blends, complex architecture and multifunctionalities were employed.

7. Conclusions and perspectives

7.1. Conclusions

Polymer materials have different roles in rechargeable LMBs, spanning from (quasi)solid-state electrolytes and electrode coatings (i.e. artificial SEI), to binders, coatings and frameworks for active materials in the electrodes. Therefore, the ability to engineer polymer structures and functionalities is key to the fabrication of safe and high-energy-density LMBs.

While liquid organic carbonates or ethers are the electrolytes of choice for LIBs, they are not ideal for lithium metal anodes. In the past decades, many efforts were put into the design of non-flammable polymer electrolytes that can prevent dendrite growth and eliminate the hazards associated with the commercial volatile

and flammable liquid electrolytes. PEO remains the most common polymer for SPEs, however its crystallinity, low t_{Li+}, and poor stability at high voltages promoted the use of other polymers, including polycarbonates, poly(ionic liquids), and polymeric charge-transfer complexes. Morphology, composition, architecture, and functional groups of these polymer electrolytes could be largely tuned, thanks to the progress in various polymerization and post-polymerization chemistries, including controlled polymerization methods. As a consequence, SPEs can exhibit room temperature conductivity of $\sim 10^{-4}$ S/cm, with oxidative stability approaching 5V. Conductivity values exceeding 10^{-3} S/cm were achieved by introducing plasticizers or functional fillers, to form gel or composite polymer electrolytes, respectively. In addition, the Li transference number and mechanical properties of polymer electrolyte are widely tunable. Single-ion conducting PEs have t_{Li+} close to unity, while crosslinked PEs have high shear modulus, and they can further display self-healing ability thanks to the introduction of dynamic bonds. Recent developments include the design of sustainable PEs that can be degraded and/or employs bio-based monomers, and the use of *in situ* polymerizations to lower manufacturing costs and improve electrode/electrolyte interfacial contact.

When a conventional organic carbonate electrolyte is used in an LMB, a passivating layer forms between the anode and the electrolyte during cycling. Its poor flexibility and homogeneity make it vulnerable to volume changes at the electrode and promote dendrite growth. In the past decade, polymer artificial solid electrolyte interphases were developed to improve the interfacial stability. Mechanical and electrochemical properties are crucial for effective ASEIs. High shear modulus polymer ASEIs can physically resist the amplification of surface roughness, and viscoelastic polymers can adapt to surface changes. Polymer ASEIs should have not only high ionic conductivity, but also high transference number and promote uniform transport of Li^+. Inorganic functional fillers were added to polymer ASEIs to improve their performance. Reactive polymers were used to ensure on-site formation of highly homogeneous and robust ASEIs, competing with detrimental side-reactions during cycling. Polymer interlayers were also applied on the surface separators or solid electrolytes to enhance interfacial stability and contact.

The “hostless” nature of conventional lithium foil leads to severe volume changes during cycling. Therefore, hosting lithium metal within a polymer matrix dramatically reduced volume fluctuations. At the same time, 3D polymer networks with lithiophilic functional groups improved the homogeneity of the Li^+ flux during stripping/plating, decreasing concentration polarization, and therefore minimizing the formation of dendrites. On the other hand, the commercialization of all-solid-state LMBs is severely limited by the poor interfacial contact between lithium metal and solid-state electrolytes. A recently proposed paradigm shift in battery research employed soft polymers to form semi-liquid Li anodes that achieved good interfacial contact with solid electrolytes, relieving volume changes and increasing active material utilization.

In addition, polymers are crucial components of cathode materials, particularly for high-energy layered metal oxide cathodes, and sulfur cathodes in Li-S batteries. Polymer binders improved the homogeneity of active material distribution, enhancing the adhesion between active material, eventual additives, and current collector, while increasing electronic and ionic conductivity. Polymer coatings on cathode active materials could enhance the conductivity and cycling stability by minimizing side reactions with the electrolyte. In Li-S batteries, polymer binders and coatings further prevented the shuttling of polysulfides. This detrimental phenomenon was also contained by designing sulfur/polymer composite cathodes. Recent efforts were directed to the development of eco-friendly and low-cost procedures to prepare cathodes avoiding toxic solvents that are typically employed for commercial LIBs.

7.2. Perspectives

In order to power electric vehicles and electronics with LMBs, it remains necessary to enhance the cycle life and reliability of these devices, under practical operating conditions, including high current densities, significant stresses and broad temperature ranges. To achieve a cell-level specific capacity of $>$ 500 Wh/Kg for a LMB that employs a NCM622 cathode and a liquid electrolyte, several requirements should be met, such as an electrolyte to capacity ratio under 2.4 g/Ah, a cathode porosity of $<$25% with a capacity of $>$ 250 mAh/g, and N/P $\sim$1 [19]. Therefore, the synergistic optimization of all cell components is crucial. Polymer materials can have beneficial impact on all cell components and on a high-energy LMB as a whole. Although valuable progress was achieved in the design of polymers for electrolytes, interlayers and electrodes, further challenges associated with materials preparation and practical applications remain to be addressed.

1. Compared to convention liquid electrolyte, most SPEs have 1-2 order of magnitudes lower conductivities. In order to achieve conductivities of $>$ 1 mS/cm^2 at room temperature, one promising strategy is to decouple the ionic conduction from polymers segmental motion. The ionic conductivity of SPEs is inversely proportional to their thickness, therefore it is important to control the thickness during manufacturing and achieve sufficiently low thickness for high-energy-density devices. While introducing challenges in the SPE preparation method, the design of thin polymer membranes must not sacrifice their mechanical strength. Furthermore, it remains challenging to develop SPEs with sufficient anodic and cathodic stability for highly oxidative and reducing electrode environments. Finally, simple synthetic approaches are needed for large-scale production with minimized batch-to-batch variations and reduced costs.
2. Several functionalities were demonstrated to improve the properties of polymer-based ASEIs, therefore multifunctional polymer materials should be designed to simultaneously increase the uniformity of ion transport, and the chemical and mechanical stability. Similar to the case of SPEs, facile manufacturing and reduced batch-to-batch variations in polymer synthesis and coating techniques are essential for commercialization. Moreover, the thickness of the ASEI and thus its weight should be considered and minimized, to avoid that the introduction of a protective coating results in a decrease of the cell-level energy density. Moreover, advanced characterization tools must be used to observe the evolution of ASEIs during cycling to guide the design of better coatings. In addition, more efforts are needed toward the development of ASEIs paired with solid electrolytes, toward the commercialization of high-energy all-solid-state LMBs.
3. The use of polymers as framework for anode active materials is nascent and promising. The poor (electro)chemical stability of several polymers in contact with Li anodes requires to develop innovative strategies toward stable polymer networks and to analyze the composition and nature of polymer degradation products. When employed with liquid electrolyte, polymer frameworks could be swelled by the electrolyte, resulting in a deterioration of their mechanical properties. Crosslinked polymers have the potential to form stable and robust composite anodes.
4. Current research on binders for cathode is largely focused on commercially available polymers. Altering the nature, composition, and morphologies of cathode binders can provide materials that exhibit sufficient mechanical strength, (electro)chemical

stability, and ionic/electronic conductivity. Importantly, high-performing water-soluble binders are urgently needed to eliminate the use of toxic NMP in the cathode slurry preparation.

5. The development of polymer coatings for cathode active materials with sufficiently high ionic and electronic conductivity remains a challenge. In addition, it is necessary to finely control the coating thickness and homogeneity. The covalent grafting of polymers chains on inorganic nanoparticles has emerged as a promising strategy to design superior hybrid materials with high homogeneity and tunable properties. Therefore, the modification of cathode active particles by grafting polymer chains onto their surface could effectively improve cathode stabilities and performance, and prevent cracking of secondary particles during cycling. Moreover, coating primary particles should be targeted to further enhance battery performance.
6. Another important application of polymers in cathode materials concern the use of redox active polymers/monomers as high-energy cathodes for direct energy storage, which have emerged as a promising area that require expertise from both polymer science and electrochemistry [420–422].
7. The integration of battery research and manufacturing with robotic automation could greatly improve the speed of experimental work and innovation. Moreover, experimental efforts to discover new materials for LMBs should be complemented by computational screening, using density functional theory and molecular dynamics, and developing predictive algorithms through machine learning to accelerate the design and deployment of safe LMBs.

Finally, as the market shares of secondary batteries continue to increase, the recycling of battery components becomes increasingly important. Therefore, bio-based and degradable or recyclable polymers needs to be employed or designed to improve the sustainability of the battery industry. Advanced polymerization and post-polymerization processes and characterization techniques have led to considerable progress in the development of polymer materials for high-energy-density Li metal batteries, which have the potential to soon enable urgently needed breakthroughs in energy storage.

Declaration of Competing Interest

The authors declare that they have no known competing financial interests or personal relationships that could have appeared to influence the work reported in this paper.

Acknowledgments

Mateusz Olszewski is sincerely acknowledged for his contributions to the graphic design;

Support from NSF (DMR 1501324) is gratefully acknowledged.

References

[1] Naber JD, Johnson JE. 8 - Internal combustion engine cycles and concepts. In: Alternative Fuels and Advanced Vehicle Technologies for Improved Environmental Performance. Woodhead Publishing; 2014. p. 197–224.
[2] Goodenough JB, Park K-S. The Li-ion rechargeable battery: a perspective. J Am Chem Soc 2013;135:1167–76.
[3] Hoekstra A. The underestimated potential of battery electric vehicles to reduce emissions. Joule 2019;3:1412–14.
[4] Stephan AK. The Age of Li-Ion Batteries. Joule 2019;3:2583–4.
[5] Whittingham MS. History, evolution, and future status of energy storage. Proc IEEE 2012;100:1518–34.
[6] Whittingham MS. Electrical energy storage and intercalation chemistry. Science 1976;192:1126–7.
[7] Mizushima K, Jones PC, Wiseman PJ, Goodenough JB. LixCoO2 (0<x<-1): a new cathode material for batteries of high energy density. Mater Res Bull 1980;15:783–9.
[8] Yoshino A. 1 - Development of the lithium-ion battery and recent technological trends. In: Lithium-Ion Batteries. Amsterdam: Elsevier; 2014. p. 1–20.
[9] Rahman MA, Wang X, Wen C. High energy density metal-air batteries: a review. J Electrochem Soc 2013;160:A1759–A1A71.
[10] Liu Z, Yu Q, Zhao Y, He R, Xu M, Feng S, et al. Silicon oxides: a promising family of anode materials for lithium-ion batteries. Chem Soc Rev 2019;48:285–309.
[11] Chae S, Choi S-H, Kim N, Sung J, Cho J. Integration of graphite and silicon anodes for the commercialization of high-energy lithium-ion batteries. Angew Chem Int Ed 2020;59:110–35.
[12] Lopez J, Mackanic DG, Cui Y, Bao Z. Designing polymers for advanced battery chemistries. Nat Rev Mater 2019;4:312–30.
[13] Goodenough JB, Kim Y. Challenges for rechargeable Li batteries. Chem Mater 2010;22:587–603.
[14] Etacheri V, Marom R, Elazari R, Salitra G, Aurbach D. Challenges in the development of advanced Li-ion batteries: a review. Energy Environ Sci 2011;4:3243–62.
[15] Lin D, Liu Y, Cui Y. Reviving the lithium metal anode for high-energy batteries. Nat Nanotech 2017;12:194.
[16] Blomgren GE. The development and future of lithium ion batteries. J Electrochem Soc 2017;164:A5019–A5A25.
[17] Lu Y, Rong X, Hu Y-S, Li H, Chen L. Research and development of advanced battery materials in China. Energy Storage Mater 2019.
[18] Xie Z, Wu Z, An X, Yue X, Wang J, Abudula A, et al. Anode-free rechargeable lithium metal batteries: progress and prospects. Energy Storage Mater 2020;32:386–401.
[19] Liu J, Bao Z, Cui Y, Dufek EJ, Goodenough JB, Khalifah P, et al. Pathways for practical high-energy long-cycling lithium metal batteries. Nat Energy 2019;4:180–6.
[20] Xu W, Wang J, Ding F, Chen X, Nasybulin E, Zhang Y, et al. Lithium metal anodes for rechargeable batteries. Energy Environ Sci 2014;7:513–37.
[21] Ren X, Zou L, Cao X, Engelhard MH, Liu W, Burton SD, et al. Enabling high-voltage lithium-metal batteries under practical conditions. Joule 2019;3:1662–76.
[22] Yu Z, Cui Y, Bao Z. Design principles of artificial solid electrolyte interphases for lithium-metal anodes. Cell Rep Phys Sci 2020;1:100119.
[23] Quartarone E, Mustarelli P. Electrolytes for solid-state lithium rechargeable batteries: recent advances and perspectives. Chem Soc Rev 2011;40:2525–2540.
[24] Manthiram A, Yu X, Wang S. Lithium battery chemistries enabled by solid-state electrolytes. Nat Rev Mater 2017;2:16103.
[25] Karayaylali P, Tatara R, Zhang Y, Chan K-L, Yu Y, Giordano L, et al. Editors' choice—coating-dependent electrode-electrolyte interface for Ni-rich positive electrodes in Li-ion batteries. J Electrochem Soc 2019;166:A1022–A1A30.
[26] Chen W, Lei T, Wu C, Deng M, Gong C, Hu K, et al. Designing safe electrolyte systems for a high-stability lithium–sulfur battery. Adv Energy Mater 2018;8:1702348.
[27] Bruce PG, Freunberger SA, Hardwick LJ, Tarascon J-M. Li–O2 and Li–S batteries with high energy storage. Nat Mater 2011;11:19.
[28] Schubert US, Zechel S. The year of polymers –100 years of macromolecular chemistry. Macromol Rapid Commun 2020;41:1900620.
[29] Nicolas J, Guillaneuf Y, Lefay C, Bertin D, Gigmes D, Charleux B. Nitroxide–mediated polymerization. Prog Polym Sci 2013;38:63–235.
[30] Lindmark-Hamberg M, Wagener KB. Acyclic metathesis polymerization: the olefin metathesis reaction of 1,5-hexadiene and 1,9-decadiene. Macromolecules 1987;20:2949–51.
[31] Breslow DS. Metathesis polymerization. Prog Polym Sci 1993;18:1141–95.
[32] Wang J-S, Matyjaszewski K. Controlled/"living" radical polymerization. atom transfer radical polymerization in the presence of transition-metal complexes. J Am Chem Soc 1995;117:5614–15.
[33] Matyjaszewski K, Xia J. Atom transfer radical polymerization. Chem Rev 2001;101:2921–90.
[34] Chiefari J, Chong YK, Ercole F, Krstina J, Jeffery J, Le TPT, et al. Living free-radical polymerization by reversible addition−fragmentation chain transfer: the RAFT process. Macromolecules 1998;31:5559–62.
[35] Finn MG, Sharpless KB. Click chemistry: diverse chemical function from a few good reactions. Angew Chem 2001;40 2004-+.
[36] Hoyle CE, Bowman CN. Thiol–Ene click chemistry. Angew Chem Int Ed 2010;49:1540–73.
[37] Moorhouse AD. The growing applications of click chemistry. Chem Soc Rev 2007;36:1249–62.
[38] Hein JE, Fokin VV. Copper-catalyzed azide–alkyne cycloaddition (CuAAC) and beyond: new reactivity of copper(i) acetylides. Chem Soc Rev 2010;39:1302–15.
[39] Laurichesse S, Avérous L. Chemical modification of lignins: towards biobased polymers. Prog Polym Sci 2014;39:1266–90.
[40] Braunecker WA, Matyjaszewski K. Controlled/living radical polymerization: f eatures, developments, and perspectives. Prog Polym Sci 2007;32:93–146.
[41] Dechy-Cabaret O, Martin-Vaca B, Bourissou D. Controlled ring-opening polymerization of lactide and glycolide. Chem Rev 2004;104:6147–76.
[42] Perrier S, Takolpuckdee P. Macromolecular design via reversible addition–fragmentation chain transfer (RAFT)/xanthates (MADIX) polymerization. J Polym Sci, Part A: Polym Chem 2005;43:5347–93.
[43] Matyjaszewski K, Tsarevsky NV. Nanostructured functional materials prepared by atom transfer radical polymerization. Nat Chem 2009;1:276–88.
[44] Lutz J-F, Ouchi M, Liu DR, Sawamoto M. Sequence-controlled polymers. Science 2013;341:1238149.

[45] Han J, Li S, Tang A, Gao C. Water-soluble and clickable segmented hyperbranched polymers for multifunctionalization and novel architecture construction. Macromolecules 2012;45:4966–77.
[46] Zheng Y, Li S, Weng Z, Gao C. Hyperbranched polymers: advances from synthesis to applications. Chem Soc Rev 2015;44:4091–130.
[47] Li S, Han J, Gao C. High-density and hetero-functional group engineering of segmented hyperbranched polymers via click chemistry. Polym Chem 2013;4:1774–87.
[48] Yan J, Bockstaller MR, Matyjaszewski K. Brush-modified materials: control of molecular architecture, assembly behavior, properties and applications. Prog Polym Sci 2020;100:101180.
[49] Barbey R, Lavanant L, Paripovic D, Schüwer N, Sugnaux C, Tugulu S, et al. Polymer brushes via surface-initiated controlled radical polymerization: synthesis, characterization, properties, and applications. Chem Rev 2009;109:5437–527.
[50] Förster S, Antonietti M. Amphiphilic block copolymers in structure-controlled nanomaterial hybrids. Adv Mater 1998;10:195–217.
[51] Rao JP, Geckeler KE. Polymer nanoparticles: preparation techniques and size–control parameters. Prog Polym Sci 2011;36:887–913.
[52] O'Reilly RK, Hawker CJ, Wooley KL. Cross-linked block copolymer micelles: functional nanostructures of great potential and versatility. Chem Soc Rev 2006;35:1068–83.
[53] Huang X, Qi X, Boey F, Zhang H. Graphene-based composites. Chem Soc Rev 2012;41:666–86.
[54] Liaw D-J, Wang K-L, Huang Y-C, Lee K-R, Lai J-Y, Ha C-S. Advanced polyimide materials: syntheses, physical properties and applications. Prog Polym Sci 2012;37:907–74.
[55] Xu Y, Jin S, Xu H, Nagai A, Jiang D. Conjugated microporous polymers: design, synthesis and application. Chem Soc Rev 2013;42:8012–31.
[56] Dawson R, Cooper AI, Adams DJ. Nanoporous organic polymer networks. Prog Polym Sci 2012;37:530–63.
[57] Mecerreyes D. Polymeric ionic liquids: broadening the properties and applications of polyelectrolytes. Prog Polym Sci 2011;36:1629–48.
[58] Whittell GR, Hager MD, Schubert US, Manners I. Functional soft materials from metallopolymers and metallosupramolecular polymers. Nat Mater 2011;10:176–88.
[59] Matyjaszewski K. Adv mater by atom transfer radical polymerization. Adv Mater 2018;30:1706441.
[60] Li S, Lorandi F, Whitacre JF, Matyjaszewski K. Polymer chemistry for improving lithium metal anodes. Macromol Chem Phys 2019;221:1900379.
[61] Zhang C, Jin T, Cheng G, Yuan S, Sun Z, Li N-W, Yu L, Ding S. Functional polymers in electrolyte optimization and interphase design for lithium metal anodes. J Mater Chem A 2021;9:13388–401.
[62] Sun Y. Lithium ion conducting membranes for lithium-air batteries. Nano Energy 2013;2:801–16.
[63] Yi J, Guo S, He P, Zhou H. Status and prospects of polymer electrolytes for solid-state Li–O2 (air) batteries. Energy Environ Sci 2017;10:860–84.
[64] Lai J, Xing Y, Chen N, Li L, Wu F, Chen R. Electrolytes for rechargeable lithium–air batteries. Angew Chem Int Ed 2020;59:2974–97.
[65] Zhang P, Ding M, Li X, Li C, Li Z, Yin L. Challenges and strategy on parasitic reaction for high-performance nonaqueous lithium–oxygen batteries. Adv Energy Mater 2020;10:2001789.
[66] Wang H, Wang X, Li M, Zheng L, Guan D, Huang X, et al. Porous materials applied in nonaqueous Li–O2 batteries: status and perspectives. Adv Mater 2020;32 2002559.
[67] Zhou J, Cheng J, Wang B, Peng H, Lu J. Flexible metal–gas batteries: a potential option for next-generation power accessories for wearable electronics. Energy Environ Sci 2020;13:1933–70.
[68] Li J, Cai Y, Wu H, Yu Z, Yan X, Zhang Q, et al. Polymers in lithium-ion and lithium metal batteries. Adv Energy Mater 2021;11:2003239.
[69] Costa CM, Lizundia E, Lanceros-Mendez S, Lanceros-Méndez S. Polymers for advanced lithium-ion batteries: State of the art and future needs on polymers for the different battery components. Prog Energy Combust Sci 2020;79:100846.
[70] Yin H, Han CJ, Tang YB, Yin H, Han C, Liu Q, et al. Recent Advances and Perspectives on the Polymer Electrolytes for Sodium/Potassium-Ion Batteries. Small 2021:2006627.
[71] Zhao QL, Whittaker AK, Zhao XS, Zhao Q, Whittaker A, Zhao X. Polymer electrode materials for sodium-ion batteries. Materials 2018;11:2567.
[72] Yang MM, Shu XX, Zhang JT, Yang M, Shu X, Pan W, et al. Toward flexible zinc–air batteries with self-supported air electrodes. Small 2021:2006773.
[73] Chen XC, Zhou Z, Chen Y, Chen X, Zhou Z, Karahan HE, et al. Recent advances in materials and design of electrochemically rechargeable zinc–air batteries. Small 2018;14:1801929.
[74] Xu CX, Yang YL, Ma JM, Xu C, Yang Y, Wang H, et al. Electrolytes for lithium- and sodium-metal batteries. Chem Asian J 2020;15:3584–98.
[75] Wong DH, Thelen JL, Fu Y, Devaux D, Pandya AA, Battaglia VS, et al. Nonflammable perfluoropolyether-based electrolytes for lithium batteries. Proc Natl Acad Sci 2014;111:3327–31.
[76] Zhou D, Shanmukaraj D, Tkacheva A, Armand M, Wang G. Polymer electrolytes for lithium-based batteries: advances and prospects. Chem 2019;5:2326–52.
[77] Tikekar MD, Choudhury S, Tu Z, Archer LA. Design principles for electrolytes and interfaces for stable lithium-metal batteries. Nat Energy 2016;1:1–7.
[78] Xia S, Wu X, Zhang Z, Cui Y, Liu W. Practical challenges and future perspectives of all-solid-state lithium-metal batteries. Chem 2018.
[79] Zhao Q, Stalin S, Zhao C-Z, Archer LA. Designing solid-state electrolytes for safe, energy-dense batteries. Nat Rev Mater 2020;5:229–52.
[80] Wang X, Kerr R, Chen F, Goujon N, Pringle JM, Mecerreyes D, et al. Toward high-energy-density lithium metal batteries: opportunities and challenges for solid organic electrolytes. Adv Mater 2020;32:1905219.
[81] Monroe C, Newman J. The impact of elastic deformation on deposition kinetics at lithium/polymer interfaces. J Electrochem Soc 2005;152:A396.
[82] Huo H, Liang J, Zhao N, Li X, Lin X, Zhao Y, et al. Dynamics of the garnet/li interface for dendrite-free solid-state batteries. ACS Energy Lett 2020;5:2156–64.
[83] https://ionicmaterials.com/the-solution/, 2021.
[84] Zhu J, Zhu P, Yan C, Dong X, Zhang X. Recent progress in polymer materials for advanced lithium-sulfur batteries. Prog Polym Sci 2019;90:118–163.
[85] Mindemark J, Lacey MJ, Bowden T, Brandell D. Beyond PEO—alternative host materials for Li+-conducting solid polymer electrolytes. Prog Polym Sci 2018;81:114–43.
[86] Tikekar MD, Archer LA, Koch DL. Stabilizing electrodeposition in elastic solid electrolytes containing immobilized anions. Sci Adv 2016;2:e1600320.
[87] Choudhury S, Vu D, Warren A, Tikekar MD, Tu Z, Archer LA. Confining electrodeposition of metals in structured electrolytes. Proc Natl Acad Sci 2018;115:6620–5.
[88] Berthier C, Gorecki W, Minier M, Armand M, Chabagno J, Rigaud P. Microscopic investigation of ionic conductivity in alkali metal salts-poly (ethylene oxide) adducts. Solid State Ion 1983;11:91–5.
[89] Nie K, Wang X, Qiu J, Wang Y, Yang Q, Xu J, et al. Increasing Poly(ethylene oxide) Stability to 4.5 V by Surface Coating of the Cathode. ACS Energy Lett 2020;5:826–32.
[90] Mecerreyes D, Porcarelli L, Casado N. Innovative Polymers for Next-Generation Batteries. Macromol Chem Phys 2020;221:1900490.
[91] Panday A, Mullin S, Gomez ED, Wanakule N, Chen VL, Hexemer A, et al. Effect of Molecular Weight and Salt Concentration on Conductivity of Block Copolymer Electrolytes. Macromolecules 2009;42:4632–7.
[92] Young WS, Kuan WF. Epps III TH. Block copolymer electrolytes for rechargeable lithium batteries. J Polym Sci B Polym Phys 2014;52:1–16.
[93] Phan TN, Issa S, Gigmes D. Poly (ethylene oxide)-based block copolymer electrolytes for lithium metal batteries. Polym Int 2019;68:7–13.
[94] Shah NJ, Dadashi-Silab S, Galluzzo MD, Chakraborty S, Loo WS, Matyjaszewski K, et al. Effect of Added Salt on Disordered Poly(ethylene oxide)-Block-Poly(methyl methacrylate) Copolymer Electrolytes. Macromolecules 2021;54:1414–24.
[95] Bouchet R, Phan T, Beaudoin E, Devaux D, Davidson P, Bertin D, et al. Charge transport in nanostructured PS–PEO–PS triblock copolymer electrolytes. Macromolecules 2014;47:2659–65.
[96] Zhang B, Zhang Y, Zhang N, Liu J, Cong L, Liu J, et al. Synthesis and interface stability of polystyrene-poly(ethylene glycol)-polystyrene triblock copolymer as solid-state electrolyte for lithium-metal batteries. J Power Sources 2019;428:93–104.
[97] Maslyn JA, Loo WS, McEntush KD, Oh HJ, Harry KJ, Parkinson DY, et al. Growth of Lithium Dendrites and Globules through a Solid Block Copolymer Electrolyte as a Function of Current Density. J Phys Chem C 2018;122:26797–804.
[98] Frenck L, Maslyn JA, Loo WS, Parkinson DY, Balsara NP. Impact of Salt Concentration on Nonuniform Lithium Electrodeposition through Rigid Block Copolymer Electrolytes. ACS Appl Mater Interfaces 2019;11:47878–85.
[99] Niitani T, Shimada M, Kawamura K, Dokko K, Rho Y-H, Kanamura K. Synthesis of Li+ ion conductive PEO-PSt block copolymer electrolyte with microphase separation structure. Electrochem Solid State Lett 2005;8:A385.
[100] Devaux D, Glé D, Phan TN, Gigmes D, Giroud E, Deschamps M, et al. Optimization of block copolymer electrolytes for lithium metal batteries. Chem Mater 2015;27:4682–92.
[101] Bergfelt A, Rubatat L, Mogensen R, Brandell D, Bowden T. d8-poly(methyl methacrylate)-poly [(oligo ethylene glycol) methyl ether methacrylate] tri-block-copolymer electrolytes: morphology, conductivity and battery performance. Polymer 2017;131:234–42.
[102] Bergfelt A, Rubatat L, Brandell D, Bowden T. Poly(benzyl methacrylate)-poly [(oligo ethylene glycol) methyl ether methacrylate] triblock-copolymers as solid electrolyte for lithium batteries. Solid State Ion 2018;321:55–61.
[103] Gao Y, Yan Z, Gray JL, He X, Wang D, Chen T, et al. Polymer–inorganic solid—electrolyte interphase for stable lithium metal batteries under lean electrolyte conditions. Nat Mater 2019;18:384–9.
[104] Xu H, Wang A, Liu X, Feng D, Wang S, Chen J, et al. A new fluorine-containing star-branched polymer as electrolyte for all-solid-state lithium-ion batteries. Polymer 2018;146:249–55.
[105] Rosenbach D, Mödl N, Hahn M, Petry J, Danzer MA, Thelakkat M. Synthesis and Comparative Studies of Solvent-Free Brush Polymer Electrolytes for Lithium Batteries. ACS Appl Energy Mater 2019;2:3373–88.
[106] Zhang Y, Costantini N, Mierzwa M, Pakula T, Neugebauer D, Matyjaszewski K. Super soft elastomers as ionic conductors. Polymer 2004;45:6333–9.
[107] Shibuya Y, Tatara R, Jiang Y, Shao-Horn Y, Johnson JA. Brush-First ROMP of poly(ethylene oxide) macromonomers of varied length: impact of polymer architecture on thermal behavior and Li+ conductivity. J Polym Sci, Part A: Polym Chem 2019;57:448–55.
[108] Nederstedt H, Jannasch P. Poly (p-phenylene) s tethered with oligo (ethylene oxide): synthesis by Yamamoto polymerization and properties as solid polymer electrolytes. Polym Chem 2020;11:2418–29.

[109] Nair JR, Shaji I, Ehteshami N, Thum A, Diddens D, Heuer A, et al. Solid polymer electrolytes for lithium metal battery via thermally induced cationic ring-opening polymerization (CROP) with an insight into the reaction mechanism. Chem Mater 2019;31:3118–33.
[110] Stalin S, Johnson HEN, Biswal P, Vu D, Zhao Q, Yin J, et al. Achieving Uniform Lithium Electrodeposition in Cross-Linked Poly(ethylene oxide) Networks: "Soft" Polymers Prevent Metal Dendrite Proliferation. Macromolecules 2020.
[111] Sakakibara T, Kitamura M, Honma T, Kohno H, Uno T, Kubo M, et al. Cross-linked polymer electrolyte and its application to lithium polymer battery. Electrochim Acta 2019;296:1018–26.
[112] Aldalur I, Armand M, Zhang H. Jeffamine-Based Polymers for Rechargeable Batteries. Batter Supercaps 2020;3:30–46.
[113] Aldalur I, Zhang H, Piszcz M, Oteo U, Rodriguez-Martinez LM, Shanmukaraj D, et al. Jeffamine® based polymers as highly conductive polymer electrolytes and cathode binder materials for battery application. J Power Sources 2017;347:37–46.
[114] Aldalur I, Martinez-Ibañez M, Krztoń-Maziopa A, Piszcz M, Armand M, Zhang H. Flowable polymer electrolytes for lithium metal batteries. J Power Sources 2019;423:218–26.
[115] Zhou W, Wang Z, Pu Y, Li Y, Xin S, Li X, et al. Double-layer polymer electrolyte for high-voltage all-solid-state rechargeable batteries. Adv Mater 2019;31:1805574.
[116] Hu P, Chai J, Duan Y, Liu Z, Cui G, Chen L. Progress in nitrile-based polymer electrolytes for high performance lithium batteries. J Mater Chem A 2016;4:10070–83.
[117] Wang Q, Zhang H, Cui Z, Zhou Q, Shangguan X, Tian S, et al. Siloxane-based polymer electrolytes for solid-state lithium batteries. Energy Storage Mater 2019;23:466–90.
[118] Pagot G, Bertasi F, Vezzù K, Nawn G, Pace G, Nale A, et al. Correlation between Properties and Conductivity Mechanism in Poly(vinyl alcohol)-based Lithium Solid Electrolytes. Solid State Ion 2018;320:177–85.
[119] Zhang J, Yang J, Dong T, Zhang M, Chai J, Dong S, et al. Aliphatic Polycarbonate-Based Solid-State Polymer Electrolytes for Advanced Lithium Batteries: Advances and Perspective. Small 2018;14:1800821.
[120] Wang C, Zhang H, Li J, Chai J, Dong S, Cui G. The interfacial evolution between polycarbonate-based polymer electrolyte and Li-metal anode. J Power Sources 2018;397:157–61.
[121] Commarieu B, Paolella A, Collin-Martin S, Gagnon C, Vijh A, Guerfi A, et al. Solid-to-liquid transition of polycarbonate solid electrolytes in Li-metal batteries. J Power Sources 2019;436:226852.
[122] Li J, Dong S, Wang C, Hu Z, Zhang Z, Zhang H, et al. A study on the interfacial stability of the cathode/polycarbonate interface: implication of overcharge and transition metal redox. J Mater Chem A 2018;6:11846–52.
[123] Ouhib F, Meabe L, Mahmoud A, Eshraghi N, Grignard B, Thomassin J-M, et al. CO 2-sourced polycarbonates as solid electrolytes for room temperature operating lithium batteries. J Mater Chem A 2019;7:9844–53.
[124] Gennen S, Grignard B, Tassaing T, Jérôme C, Detrembleur C. CO2-Sourced α-Alkylidene Cyclic Carbonates: a Step Forward in the Quest for Functional Regioregular Poly(urethane)s and Poly(carbonate)s. Angew Chem Int Ed 2017;56:10394–8.
[125] Ouhib F, Meabe L, Mahmoud A, Grignard B, Thomassin J-M, Boschini F, et al. Influence of the Cyclic versus Linear Carbonate Segments in the Properties and Performance of CO2-Sourced Polymer Electrolytes for Lithium Batteries. ACS Appl Polym Mater 2020;2:922–31.
[126] Meabe L, Huynh TV, Lago N, Sardon H, Li C, O'Dell LA, et al. Poly (ethylene oxide carbonates) solid polymer electrolytes for lithium batteries. Electrochim Acta 2018;264:367–75.
[127] Meabe L, Huynh TV, Mantione D, Porcarelli L, Li C, O'Dell LA, et al. UV-cross-linked poly (ethylene oxide carbonate) as free standing solid polymer electrolyte for lithium batteries. Electrochim Acta 2019;302:414–21.
[128] Mindemark J, Sun B, Törmä E, Brandell D. High-performance solid polymer electrolytes for lithium batteries operational at ambient temperature. J Power Sources 2015;298:166–70.
[129] Johansson IL, Brandell D, Mindemark J. Mechanically Stable UV-Crosslinked Polyester-Polycarbonate Solid Polymer Electrolyte for High-Temperature Batteries. Batter Supercaps 2020.
[130] Bergfelt A, Hernández G, Mogensen R, Lacey MJ, Mindemark J, Brandell D, et al. Mechanically Robust Yet Highly Conductive Diblock Copolymer Solid Polymer Electrolyte for Ambient Temperature Battery Applications. ACS Appl Polym Mater 2020;2:939–48.
[131] Eshetu GG, Mecerreyes D, Forsyth M, Zhang H, Armand M. Polymeric ionic liquids for lithium-based rechargeable batteries. Mol Syst Des Eng 2019;4:294–309.
[132] Wang X, Chen F, Girard GMA, Zhu H, MacFarlane DR, Mecerreyes D, et al. Poly(Ionic Liquid)s-in-Salt Electrolytes with Co-coordination-Assisted Lithium-Ion Transport for Safe Batteries. Joule 2019;3:2687–702.
[133] Zimmerman MANA, Ma US), Gavrilov Alexei B. (Woburn, MA, US). Solid, ionically conducting polymer material, and methods and applications for same. United States: IONIC MATERIALS, INC (Woburn, MA, US); 2020.
[134] Hatakeyama-Sato K, Tezuka T, Umeki M, Oyaizu K. AI-Assisted Exploration of Superionic Glass-Type Li+ Conductors with Aromatic Structures. J Am Chem Soc 2020;142:3301–5.
[135] Torrance JB. An Overview of Organic Charge-Transfer Solids: Insulators, Metals, and the Neutral-Ionic Transition. Mol Cryst Liq Cryst 1985;126:55–67.
[136] Hatakeyama-Sato K, Umeki M, Tezuka T, Oyaizu K. Charge-Transfer Complexes for Solid-State Li+ Conduction. ACS Appl Electron Mater 2020;2:2211–17.
[137] Patil N, Jérôme C, Detrembleur C. Recent advances in the synthesis of catechol-derived (bio)polymers for applications in energy storage and environment. Prog Polym Sci 2018;82:34–91.
[138] Liu J, Yuan H, Cheng XB, Chen WJ, Titirici MM, Huang JQ, et al. A review of naturally derived nanostructured materials for safe lithium metal batteries. Mater Today Nano 2019;8:100049.
[139] Quartarone E, Mustarelli P. Review—Emerging Trends in the Design of Electrolytes for Lithium and Post-Lithium Batteries. J Electrochem Soc 2020;167:050508.
[140] Nematdoust S, Najjar R, Bresser D, Passerini S. Partially Oxidized Cellulose grafted with Polyethylene Glycol mono-Methyl Ether (m-PEG) as Electrolyte Material for Lithium Polymer Battery. Carbohydr Polym 2020;240:116339.
[141] Wang S, Zhang L, Zeng Q, Liu X, Lai W-Y, Zhang L. Cellulose Microcrystals with Brush-Like Architectures as Flexible All-Solid-State Polymer Electrolyte for Lithium-Ion Battery. ACS Sustain Chem Eng 2020;8:3200–7.
[142] Jeong D, Shim J, Shin H, Lee J-C. Sustainable lignin-derived cross-linked graft polymers as electrolyte and binder materials for lithium metal battery. ChemSusChem 2020.
[143] Cheng X, Pan J, Zhao Y, Liao M, Peng H. Gel polymer electrolytes for electrochemical energy storage. Adv Energy Mater 2018;8:1702184.
[144] Burba CM, Butson ED, Atchley JR, Johnson MS. Thermal Properties and Ionic Conductivities of Confined LiBF4 Dimethyl Carbonate Solutions. J Phys Chem C 2014;118:366–75.
[145] Porcarelli L, Gerbaldi C, Bella F, Nair JR. Super soft all-ethylene oxide polymer electrolyte for safe all-solid lithium batteries. Sci Rep 2016;6:19892.
[146] Mackanic DG, Michaels W, Lee M, Feng D, Lopez J, Qin J, et al. Crosslinked Poly(tetrahydrofuran) as a Loosely Coordinating Polymer Electrolyte. Adv Energy Mater 2018;8:1800703.
[147] Wu H, Cao Y, Su H, Wang C. Tough gel electrolyte using double polymer network design for the safe, stable cycling of lithium metal anode. Angew Chem Int Ed 2018;57:1361–5.
[148] Wehbi M, Dolphijn G, Brassinne J, Gohy J-F, Ameduri B. Synthesis of Vinylidene Fluoride-Based Copolymers Bearing Perfluorinated Ether Pendant Groups and Their Application in Gel Polymer Electrolytes. Macromolecules 2019;52:3056–65.
[149] Lodge TP. A Unique Platform for Materials Design. Science 2008;321:50–1.
[150] Schulze MW, McIntosh LD, Hillmyer MA, Lodge TP. High-Modulus, High–Conductivity Nanostructured Polymer Electrolyte Membranes via Polymerization-Induced Phase Separation. Nano Lett 2014;14:122–6.
[151] Zhao Q, Liu X, Stalin S, Khan K, Archer LA. Solid-state polymer electrolytes with in-built fast interfacial transport for secondary lithium batteries. Nat Energy 2019;4:365.
[152] Liu Q, Cresce A, Schroeder M, Xu K, Mu D, Wu B, et al. Insight on lithium metal anode interphasial chemistry: reduction mechanism of cyclic ether solvent and SEI film formation. Energy Storage Mater 2019;17:366–73.
[153] Zhao CZ, Zhao Q, Liu X, Zheng J, Stalin S, Zhang Q, et al. Rechargeable Lithium Metal Batteries with an In-Built Solid-State Polymer Electrolyte and a High Voltage/Loading Ni-Rich Layered Cathode. Adv Mater 2020;32:1905629.
[154] Liu F, Li T, Yang Y, Yan J, Li N, Xue J, et al. Investigation on the Copolymer Electrolyte of Poly (1, 3-dioxolane-co-formaldehyde). Macromol Rapid Commun 2020;41:2000047.
[155] Chai J, Liu Z, Ma J, Wang J, Liu X, Liu H, et al. Situ Generation of Poly (Vinylene Carbonate) Based Solid Electrolyte with Interfacial Stability for LiCoO2 Lithium Batteries. Adv Sci 2017;4:1600377.
[156] Huang S, Cui Z, Qiao L, Xu G, Zhang J, Tang K, et al. An in-situ polymerized solid polymer electrolyte enables excellent interfacial compatibility in lithium batteries. Electrochim Acta 2019;299:820–7.
[157] Tamura T, Yoshida K, Hachida T, Tsuchiya M, Nakamura M, Kazue Y, et al. Physicochemical Properties of Glyme–Li Salt Complexes as a New Family of Room-temperature Ionic Liquids. Chem Lett 2010;39:753–5.
[158] Eyckens DJ, Henderson LC. A Review of Solvate Ionic Liquids: Physical Parameters and Synthetic Applications. Front Chem 2019;7:263.
[159] Watanabe M, Dokko K, Ueno K, Thomas ML. From Ionic Liquids to Solvate Ionic Liquids: Challenges and Opportunities for Next Generation Battery Electrolytes. Bull Chem Soc Jpn 2018;91:1660–82.
[160] Dokko K, Tachikawa N, Yamauchi K, Tsuchiya M, Yamazaki A, Takashima E, et al. Solvate Ionic Liquid Electrolyte for Li–S Batteries. J Electrochem Soc 2013;160:A1304–A1A10.
[161] Kitazawa Y, Iwata K, Imaizumi S, Ahn H, Kim SY, Ueno K, et al. Gelation of Solvate Ionic Liquid by Self-Assembly of Block Copolymer and Characterization as Polymer Electrolyte. Macromolecules 2014;47:6009–16.
[162] Wan J, Xie J, Mackanic DG, Burke W, Bao Z, Cui Y. Status, promises, and challenges of nanocomposite solid-state electrolytes for safe and high performance lithium batteries. Mater Today Nano 2018;4:1–16.
[163] Liang CC. Conduction Characteristics of the Lithium Iodide-Aluminum Oxide Solid Electrolytes. J Electrochem Soc 1973;120:1289.
[164] Khandkar AC, Wagner JB. Fast ion transport in composites. Solid State Ion 1986;18-19:1100–4.
[165] Liu W, Lin D, Sun J, Zhou G, Cui Y. Improved Lithium Ionic Conductivity in Composite Polymer Electrolytes with Oxide-Ion Conducting Nanowires. ACS Nano 2016;10:11407–13.
[166] Zhao R, Wu Y, Liang Z, Gao L, Xia W, Zhao Y, et al. Metal-organic frameworks for solid-state electrolytes. Energy Environ Sci 2020.

[167] Nematdoust S, Najjar R, Bresser D, Passerini S. Understanding the Role of Nanoparticles in PEO-Based Hybrid Polymer Electrolytes for Solid-State Lithium–Polymer Batteries. J Phys Chem C 2020;124:27907–15.
[168] Jin S, Ye Y, Niu Y, Xu Y, Jin H, Wang J, et al. Solid–Solution-Based Metal Alloy Phase for Highly Reversible Lithium Metal Anode. J Am Chem Soc 2020;142:8818–26.
[169] Lin D, Liu W, Liu Y, Lee HR, Hsu P-C, Liu K, et al. High ionic conductivity of composite solid polymer electrolyte via in situ synthesis of monodispersed SiO2 nanospheres in poly (ethylene oxide). Nano Lett 2016;16:459–65.
[170] Blensdorf T, Joenathan A, Hunt M, Werner-Zwanziger U, Stein BD, Mahmoud WE, et al. Hybrid composite polymer electrolytes: ionic liquids as a magic bullet for the poly (ethylene glycol)–silica network. J Mater Chem A 2017;5:3493–502.
[171] Zhu Y, Cao J, Chen H, Yu Q, Li B. High electrochemical stability of a 3D cross-linked network PEO@nano-SiO2 composite polymer electrolyte for lithium metal batteries. J Mater Chem A 2019;7:6832–9.
[172] Lin D, Yuen PY, Liu Y, Liu W, Liu N, Dauskardt RH, et al. A silica-aerogel-reinforced composite polymer electrolyte with high ionic conductivity and high modulus. Adv Mater 2018;30:1802661.
[173] Bai M, Xie K, Yuan K, Zhang K, Li N, Shen C, et al. A Scalable Approach to Dendrite-Free Lithium Anodes via Spontaneous Reduction of Spray-Coated Graphene Oxide Layers. Adv Mater 2018;30:1801213.
[174] Sethi GK, Jung HY, Loo WS, Sawhney S, Park MJ, Balsara NP, et al. Structure and thermodynamics of hybrid organic–inorganic diblock copolymers with salt. Macromolecules 2019;52:3165–75.
[175] Wang A, Zhang X, Yang Y-W, Huang J, Liu X, Luo J. Horizontal Centripetal Plating in the Patterned Voids of Li/Graphene Composites for Stable Lithium-Metal Anodes. Chem 2018;4:2192–200.
[176] Chinnam PR, Wunder SL. Polyoctahedral Silsesquioxane-Nanoparticle Electrolytes for Lithium Batteries: POSS-Lithium Salts and POSS-PEGs. Chem Mater 2011;23:5111–21.
[177] Zhang W, Müller AH. Architecture, self-assembly and properties of well-defined hybrid polymers based on polyhedral oligomeric silsequioxane (POSS). Prog Polym Sci 2013;38:1121–62.
[178] Lu Q, Fu J, Chen L, Shang D, Li M, Xu Y, et al. Polymeric polyhedral oligomeric silsesquioxane ionic liquids based solid polymer electrolytes for lithium ion batteries. J Power Sources 2019;414:31–40.
[179] Pyun J, Matyjaszewski K, Kowalewski T, Savin D, Patterson G, Kickelbick G, et al. Synthesis of Well-Defined Block Copolymers Tethered to Polysilsesquioxane Nanoparticles and Their Nanoscale Morphology on Surfaces. J Am Chem Soc 2001;123:9445–6.
[180] Pyun J, Matyjaszewski K. The Synthesis of Hybrid Polymers Using Atom Transfer Radical Polymerization: Homopolymers and Block Copolymers from Polyhedral Oligomeric Silsesquioxane Monomers. Macromolecules 2000;33:217–20.
[181] Sethi GK, Jiang X, Chakraborty R, Loo WS, Villaluenga I, Balsara NP. Anomalous self-assembly and ion transport in nanostructured organic–inorganic solid electrolytes. ACS Macro Lett 2018;7:1056–61.
[182] Zhang K, Kirlikovali KO, Varma RS, Jin Z, Jang HW, Farha OK, et al. Covalent organic frameworks: emerging organic solid materials for energy and electrochemical applications. ACS Appl Mater Interfaces 2020.
[183] Gerbaldi C, Nair JR, Kulandainathan MA, Kumar RS, Ferrara C, Mustarelli P, et al. Innovative high performing metal organic framework (MOF)-laden nanocomposite polymer electrolytes for all-solid-state lithium batteries. J Mater Chem A 2014;2:9948–54.
[184] Falco M, Castro L, Nair JR, Bella F, Bardé F, Meligrana G, et al. UV-cross-linked composite polymer electrolyte for high-rate, ambient temperature lithium batteries. ACS Appl Energy Mater 2019;2:1600–7.
[185] Wu S, Jiao T, Yang S, Liu B, Zhang W, Zhang K. Lithiophilicity conversion of the Cu surface through facile thermal oxidation: boosting a stable Li–Cu composite anode through melt infusion. J Mater Chem A 2019;7:5726–5732.
[186] Xia S, Lopez J, Liang C, Zhang Z, Bao Z, Cui Y, et al. High-Rate and Large-Capacity Lithium Metal Anode Enabled by Volume Conformal and Self-Healable Composite Polymer Electrolyte. Adv Sci 2019;6:1802353.
[187] Chen L, Li Y, Li S-P, Fan L-Z, Nan C-W, Goodenough JB. PEO/garnet composite electrolytes for solid-state lithium batteries: from “ceramic-in-polymer” to “polymer-in-ceramic. Nano Energy 2018;46:176–84.
[188] Pan R, Sun R, Wang Z, Lindh J, Edström K, Strømme M, et al. Sandwich-structured nano/micro fiber-based separators for lithium metal batteries. Nano Energy 2019;55:316–26.
[189] Villaluenga I, Wujcik KH, Tong W, Devaux D, Wong DHC, DeSimone JM, et al. Compliant glass–polymer hybrid single ion-conducting electrolytes for lithium batteries. Proc Natl Acad Sci USA 2016;113:52.
[190] Li C, Liu S, Shi C, Liang G, Lu Z, Fu R, et al. Two-dimensional molecular brush–functionalized porous bilayer composite separators toward ultrastable high--current density lithium metal anodes. Nat Commun 2019;10:1363.
[191] Liu W, Lee SW, Lin D, Shi F, Wang S, Sendek AD, et al. Enhancing ionic conductivity in composite polymer electrolytes with well-aligned ceramic nanowires. Nat Energy 2017;2:1–7.
[192] Fu KK, Gong Y, Dai J, Gong A, Han X, Yao Y, et al. Flexible, solid-state, ion-conducting membrane with 3D garnet nanofiber networks for lithium batteries. Proc Natl Acad Sci USA 2016;113:7094–9.
[193] Yan C, Zhu P, Jia H, Du Z, Zhu J, Orenstein R, et al. Garnet-rich composite solid electrolytes for dendrite-free, high-rate, solid-state lithium-metal batteries. Energy Storage Mater 2020;26:448–56.
[194] Zhou Y, Wang X, Zhu H, Armand M, Forsyth M, Greene GW, et al. Ternary lithium-salt organic ionic plastic crystal polymer composite electrolytes for high voltage, all-solid-state batteries. Energy Storage Mater 2018;15:407–14.
[195] Zhang H, Li C, Piszcz M, Coya E, Rojo T, Rodriguez-Martinez LM, et al. Single lithium-ion conducting solid polymer electrolytes: advances and perspectives. Chem Soc Rev 2017;46:797–815.
[196] Diederichsen KM, McShane EJ, McCloskey BD. Promising Routes to a High Li+ Transference Number Electrolyte for Lithium Ion Batteries. ACS Energy Lett 2017;2:2563–75.
[197] Tintaru A, Rollet M, Gigmes D, Phan TN. A post-polymerization functionalization strategy for the synthesis of sulfonyl (trifluoromethanesulfonyl) imide functionalized (co) polymers. Polym Chem 2017;8:5660–5.
[198] Bouchet R, Maria S, Meziane R, Aboulaich A, Lienafa L, Bonnet J-P, et al. Single-ion BAB triblock copolymers as highly efficient electrolytes for lithium-metal batteries. Nat Mater 2013;12:452–7.
[199] Li S, Mohamed AI, Pande V, Wang H, Cuthbert J, Pan X, et al. Single-ion homopolymer electrolytes with high transference number prepared by click chemistry and photoinduced metal-free atom-transfer radical polymerization. ACS Energy Lett 2017;3:20–7.
[200] Rojas AA, Inceoglu S, Mackay NG, Thelen JL, Devaux D, Stone GM, et al. Effect of lithium-ion concentration on morphology and ion transport in single-ion–conducting block copolymer electrolytes. Macromolecules 2015;48:6589–95.
[201] Porcarelli L, Aboudzadeh MA, Rubatat L, Nair JR, Shaplov AS, Gerbaldi C, et al. Single-ion triblock copolymer electrolytes based on poly (ethylene oxide) and methacrylic sulfonamide blocks for lithium metal batteries. J Power Sources 2017;364:191–9.
[202] Meabe L, Goujon N, Li C, Armand M, Forsyth M, Mecerreyes D. Single-Ion Conducting Poly (Ethylene Oxide Carbonate) as Solid Polymer Electrolyte for Lithium Batteries. Batter Supercaps 2020;3:68–75.
[203] Porcarelli L, Manojkumar K, Sardon H, Llorente O, Shaplov AS, Vijayakrishna K, et al. Single ion conducting polymer electrolytes based on versatile polyurethanes. Electrochim Acta 2017;241:526–34.
[204] Cao P-F, Li B, Yang G, Zhao S, Townsend J, Xing K, et al. Elastic Single-Ion Conducting Polymer Electrolytes: Toward a Versatile Approach for Intrinsically Stretchable Functional Polymers. Macromolecules 2020;53:3591–601.
[205] Ahmed F, Choi I, Rahman MM, Jang H, Ryu T, Yoon S, et al. Remarkable Conductivity of a Self-Healing Single-Ion Conducting Polymer Electrolyte, Poly(ethylene-co-acrylic lithium (fluoro sulfonyl)imide), for All-Solid-State Li-Ion Batteries. ACS Appl Mater Interfaces 2019;11:34930–8.
[206] Deng K, Qin J, Wang S, Ren S, Han D, Xiao M, et al. Effective Suppression of Lithium Dendrite Growth Using a Flexible Single-Ion Conducting Polymer Electrolyte. Small 2018;14:1801420.
[207] Kim Y, Kwon SJ, Jang H-kK, Jung BM, Lee SB, Choi UH. High Ion Conducting Nanohybrid Solid Polymer Electrolytes via Single-Ion Conducting Mesoporous Organosilica in Poly(ethylene oxide). Chem Mater 2017;29:4401–10.
[208] Huang M, Feng S, Zhang W, Giordano L, Chen M, Amanchukwu CV, et al. Fluorinated Aryl Sulfonimide Tagged (FAST) salts: modular synthesis and structure–property relationships for battery applications. Energy Environ Sci 2018;11:1326–34.
[209] Huang M, Feng S, Zhang W, Lopez J, Qiao B, Tatara R, et al. Design of S-Substituted Fluorinated Aryl Sulfonamide-Tagged (S-FAST) Anions To Enable New Solvate Ionic Liquids for Battery Applications. Chem Mater 2019;31:7558–64.
[210] Zhang W, Feng S, Huang M, Qiao B, Shigenobu K, Giordano L, et al. Molecularly Tunable Polyanions for Single-Ion Conductors and Poly(solvate ionic liquids). Chem Mater 2021;33:524–34.
[211] Savoie BM, Webb MA, Miller TF. Enhancing cation diffusion and suppressing anion diffusion via lewis-acidic polymer electrolytes. J Phys Chem Lett 2017;8:641–6.
[212] Li D, Ji X, Gong X, Tsai F, Zhang Q, Yao L, et al. The synergistic effect of poly(ethylene glycol)-borate ester on the electrochemical performance of all solid state Si doped-poly(ethylene glycol) hybrid polymer electrolyte for lithium ion battery. J Power Sources 2019;423:349–57.
[213] Dai K, Zheng Y, Wei W. Organoboron-containing polymer electrolytes for high-performance lithium batteries. Adv Funct Mater 2021;31:2008632.
[214] Matsumi N, Sugai K, Ohno H. Ion conductive characteristics of alkylborane type and boric ester type polymer electrolytes derived from mesitylborane. Macromolecules 2003;36:2321–6.
[215] Tabata S-i, Hirakimoto T, Tokuda H, Susan MABH, Watanabe M. Effects of novel boric acid esters on ion transport properties of lithium salts in nonaqueous electrolyte solutions and polymer electrolytes. Phys Chem B 2004;108:19518–26.
[216] Matsumi N, Sugai K, Miyake M, Ohno H. Polymerized ionic liquids via hydroboration polymerization as single ion conductive polymer electrolytes. Macromolecules 2006;39:6924–7.
[217] Bapat AP, Sumerlin BS, Sutti A. Bulk network polymers with dynamic B–O bonds: healable and reprocessable materials. Mater Horiz 2020;7:694–714.
[218] Dai K, Ma C, Feng Y, Zhou L, Kuang G, Zhang Y, et al. A borate-rich, cross-linked gel polymer electrolyte with near-single ion conduction for lithium metal batteries. J Mater Chem A 2019;7:18547–57.
[219] Kaskhedikar N, Karatas Y, Cui G, Maier J, Wiemhöfer HD. Nanocomposites based on borate esters as improved lithium-ion electrolytes. J Mater Chem 2011;21:11838–43.
[220] Cong L, Liu J, Armand M, Mauger A, Julien CM, Xie H, et al. Role of perfluoropolyether-based electrolytes in lithium metal batteries: Implication for suppressed Al current collector corrosion and the stability of Li metal/electrolytes interfaces. J Power Sources 2018;380:115–25.

[221] Devaux D, Villaluenga I, Bhatt M, Shah D, Chen XC, Thelen JL, et al. Crosslinked perfluoropolyether solid electrolytes for lithium ion transport. Solid State Ion 2017;310:71–80.
[222] Chintapalli M, Timachova K, Olson KR, Mecham SJ, DeSimone JM, Balsara NP. Lithium Salt Distribution and Thermodynamics in Electrolytes Based on Short Perfluoropolyether-block-Poly (ethylene oxide) Copolymers. Macromolecules 2020;53:1142–53.
[223] Amanchukwu CV, Yu Z, Kong X, Qin J, Cui Y, Bao Z. A new class of ionically conducting fluorinated ether electrolytes with high electrochemical stability. J Am Chem Soc 2020;142:7393–403.
[224] Roy N, Bruchmann B, Lehn J-M. DYNAMERS: dynamic polymers as self-healing materials. Chem Soc Rev 2015;44:3786–807.
[225] Podgórski M, Fairbanks BD, Kirkpatrick BE, McBride M, Martinez A, Dobson A, et al. Covalent Adaptable Networks: toward Stimuli-Responsive Dynamic Thermosets through Continuous Development and Improvements in Covalent Adaptable Networks (CANs) (Adv. Mater. 20/2020). Adv Mater 2020;32:2070158.
[226] Van Zee NJ, Nicolaÿ R. Vitrimers: permanently crosslinked polymers with dynamic network topology. Prog Polym Sci 2020:101233.
[227] Chen D, Wang D, Yang Y, Huang Q, Zhu S, Zheng Z. Self-healing materials for next-generation energy harvesting and storage devices. Adv Energy Mater 2017;7:1700890.
[228] Zhou B, He D, Hu J, Ye Y, Peng H, Zhou X, et al. A flexible, self-healing and highly stretchable polymer electrolyte via quadruple hydrogen bonding for lithium-ion batteries. J Mater Chem A 2018;6:11725–33.
[229] Zhou B, Jo YH, Wang R, He D, Zhou X, Xie X, et al. Self-healing composite polymer electrolyte formed via supramolecular networks for high-performance lithium-ion batteries. J Mater Chem A 2019;7:10354–62.
[230] Zhou B, Zuo C, Xiao Z, Zhou X, He D, Xie X, et al. Self-healing polymer electrolytes formed via dual-networks: a new strategy for flexible lithium metal batteries. Chemistry 2018;24:19200–7.
[231] Guo P, Su A, Wei Y, Liu X, Li Y, Guo F, et al. Healable, highly conductive, flexible, and nonflammable supramolecular ionogel electrolytes for lithium-ion batteries. ACS Appl Mater Interfaces 2019;11:19413–20.
[232] Tamate R, Hashimoto K, Horii T, Hirasawa M, Li X, Shibayama M, et al. Self-healing micellar ion gels based on multiple hydrogen bonding. Adv Mater 2018;30:1802792.
[233] Jo YH, Li S, Zuo C, Zhang Y, Gan H, Li S, et al. Self-healing solid polymer electrolyte facilitated by a dynamic cross-linked polymer matrix for lithium-ion batteries. Macromolecules 2020;53:1024–32.
[234] Jing BB, Evans CM. Catalyst-free dynamic networks for recyclable, self-healing solid polymer electrolytes. J Am Chem Soc 2019;141:18932–7.
[235] Wu N, Shi YR, Lang SY, Zhou JM, Liang JY, Wang W, et al. Self-Healable Solid Polymeric Electrolytes for Stable and Flexible Lithium Metal Batteries. Angew Chem Int Ed 2019;58:18146–9.
[236] Kato R, Mirmira P, Sookezian A, Grocke GL, Patel SN, Rowan SJ. Ion–Conducting Dynamic Solid Polymer Electrolyte Adhesives. ACS Macro Lett 2020;9:500–6.
[237] Peled E. The electrochemical behavior of alkali and alkaline earth metals in nonaqueous battery systems—the solid electrolyte interphase model. J Electrochem Soc 1979;126:2047–51.
[238] Peled E, Golodnitsky D, Ardel G. Advanced model for solid electrolyte interphase electrodes in liquid and polymer electrolytes. J Electrochem Soc 1997;144:L208–LL10.
[239] Aurbach D, Markovsky B, Levi MD, Levi E, Schechter A, Moshkovich M, et al. New insights into the interactions between electrode materials and electrolyte solutions for advanced nonaqueous batteries. J Power Sources 1999;81-82:95–111.
[240] Winter M. The Solid Electrolyte Interphase – The Most Important and the Least Understood Solid Electrolyte in Rechargeable Li Batteries. Z Phys Chem 2009:1395.
[241] Verma P, Maire P, Novák P. A review of the features and analyses of the solid electrolyte interphase in Li-ion batteries. Electrochim Acta 2010;55:6332–41.
[242] Yang C, Fu K, Zhang Y, Hitz E, Hu L. Protected Lithium-Metal Anodes in Batteries: From Liquid to Solid. Adv Mater 2017;29:1701169.
[243] Zhang X-Q, Cheng X-B, Zhang Q. Advances in Interfaces between Li Metal Anode and Electrolyte. Adv Mater Interfaces 2018;5:1701097.
[244] Peled E, Menkin S. Review—SEI: past, present and future. J Electrochem Soc 2017;164:A1703–A1A19.
[245] Soto FA, Ma Y, Martinez de la Hoz JM, Seminario JM, Balbuena PB. Formation and growth mechanisms of solid-electrolyte interphase layers in rechargeable batteries. Chem Mater 2015;27:7990–8000.
[246] Tung S-O, Ho S, Yang M, Zhang R, Kotov NA. A dendrite-suppressing composite ion conductor from aramid nanofibres. Nat Commun 2015;6:6152.
[247] Lee H, Lee DJ, Kim Y-J, Park J-K, Kim H-T. A simple composite protective layer coating that enhances the cycling stability of lithium metal batteries. J Power Sources 2015;284:103–8.
[248] Yan K, Lee H-W, Gao T, Zheng G, Yao H, Wang H, et al. Ultrathin two-dimensional atomic crystals as stable interfacial layer for improvement of lithium metal anode. Nano Lett 2014;14:6016–22.
[249] Liu W, Li W, Zhuo D, Zheng G, Lu Z, Liu K, et al. Core–shell nanoparticle coating as an interfacial layer for dendrite-free lithium metal anodes. ACS Central Sci 2017;3:135–40.
[250] Kong X, Rudnicki PE, Choudhury S, Bao Z, Qin J. Dendrite Suppression by a Polymer Coating: a Coarse-Grained Molecular Study. Adv Funct Mater 2020;30:1910138.
[251] Zhu B, Jin Y, Hu X, Zheng Q, Zhang S, Wang Q, et al. Poly(dimethylsiloxane) Thin Film as a Stable Interfacial Layer for High-Performance Lithium-Metal Battery Anodes. Adv Mater 2017;29:1603755.
[252] Pang Q, Zhou L, Nazar LF. Elastic and Li-ion–percolating hybrid membrane stabilizes Li metal plating. Proc Natl Acad Sci 2018;115:12389.
[253] Liu K, Pei A, Lee HR, Kong B, Liu N, Lin D, et al. Lithium Metal Anodes with an Adaptive "Solid-Liquid" Interfacial Protective Layer. J Am Chem Soc 2017;139:4815–20.
[254] Zheng G, Wang C, Pei A, Lopez J, Shi F, Chen Z, et al. High-performance lithium metal negative electrode with a soft and flowable polymer coating. ACS Energy Lett 2016;1:1247–55.
[255] Cordier P, Tournilhac F, Soulié-Ziakovic C, Leibler L. Self-healing and thermoreversible rubber from supramolecular assembly. Nature 2008;451:977–80.
[256] Chen H, Pei A, Lin D, Xie J, Yang A, Xu J, et al. Uniform high ionic conducting lithium sulfide protection layer for stable lithium metal anode. Adv Energy Mater 2019;9:1900858.
[257] Lopez J, Pei A, Oh JY, Wang G-JN, Cui Y, Bao Z. Effects of polymer coatings on electrodeposited lithium metal. J Am Chem Soc 2018;140:11735–44.
[258] Luo J, Fang C-C, Wu N-L. High polarity poly(vinylidene difluoride) thin coating for dendrite-free and high-performance lithium metal anodes. Adv Energy Mater 2018;8:1701482.
[259] Fan L, Guo Z, Zhang Y, Wu X, Zhao C, Sun X, et al. Stable artificial solid electrolyte interphase films for lithium metal anode via metal–organic frameworks cemented by polyvinyl alcohol. J Mater Chem A 2020;8:251–8.
[260] Yan J, Pan X, Wang Z, Lu Z, Wang Y, Liu L, et al. A fatty acid-inspired tetherable initiator for surface-initiated atom transfer radical polymerization. Chem Mater 2017;29:4963–9.
[261] Yan J, Malakooti MH, Lu Z, Wang Z, Kazem N, Pan C, et al. Solution processable liquid metal nanodroplets by surface-initiated atom transfer radical polymerization. Nat Nanotech 2019;14:684–90.
[262] Liu W, Lin D, Pei A, Cui Y. Stabilizing lithium metal anodes by uniform li-ion flux distribution in nanochannel confinement. J Am Chem Soc 2016;138:15443–50.
[263] Jorne J. Transference number approaching unity in nanocomposite electrolytes. Nano Lett 2006;6:2973–6.
[264] Carta M, Msayib KJ, McKeown NB. Novel polymers of intrinsic microporosity (PIMs) derived from 1,1-spiro-bis(1,2,3,4-tetrahydronaphthalene)-based monomers. Tetrahedron Lett 2009;50:5954–7.
[265] Kopeć M, Lamson M, Yuan R, Tang C, Kruk M, Zhong M, et al. Polyacrylonitrile-derived nanostructured carbon materials. Prog Polym Sci 2019;92:89–134.
[266] Moon GH, Kim HJ, Chae IS, Park SC, Kim BS, Jang J, et al. An artificial solid interphase with polymers of intrinsic microporosity for highly stable Li metal anodes. Chem Commun 2019;55:6313–16.
[267] Baran MJ, Carrington ME, Sahu S, Baskin A, Song J, Baird MA, et al. Diversity-oriented synthesis of polymer membranes with ion solvation cages. Nature 2021;592:225–31.
[268] Tu Z, Choudhury S, Zachman MJ, Wei S, Zhang K, Kourkoutis LF, et al. Designing artificial solid-electrolyte interphases for single-ion and high-efficiency transport in batteries. Joule 2017;1:394–406.
[269] Yu Z, Mackanic DG, Michaels W, Lee M, Pei A, Feng D, Dynamic A, et al. Electrolyte-blocking, and single-ion-conductive network for stable lithium-metal anodes. Joule 2019;3:2761–76.
[270] Li J, Le D-B, Ferguson PP, Dahn JR. Lithium polyacrylate as a binder for tin—cobalt–carbon negative electrodes in lithium-ion batteries. Electrochim Acta 2010;55:2991–5.
[271] Pieczonka NPW, Borgel V, Ziv B, Leifer N, Dargel V, Aurbach D, et al. Lithium Polyacrylate (LiPAA) as an Advanced Binder and a Passivating Agent for High-Voltage Li-Ion Batteries. Adv Energy Mater 2015;5:1501008.
[272] Li N-W, Shi Y, Yin Y-X, Zeng X-X, Li J-Y, Li C-J, et al. A flexible solid electrolyte interphase layer for long-life lithium metal anodes. Angew Chem Int Ed 2018;57:1505–9.
[273] Zhao Y, Wang D, Gao Y, Chen T, Huang Q, Wang D. Stable Li metal anode by a polyvinyl alcohol protection layer via modifying solid-electrolyte interphase layer. Nano Energy 2019;64:103893.
[274] Zhao Q, Tu Z, Wei S, Zhang K, Choudhury S, Liu X, et al. Building organic/inorganic hybrid interphases for fast interfacial transport in rechargeable metal batteries. Angew Chem Int Ed 2018;57:992–6.
[275] Zhao Y, Li G, Gao Y, Wang D, Huang Q, Wang D. Stable Li Metal Anode by a Hybrid Lithium Polysulfidophosphate/Polymer Cross-Linking Film. ACS Energy Lett 2019;4:1271–8.
[276] Liu Y, Lin D, Yuen PY, Liu K, Xie J, Dauskardt RH, et al. An Artificial Solid Electrolyte Interphase with High Li-Ion Conductivity, Mechanical Strength, and Flexibility for Stable Lithium Metal Anodes. Adv Mater 2017;29:1605531.
[277] Gao Y, Zhao Y, Li YC, Huang Q, Mallouk TE, Wang D. Interfacial Chemistry Regulation via a Skin-Grafting Strategy Enables High-Performance Lithium-Metal Batteries. J Am Chem Soc 2017;139:15288–91.
[278] Lu Y, Tu Z, Archer LA. Stable lithium electrodeposition in liquid and nanoporous solid electrolytes. Nat Mater 2014;13:961–9.
[279] Pu J, Li J, Shen Z, Zhong C, Liu J, Ma H, et al. Interlayer Lithium Plating in Au Nanoparticles Pillared Reduced Graphene Oxide for Lithium Metal Anodes. Adv Funct Mater 2018;28:1804133.

[280] Chen Y-T, Abbas SA, Kaisar N, Wu SH, Chen H-A, Boopathi KM, et al. Mitigating Metal Dendrite Formation in Lithium–Sulfur Batteries via Morphology-Tunable Graphene Oxide Interfaces. ACS Appl Mater Interfaces 2019;11:2060–70.
[281] Liu H, Cheng X-B, Huang J-Q, Kaskel S, Chou S, Park HS, et al. Alloy anodes for rechargeable alkali-metal batteries: progress and challenge. ACS Mater Lett 2019;1:217–29.
[282] Jiang Z, Jin L, Han Z, Hu W, Zeng Z, Sun Y, et al. Facile generation of polymer–alloy hybrid layers for dendrite-free lithium-metal anodes with improved moisture stability. Angew Chem Int Ed 2019;58:11374–8.
[283] Lagadec MF, Zahn R, Wood V. Characterization and performance evaluation of lithium-ion battery separators. Nat Energy 2019;4:16–25.
[284] Pan R, Xu X, Sun R, Wang Z, Lindh J, Edström K, et al. Nanocellulose Modified Polyethylene Separators for Lithium Metal Batteries. Small 2018;14:1704371.
[285] Kim PJH, Pol VG. Surface functionalization of a conventional polypropylene separator with an aluminum nitride layer toward ultrastable and high-rate lithium metal anodes. ACS Appl Mater Interfaces 2019;11:3917–24.
[286] Kim J-K, Kim DH, Joo SH, Choi B, Cha A, Kim KM, et al. Hierarchical chitin fibers with aligned nanofibrillar architectures: a nonwoven-mat separator for lithium metal batteries. ACS Nano 2017;11:6114–21.
[287] Kim PJ, Pol VG. High performance lithium metal batteries enabled by surface tailoring of polypropylene separator with a polydopamine/graphene layer. Adv Energy Mater 2018;8:1802665.
[288] Wu J, Liu S, Huang J, Cui Y, Ma P, Wu D, et al. Fabrication of Advanced Hierarchical Porous Polymer Nanosheets and Their Application in Lithium–Sulfur Batteries. Macromolecules 2021.
[289] Wang Z, Pan R, Xu C, Ruan C, Edström K, Strømme M, et al. Conducting polymer paper-derived separators for lithium metal batteries. Energy Storage Mater 2018;13:283–92.
[290] Huo H, Li X, Chen Y, Liang J, Deng S, Gao X, et al. Bifunctional composite separator with a solid-state-battery strategy for dendrite-free lithium metal batteries. Energy Storage Mater 2020;29:361–6.
[291] Fu C, Venturi V, Kim J, Ahmad Z, Ells AW, Viswanathan V, et al. Universal chemomechanical design rules for solid-ion conductors to prevent dendrite formation in lithium metal batteries. Nat Mater 2020;19:758–66.
[292] Wang S, Xu H, Li W, Dolocan A, Manthiram A. Interfacial Chemistry in Solid-State Batteries: Formation of Interphase and Its Consequences. J Am Chem Soc 2018;140:250–7.
[293] Famprikis T, Canepa P, Dawson JA, Islam MS, Masquelier C. Fundamentals of inorganic solid-state electrolytes for batteries. Nat Mater 2019;18:1278–1291.
[294] Wang Y, Wang G, He P, Hu J, Jiang J, Fan L-Z. Sandwich structured NASICON-type electrolyte matched with sulfurized polyacrylonitrile cathode for high performance solid-state lithium-sulfur batteries. Chem Eng J 2020;393:124705.
[295] Renna LA, Blanc F-G, Giordani V. Interface Modification of lithium Metal Anode and Solid-state Electrolyte with Gel Electrolyte. J Electrochem Soc 2020;167:070542.
[296] Xie Z, Wu Z, An X, Yue X, Xiaokaiti P, Yoshida A, et al. A sandwich-type composite polymer electrolyte for all-solid-state lithium metal batteries with high areal capacity and cycling stability. J Membr Sci 2020;596:117739.
[297] Liang J-Y, Zeng X-X, Zhang X-D, Zuo T-T, Yan M, Yin Y-X, et al. Engineering Janus Interfaces of Ceramic Electrolyte via Distinct Functional Polymers for Stable High-Voltage Li-Metal Batteries. J Am Chem Soc 2019;141:9165–9.
[298] Zhou W, Wang S, Li Y, Xin S, Manthiram A, Goodenough JB. Plating a Dendrite-Free Lithium Anode with a Polymer/Ceramic/Polymer Sandwich Electrolyte. J Am Chem Soc 2016;138:9385–8.
[299] Chinnam PR, Wunder SL. Engineered Interfaces in Hybrid Ceramic–Polymer Electrolytes for Use in All-Solid-State Li Batteries. ACS Energy Lett 2017;2:134–8.
[300] Li H, Li M, Siyal SH, Zhu M, Lan J-L, Sui G, et al. A sandwich structure polymer/polymer-ceramics/polymer gel electrolytes for the safe, stable cycling of lithium metal batteries. J Membr Sci 2018;555:169–76.
[301] Liu B, Gong Y, Fu K, Han X, Yao Y, Pastel G, et al. Garnet Solid Electrolyte Protected Li-Metal Batteries. ACS Appl Mater Interfaces 2017;9:18809–15.
[302] Lin D, Liu Y, Pei A, Cui Y. Nanoscale perspective: materials designs and understandings in lithium metal anodes. Nano Res 2017;10:4003–26.
[303] Shi P, Zhang X-Q, Shen X, Zhang R, Liu H, Zhang Q. A review of composite lithium metal anode for practical applications. Adv Mater Tech 2020;5:1900806.
[304] Lin D, Liu Y, Liang Z, Lee H-W, Sun J, Wang H, et al. Layered reduced graphene oxide with nanoscale interlayer gaps as a stable host for lithium metal anodes. Nat Nanotech 2016;11:626–32.
[305] Ye H, Xin S, Yin Y-X, Li J-Y, Guo Y-G, Wan L-J. Stable Li Plating/Stripping Electrochemistry Realized by a Hybrid Li Reservoir in Spherical Carbon Granules with 3D Conducting Skeletons. J Am Chem Soc 2017;139:5916–22.
[306] Yang C, Zhang L, Liu B, Xu S, Hamann T, McOwen D, et al. Continuous plating/stripping behavior of solid-state lithium metal anode in a 3D ion-conductive framework. Proc Natl Acad Sci USA 2018;115:3770.
[307] Li B, Zhang D, Liu Y, Yu Y, Li S, Yang S. Flexible Ti3C2 MXene-lithium film with lamellar structure for ultrastable metallic lithium anodes. Nano Energy 2017;39:654–61.
[308] Zhang R, Chen X, Shen X, Zhang X-Q, Chen X-R, Cheng X-B, et al. Coralloid Carbon Fiber-Based Composite Lithium Anode for Robust Lithium Metal Batteries. Joule 2018;2:764–77.
[309] Wang S-H, Yin Y-X, Zuo T-T, Dong W, Li J-Y, Shi J-L, et al. Stable Li Metal Anodes via Regulating Lithium Plating/Stripping in Vertically Aligned Microchannels. Adv Mater 2017;29:1703729.
[310] Chi S-S, Liu Y, Song W-L, Fan L-Z, Zhang Q. Prestoring Lithium into Stable 3D Nickel Foam Host as Dendrite-Free Lithium Metal Anode. Adv Funct Mater 2017;27:1700348.
[311] Vlad A, Reddy ALM, Ajayan A, Singh N, Gohy J-F, Melinte S, et al. Roll up nanowire battery from silicon chips. Proc Natl Acad Sci USA 2012.
[312] Liang Z, Zheng G, Liu C, Liu N, Li W, Yan K, et al. Polymer nanofiber-guided uniform lithium deposition for battery electrodes. Nano Lett 2015;15:2910–16.
[313] Li G, Liu Z, Huang Q, Gao Y, Regula M, Wang D, et al. Stable metal battery anodes enabled by polyethylenimine sponge hosts by way of electrokinetic effects. Nat Energy 2018;3:1076–83.
[314] Liang Z, Yan K, Zhou G, Pei A, Zhao J, Sun Y, et al. Composite lithium electrode with mesoscale skeleton via simple mechanical deformation. Sci Adv 2019;5:eaau5655.
[315] Liu Y, Lin D, Jin Y, Liu K, Tao X, Zhang Q, et al. Transforming from planar to three-dimensional lithium with flowable interphase for solid lithium metal batteries. Sci Adv 2017;3 eaao0713.
[316] Zhao N, Khokhar W, Bi Z, Shi C, Guo X, Fan L-Z, et al. Solid garnet batteries. Joule 2019;3:1190–9.
[317] Li S, Wang H, Wu W, Lorandi F, Whitacre JF, Matyjaszewski K. Solvent-processed metallic lithium microparticles for lithium metal batteries. ACS Appl Energy Mater 2019;2:1623–8.
[318] Albertus P, Babinec S, Litzelman S, Newman A. Status and challenges in enabling the lithium metal electrode for high-energy and low-cost rechargeable batteries. Nat Energy 2018;3:16–21.
[319] Lux SF, Schappacher F, Balducci A, Passerini S, Winter M. Low cost, environmentally benign binders for lithium-ion batteries. J Electrochem Soc 2010;157:A320 -A5.
[320] Xu JT, Chou SL, Gu QF, Liu HK, Dou SX. The effect of different binders on electrochemical properties of LiNi1/3Mn1/3C1/3O2 cathode material in lithium ion batteries. J Power Sources 2013;225:172–8.
[321] Li J, Klopsch R, Nowak S, Kunze M, Winter M, Passerini S. Investigations on cellulose-based high voltage composite cathodes for lithium ion batteries. J Power Sources 2011;196:7687–91.
[322] Ibing L, Gallasch T, Schneider P, Niehoff P, Hintennach A, Winter M, et al. Towards water based ultra-thick Li ion battery electrodes - a binder approach. J Power Sources 2019;423:183–91.
[323] Tran B, Oladeji IO, Wang ZD, Calderon J, Chai GY, Atherton D, et al. Thick LiCoO2/Nickel Foam Cathode Prepared by an Adhesive and Water-Soluble PEG-Based Copolymer Binder. J Electrochem Soc 2012;159:A1928–A1A33.
[324] Guerfi A, Kaneko M, Petitclerc M, Mori M, Zaghib K. LiFePO4 water-soluble binder electrode for Li-ion batteries. J Power Sources 2007;163:1047–52.
[325] Sun JC, Ren X, Li ZF, Tian WC, Zheng Y, Wang L, et al. Effect of poly (acrylic acid)/Poly (vinyl alcohol) blending binder on electrochemical performance for lithium iron phosphate cathodes. J Alloys Compd 2019;783:379–86.
[326] Cai ZP, Liang Y, Li WS, Xing LD, Liao YH. Preparation and performances of LiFePO4 cathode in aqueous solvent with polyacrylic acid as a binder. J Power Sources 2009;189:547–51.
[327] Li C-C, Lee J-T, Peng X-W. Improvements of Dispersion Homogeneity and Cell Performance of Aqueous-Processed LiCoO [sub 2] Cathodes by Using Dispersant of PAA–NH [sub 4]. J Electrochem Soc 2006;153:A809.
[328] Lee JH, Kim JS, Kim YC, Zang DS, Choi YM, Park WI, et al. Effect of carboxymethyl cellulose on aqueous processing of LiFePO4 cathodes and their electrochemical performance. Electrochem Solid State Lett 2008;11:A175–A1A8.
[329] Porcher W, Lestriez B, Jouanneau S, Guyomard D. Design of Aqueous Processed Thick LiFePO4 Composite Electrodes for High-Energy Lithium Battery. J Electrochem Soc 2009;156:A133–AA44.
[330] Guy D, Lestriez B, Bouchet R, Guyomard D. Critical role of polymeric binders on the electronic transport properties of composites electrode. J Electrochem Soc 2006;153:A679–AA88.
[331] Choi NS, Lee YG, Park JK. Effect of cathode binder on electrochemical properties of lithium rechargeable polymer batteries. J Power Sources 2002;112:61–6.
[332] Li CC, Lee JT, Peng XW. Improvements of dispersion homogeneity and cell performance of aqueous-processed LiCoO2 cathodes by using dispersant of PAA-NH4. J Electrochem Soc 2006;153:A809–AA15.
[333] Clement RJ, Lun Z, Ceder G. Cation-disordered rocksalt transition metal oxides and oxyfluorides for high energy lithium-ion cathodes. Energy Environ Sci 2020;13:345–73.
[334] Xu GL, Liu Q, Lau KKS, Liu Y, Liu X, Gao H, et al. Building ultraconformal protective layers on both secondary and primary particles of layered lithium transition metal oxide cathodes. Nat Energy 2019;4:484–94.
[335] Su LS, Smith PM, Anand P, Reeja-Jayan B. Surface Engineering of a LiMn2O4 Electrode Using Nanoscale Polymer Thin Films via Chemical Vapor Deposition Polymerization. ACS Appl Mater Interfaces 2018;10:27063–73.
[336] Ju SH, Kang IS, Lee YS, Shin WK, Kim S, Shin K, et al. Improvement of the Cycling Performance of LiNi0.6Co0.2Mn0.2O2 Cathode Active Materials by a Dual-Conductive Polymer Coating. ACS Appl Mater Interfaces 2014;6:2546–52.
[337] Gan QM, Qin N, Zhu YH, Huang ZX, Zhang FC, Gu S, et al. Polyvinylpyrrolidone-Induced Uniform Surface-Conductive Polymer Coating Endows Ni-Rich LiNi0.8Co0.1Mn0.1O2 with Enhanced Cyclability for Lithium-Ion Batteries. ACS Appl Mater Interfaces 2019;11:12594–604.

[338] Wu F, Liu JR, Li L, Zhang XX, Luo R, Ye YS, et al. Surface Modification of Li-Rich Cathode Materials for Lithium-Ion Batteries with a PEDOT:PSS Conducting 0Polymer. ACS Appl Mater Interfaces 2016;8:23095–104.
[339] Kwon Y, Lee Y, Kim SO, Kim HS, Kim KJ, Byun D, et al. Conducting Polymer Coating on a High-Voltage Cathode Based on Soft Chemistry Approach toward Improving Battery Performance. ACS Appl Mater Interfaces 2018;10:29457–66.
[340] Kim JM, Park JH, Lee CK, Lee SY. Multifunctional semi-interpenetrating polymer network-nanoencapsulated cathode materials for high-performance lithium-ion batteries. Sci Rep 2014;4.
[341] Park JH, Cho JH, Kim JS, Shim EG, Lee SY. High-voltage cell performance and thermal stability of nanoarchitectured polyimide gel polymer electrolyte–coated LiCoO2 cathode materials. Electrochim Acta 2012;86:346–51.
[342] Lee EH, Park JH, Kim JM, Lee SY. Direct surface modification of high-voltage LiCoO2 cathodes by UV-cured nanothickness poly(ethylene glycol diacrylate) gel polymer electrolytes. Electrochim Acta 2013;104:249–54.
[343] Yang XH, Shen LY, Wu B, Zuo ZC, Mu DB, Wu BR, et al. Improvement of the cycling performance of LiCoO2 with assistance of cross-linked PAN for lithium ion batteries. J Alloys Compd 2015;639:458–64.
[344] Cao JC, Hu GR, Peng ZD, Du K, Cao YB. Polypyrrole-coated LiCoO2 nanocomposite with enhanced electrochemical properties at high voltage for lithium-ion batteries. J Power Sources 2015;281:49–55.
[345] Cheng L, Du X, Jiang Y, Vlad A. Mechanochemical assembly of 3D mesoporous conducting-polymer aerogels for high performance hybrid electrochemical energy storage. Nano Energy 2017;41:193–200.
[346] Park KS, Schougaard SB, Goodenough JB. Conducting-polymer/iron-redox-couple composite cathodes for lithium secondary batteries. Adv Mater 2007;19:848 -+.
[347] Kim T, Ono LK, Qi YB. Elucidating the Mechanism Involved in the Performance Improvement of Lithium-Ion Transition Metal Oxide Battery by Conducting Polymer. Adv Mater Interfaces 2019;6.
[348] Gao XW, Deng YF, Wexler D, Chen GH, Chou SL, Liu HK, et al. Improving the electrochemical performance of the LiNi0.5Mn1.5O4 spinel by polypyrrole coating as a cathode material for the lithium-ion battery. J Mater Chem A 2015;3:404–11.
[349] Wang J, Chen J, Konstantinov K, Zhao L, Ng SH, Wang GX, et al. Sulphur-polypyrrole composite positive electrode materials for rechargeable lithium batteries. Electrochim Acta 2006;51:4634–8.
[350] Wei WL, Du PC, Liu D, Wang Q, Liu P. Facile one-pot synthesis of well-defined coaxial sulfur/polypyrrole tubular nanocomposites as cathodes for long-cycling lithium-sulfur batteries. Nanoscale 2018;10:13037–44.
[351] Liu Y, Yan WJ, An XW, Du X, Wang ZD, Fan HL, et al. A polypyrrole hollow nanosphere with ultra-thin wrinkled shell: synergistic trapping of sulfur in Lithium-Sulfur batteries with excellent elasticity and buffer capability. Electrochim Acta 2018;271:67–76.
[352] Yin FX, Liu XY, Zhang YG, Zhao Y, Menbayeva A, Bakenov Z, et al. Well-dispersed sulfur anchored on interconnected polypyrrole nanofiber network as high performance cathode for lithium-sulfur batteries. Solid State Sci 2017;66:44–9.
[353] Fu YZ, Manthiram A. Core-shell structured sulfur-polypyrrole composite cathodes for lithium-sulfur batteries. Rsc Adv 2012;2:5927–9.
[354] Ansari Y, Zhang S, Wen BH, Fan F, Chiang YM. Stabilizing Li-S Battery Through Multilayer Encapsulation of Sulfur. Adv Energy Mater 2019;9.
[355] Zhang J, Shi Y, Ding Y, Zhang W, Yu G. In Situ Reactive Synthesis of Polypyrrole-MnO2 Coaxial Nanotubes as Sulfur Hosts for High-Performance Lithium–Sulfur Battery. Nano Lett 2016;16:7276–81.
[356] Li F, Kaiser MR, Ma J, Hou Y, Zhou T, Han Z, et al. Uniform Polypyrrole Layer-Coated Sulfur/Graphene Aerogel via the Vapor-Phase Deposition Technique as the Cathode Material for Li–S Batteries. ACS Appl Mater Interfaces 2020;12:5958–67.
[357] Jiang H, Liu X-C, Wu Y, Shu Y, Gong X, Ke F-S, et al. Metal–Organic Frameworks for High Charge–Discharge Rates in Lithium–Sulfur Batteries. Angew Chem Int Ed 2018;57:3916–21.
[358] Li GC, Li GR, Ye SH, Gao XP. A Polyaniline-Coated Sulfur/Carbon Composite with an Enhanced High-Rate Capability as a Cathode Material for Lithium/Sulfur Batteries. Adv Energy Mater 2012;2:1238–45.
[359] Zhou WD, Yu YC, Chen H, DiSalvo FJ, Abruna HD. Yolk-Shell Structure of Polyaniline-Coated Sulfur for Lithium-Sulfur Batteries. J Am Chem Soc 2013;135:16736–43.
[360] Li X, Rao M, Lin H, Chen D, Liu Y, Liu S, et al. Sulfur loaded in curved graphene and coated with conductive polyaniline: preparation and performance as a cathode for lithium–sulfur batteries. J Mater Chem A 2015;3:18098–104.
[361] Ding K, Bu Y, Liu Q, Li T, Meng K, Wang Y. Ternary-layered nitrogen–doped graphene/sulfur/polyaniline nanoarchitecture for the high-performance of lithium–sulfur batteries. J Mater Chem A 2015;3:8022–7.
[362] Yan J, Liu X, Yao M, Wang X, Wafle TK, Li B. Long-Life, High-Efficiency Lithium–Sulfur Battery from a Nanoassembled Cathode. Chem Mater 2015;27:5080–7.
[363] Zhu P, Zhu J, Yan C, Dirican M, Zang J, Jia H, et al. Situ Polymerization of Nanostructured Conductive Polymer on 3D Sulfur/Carbon Nanofiber Composite Network as Cathode for High-Performance Lithium–Sulfur Batteries. Adv Mater Interfaces 2018;5:1701598.
[364] Yan JH, Li BY, Liu XB. Nano-porous sulfur-polyaniline electrodes for lithium–sulfurbatteries. Nano Energy 2015;18:245–52.
[365] Anilkumar KM, Jinisha B, Manoj M, Pradeep VS, Jayalekshmi S. Layered sulfur/PEDOT:PSS nano composite electrodes for lithium sulfur cell applications. Appl Surf Sci 2018;442:556–64.
[366] Yan M, Zhang Y, Li Y, Huo Y, Yu Y, Wang C, et al. Manganese dioxide nanosheet functionalized sulfur@PEDOT core–shell nanospheres for advanced lithium–sulfur batteries. J Mater Chem A 2016;4:9403–12.
[367] Zhang M, Meng Q, Ahmad A, Mao L, Yan W, Wei Z. Poly(3,4-ethylenedioxythiophene)-coated sulfur for flexible and binder-free cathodes of lithium–sulfur batteries. J Mater Chem A 2017;5:17647–52.
[368] Xiao P, Bu F, Yang G, Zhang Y, Xu Y. Integration of graphene, nano sulfur, and conducting polymer into compact, flexible lithium–sulfur battery cathodes with ultrahigh volumetric capacity and superior cycling stability for foldable devices. Adv Mater 2017;29:1703324.
[369] Wang T, Zhu J, Wei Z, Yang H, Ma Z, Ma R, et al. Bacteria-Derived Biological Carbon Building Robust Li–S Batteries. Nano Lett 2019;19:4384–90.
[370] Su D, Cortie M, Fan H, Wang G. Prussian Blue Nanocubes with an Open Framework Structure Coated with PEDOT as High-Capacity Cathodes for Lithium–Sulfur Batteries. Adv Mater 2017;29:1700587.
[371] Li WY, Zhang QF, Zheng GY, Seh ZW, Yao HB, Cui Y. Understanding the Role of Different Conductive Polymers in Improving the Nanostructured Sulfur Cathode Performance. Nano Lett 2013;13:5534–40.
[372] Huang L, Cheng J, Li X, Yuan D, Ni W, Qu G, et al. Sulfur quantum dots wrapped by conductive polymer shell with internal void spaces for high-performance lithium–sulfur batteries. J Mater Chem A 2015;3:4049–57.
[373] Moon S, Jung YH, Kim DK. Enhanced electrochemical performance of a crosslinked polyaniline-coated graphene oxide-sulfur composite for rechargeable lithium-sulfur batteries. J Power Sources 2015;294:386–92.
[374] Oh EJ, Jang KS, MacDiarmid AG. High molecular weight soluble polypyrrole. Synth Met 2001;125:267–72.
[375] Nakayama M, Yano J, Nakaoka K, Ogura K. Electrodeposition of composite films consisting of polypyrrole and mesoporous silica. Synth Met 2002;128:57–62.
[376] Liu Y, Chu Y, Yang L. Adjusting the inner-structure of polypyrrole nanoparticles through microemulsion polymerization. Mater Chem Phys 2006;98:304–8.
[377] Hong X, Fu J, Liu Y, Li S, Wang X, Dong W, et al. Recent Progress on Graphene/Polyaniline Composites for High-performance Supercapacitors. Materials 2019:12.
[378] Souza VHR, Oliveira MM, Zarbin AJG. Bottom-up synthesis of graphene/polyaniline nanocomposites for flexible and transparent energy storage devices. J Power Sources 2017;348:87–93.
[379] Yu J, Xie F, Wu Z, Huang T, Wu J, Yan D, et al. Flexible metallic fabric supercapacitor based on graphene/polyaniline composites. Electrochim Acta 2018;259:968–74.
[380] Ma P, Zhang B-hH, Xu Y-hH, Gong G. Study on improving properties of elemental sulfur cathode materials by coating PANi. Mod Chem Ind 2007;27:30.
[381] Qiu LL, Zhang SC, Zhang L, Sun MM, Wang WK. Preparation and enhanced electrochemical properties of nano-sulfur/poly(pyrrole-co-aniline) cathode material for lithium/sulfur batteries. Electrochim Acta 2010;55:4632–6.
[382] Kirchmeyer S, Reuter K. Scientific importance, properties and growing applications of poly(3,4-ethylenedioxythiophene). J Mater Chem 2005;15:2077–88.
[383] Sun K, Zhang S, Li P, Xia Y, Zhang X, Du D, et al. Review on application of PEDOTs and PEDOT:PSS in energy conversion and storage devices. J Mater Sci: Mater Electron 2015;26:4438–62.
[384] Shadike Z, Tan S, Wang Q-C, Lin R, Hu E, Qu D, et al. Review on organosulfur materials for rechargeable lithium batteries. Mater Horiz 2021;8:471–500.
[385] Dong CW, Gao W, Jin B, Jiang Q. Advances in Cathode Materials for High-Performance Lithium-Sulfur Batteries. Iscience 2018;6:151–98.
[386] Chung WJ, Griebel JJ, Kim ET, Yoon H, Simmonds AG, Ji HJ, et al. The use of elemental sulfur as an alternative feedstock for polymeric materials. Nat Chem 2013;5:518–24.
[387] Fanous J, Wegner M, Grimminger J, Andresen A, Buchmeiser MR. Structure-Related Electrochemistry of Sulfur-Poly(acrylonitrile) Composite Cathode Materials for Rechargeable Lithium Batteries. Chem Mater 2011;23:5024–8.
[388] Kim H, Lee J, Ahn H, Kim O, Park MJ. Synthesis of three-dimensionally interconnected sulfur-rich polymers for cathode materials of high-rate lithium–sulfur batteries. Nat Commun 2015;6.
[389] Li X, Liang J, Lu Y, Hou Z, Cheng Q, Zhu Y, et al. Sulfur-Rich Phosphorus Sulfide Molecules for Use in Rechargeable Lithium Batteries. Angew Chem Int Ed 2017;56:2937–41.
[390] Simmonds AG, Griebel JJ, Park J, Kim KR, Chung WJ, Oleshko VP, et al. Inverse Vulcanization of Elemental Sulfur to Prepare Polymeric Electrode Materials for Li–S Batteries. ACS Macro Lett 2014;3:229–32.
[391] Liu X, Lu Y, Zeng Q, Chen P, Li Z, Wen X, et al. Trapping of polysulfides with sulfur-rich poly ionic liquid cathode materials for ultralong-life lithium–sulfur batteries. ChemSusChem 2020;13:715–23.
[392] Matyjaszewski K, Mu Jo S, Paik H-jJ, Gaynor SG. Synthesis of well-defined polyacrylonitrile by atom transfer radical polymerization. Macromolecules 1997;30:6398–400.
[393] Lamson M, Kopeć M, Ding H, Zhong M, Matyjaszewski K. Synthesis of well-defined polyacrylonitrile by ICAR ATRP with low concentrations of catalyst. J Polym Sci, Part A: Polym Chem 2016;54:1961–8.
[394] Pan X, Lamson M, Yan J, Matyjaszewski K. Photoinduced Metal-Free Atom Transfer Radical Polymerization of Acrylonitrile. ACS Macro Lett 2015;4:192–6.

[395] Yuan R, Wang H, Sun M, Damodaran K, Gottlieb E, Kopeć M, et al. Well-Defined N/S Co-Doped Nanocarbons from Sulfurized PAN-b-PBA Block Copolymers: Structure and Supercapacitor Performance. ACS Appl Nano Mater 2019;2:2467–74.
[396] Zhang J, Song Y, Kopeć M, Lee J, Wang Z, Liu S, et al. Facile Aqueous Route to Nitrogen-Doped Mesoporous Carbons. J Am Chem Soc 2017;139:12931–4.
[397] Wang JL, Yang J, Xie JY, Xu NX. A novel conductive polymer-sulfur composite cathode material for rechargeable lithium batteries. Adv Mater 2002;14:963 -+.
[398] Yu XG, Xie JY, Yang J, Huang HJ, Wang K, Wen ZS. Lithium storage in conductive sulfur-containing polymers. J Electroanal Chem 2004;573:121–8.
[399] Wei SY, Ma L, Hendrickson KE, Tu ZY, Archer LA. Metal-Sulfur Battery Cathodes Based on PAN Sulfur Composites. J Am Chem Soc 2015;137:12143–52.
[400] Chen X, Peng LF, Wang LH, Yang JQ, Hao ZX, Xiang JW, et al. Ether-compatible sulfurized polyacrylonitrile cathode with excellent performance enabled by fast kinetics via selenium doping. Nat Commun 2019;10.
[401] Je SH, Hwang TH, Talapaneni SN, Buyukcakir O, Kim HJ, Yu JS, et al. Rational sulfur cathode design for lithium-sulfur batteries: sulfur-embedded benzoxazine polymers. ACS Energy Lett 2016;1:566–72.
[402] Han P, Chung SH, Chang CH, Manthiram A. Bifunctional Binder with Nucleophilic Lithium Polysulfide Immobilization Ability for High-Loading, High-Thickness Cathodes in Lithium-Sulfur Batteries. ACS Appl Mater Interfaces 2019;11:17393–9.
[403] Liu FQ, Hu ZY, Xue JX, Huo H, Zhou JJ, Li L. Stabilizing cathode structure via the binder material with high resilience for lithium-sulfur batteries. Rsc Advances 2019;9:40471–7.
[404] Lacey MJ, Jeschull F, Edstrom K, Brandell D. Porosity Blocking in Highly Porous Carbon Black by PVdF Binder and Its Implications for the Li-S System. Journal of Physical Chemistry C 2014;118:25890–8.
[405] Xu GY, Yan QB, Kushima A, Zhang XG, Pan J, Li J. Conductive graphene oxide-polyacrylic acid (GOPAA) binder for lithium-sulfur battery. Nano Energy 2017;31:568–74.
[406] Pang Q, Liang X, Kwok CY, Kulisch J, Nazar LF. A Comprehensive Approach toward Stable Lithium-Sulfur Batteries with High Volumetric Energy Density. Adv Energy Mater 2017;7.
[407] Chen W, Lei TY, Qian T, Lv WQ, He WD, Wu CY, et al. A New Hydrophilic Binder Enabling Strongly Anchoring Polysulfides for High-Performance Sulfur Electrodes in Lithium-Sulfur Battery. Adv Energy Mater 2018;8.
[408] Li GR, Ling M, Ye YF, Li ZP, Guo JH, Yao YF, et al. Acacia Senegal-Inspired Bifunctional Binder for Longevity of Lithium-Sulfur Batteries. Adv Energy Mater 2015;5.
[409] Jin BY, Yang LF, Zhang JW, Cai YJ, Zhu J, Lu JG, et al. Bioinspired binders actively controlling ion migration and accommodating volume change in high sulfur loading lithium-sulfur batteries. Adv Energy Mater 2019;9.
[410] Lacey MJ, Jeschull F, Edstrom K, Brandell D. Functional, water-soluble binders for improved capacity and stability of lithium-sulfur batteries. J Power Sources 2014;264:8–14.
[411] He M, Yuan LX, Zhang WX, Hu XL, Huang YH. Enhanced cyclability for sulfur cathode achieved by a water-soluble binder. J Phys Chem C 2011;115:15703–9.
[412] Hwa Y, Cairns EJ. Polymeric binders for the sulfur electrode compatible with ionic liquid containing electrolytes. Electrochim Acta 2018;271:103–9.
[413] Cheng M, Liu YA, Guo XD, Wu ZG, Chen YX, Li JS, et al. A novel binder-sulfonated polystyrene for the sulfur cathode of Li-S batteries. Ionics 2017;23:2251–8.
[414] Milroy C, Manthiram A. An elastic, conductive, electroactive nanocomposite binder for flexible sulfur cathodes in lithium-sulfur batteries. Adv Mater 2016;28:9744 -+.
[415] Zeng FL, Wang WK, Wang AB, Yuan KG, Jin ZQ, Yang YS. Multidimensional Polycation beta-Cyclodextrin Polymer as an Effective Aqueous Binder for High Sulfur Loading Cathode in Lithium-Sulfur Batteries. ACS Appl Mater Interfaces 2015;7:26257–65.
[416] Zhang L, Ling M, Feng J, Liu G, Guo JH. Effective electrostatic confinement of polysulfides in lithium/sulfur batteries by a functional binder. Nano Energy 2017;40:559–65.
[417] Su HP, Fu CY, Zhao YF, Long DH, Ling LC, Wong BM, et al. Polycation binders: an effective approach toward lithium polysulfide sequestration in Li-S batteries. ACS Energy Lett 2017;2:2591–7.
[418] Ling M, Yan WJ, Kawase A, Zhao H, Fu YB, Battaglia VS, et al. Electrostatic polysulfides confinement to inhibit redox shuttle process in the lithium sulfur batteries. ACS Appl Mater Interfaces 2017;9:31741–5.
[419] Chen W, Qian T, Xiong J, Xu N, Liu XJ, Liu J, et al. A new type of multifunctional polar binder: toward practical application of high energy lithium sulfur batteries. Adv Mater 2017;29.
[420] Muench S, Wild A, Schubert US, Muench S, Wild A, Friebe C, et al. Polymer-based organic batteries. Chem Rev 2016;116:9438–84.
[421] Wang J, Lakraychi AE, Liu X, Sieuw L, Morari C, Poizot P, et al. Conjugated sulfonamides as a class of organic lithium-ion positive electrodes. Nat Mater 2021;20:665–73.
[422] Dolphijn G, Isikli S, Gauthy F, Vlad A, Gohy JF. Hybrid LiMn2O4–radical polymer cathodes for pulse power delivery applications. Electrochim Acta 2017;255:442–8.